# Multiple approaches towards understanding virulence in *Clavibacter michiganensis* subsp. *sepedonicus*, causal agent of bacterial ring rot of potato

A DISSERTATION
SUBMITTED TO THE FACULTY OF THE GRADUATE SCHOOL
OF THE UNIVERSITY OF MINNESOTA
BY

Ryan L. Syverson

IN PARTIAL FULFILLMENT OF THE REQUIREMENTS
FOR THE DEGREE OF
DOCTOR OF PHILOSOPHY
IN PLANT PATHOLOGY

Dr. Carol A. Ishimaru

December, 2011

# Acknowledgements

I would like to thank my advisor Dr. Carol Ishimaru for her encouragement, support and advice. She has been an excellent mentor and a positive influence throughout my research and academic pursuits. I would also like to thank the members of my thesis committee Dr. Jim Bradeen, Dr. Deb Samac and Dr. Mike Sadowsky for their suggestions and collaboration. Thank you to all of the people in the Bacteriology Lab for your encouragement, assistance and friendship during my time in the lab. In particular, thanks to Rebecca Curland for your contributions and assistance with greenhouse disease assessments and IFAS experiments and Justin Stanton for your assistance with the biofilm assay optimization. Additionally, I would like to thank the entire faculty, staff and graduate students of the Department of Plant Pathology for their support and contributions to my research and academic pursuits, especially to Joel Jurgens and Ben Held for their help with the fluorescence microscopy.

I am very grateful for the encouragement of all of my family and friends, particularly my wife Tara, my parents Robert and Joni, and my sister Lyndsay. You all have been very supportive and caring in times of success and stress.

# Abstract

Recent discoveries related to pathogenesis of *Clavibacter michiganensis* subsp. *sepedonicus* (*Cms*), causal agent of bacterial ring rot of potato, are beginning to shed light on the virulence strategies of this species. The chromosomal homologue of *pat-1*, *chp7*, was found to be necessary for HR elicitation in tobacco and virulence of *Cms* in eggplant and potato. Multiple chromosomal and plasmid-encoded homologues of *pat-1* (*chp* and *php* genes, respectively) are present in *Cms*, yet only the function of *chp7* has been evaluated. The development of molecular resources and techniques for genetic manipulation of *Cms* are needed to facilitate studies aimed at building a more comprehensive understanding of the role of *pat-1* homologues in pathogenesis.

Knockout mutants *chp7* and *php3* of *Cms* were generated via targeted mutagenesis. The virulence of *chp7* and *php3* mutants of *Cms* were evaluated on eggplant and potato. Significant reductions in virulence of *Cms* were observed for *chp7* and *php3* mutants in both eggplant and potato. Mutation of *chp7* also resulted in the loss of non-hostHR induction and an observed reduction in bacterial titer of infected plants. These phenotypes however, were not observed in *php3* mutants of *Cms*.

A mutant of *chp8* was identified in a newly generated *EzTn5* transposon library of *Cms*. The virulence of the *chp8* mutant of *Cms* was evaluated in eggplant. Significant reductions in both bacterial titer of infected plant tissue and virulence of *Cms* were observed for the *chp8* mutant. In summary, three *pat-1* homologues from *Cms* have now been evaluated for their relative contributions to virulence, and these studies indicate that each is likely contributing differently to pathogenesis of *Cms*.

The formation of biofilms has been demonstrated in *Cms* both *in vitro* and *in planta*. Development of an appropriate assay for assessing biofilm formation by *Cms* is a necessary first step towards addressing the role of biofilms in bacterial ring rot. Two of the biofilm assays examined in this study could be considered as potential strategies for future assessment of biofilm formation by *Cms*. Currently, both of these assays are still diminished in their utility, given issues with inconsistencies and reproducibility.

# Table of Contents

# List of Tables

# List of Figures

# Chapter 1

# Literature Review

## Introduction to bacterial plant pathogens

Generally, bacterial plant pathogens can be separated into two major groups, gram-positive and gram-negative, based primarily on cell wall structure (41). Pathogens belonging to these two groups have evolved diverse and complex mechanisms for interacting with their respective hosts. The most clearly understood example of such an interaction can be seen in the utilization of the type III secretion system (TTSS) and its associated effectors by gram-negative bacteria. The TTSS cellular machinery allows for the direct injection of effectors into the host cell and is an essential component of host-microbe interactions of these bacteria (1). In contrast, gram-positive phytopathogens lack the outer membrane found in gram-negative bacteria and do not require or possess a TTSS for translocating effectors. Thus, gram-positive bacteria have evolved alternative strategies to induce disease. For example, the utilization of phytotoxins, pathogen-produced plant hormones and secreted virulence proteins are among the mechanisms observed in pathogenesis of gram-positive plant pathogens (18).

## Role of effectors in pathogenesis

Recently, the term "effector" has become more widely utilized in discussions of plant-microbe interactions. Hogenhout *et al.* (19) broadly define effectors as all pathogen-derived proteins or small molecules that produce changes to host cellular structure or function. When considering the role of effectors in plant-microbe interactions related to virulence, host responses to the presence of microbes can generally by classified into three categories in which effectors can play a pivotal role: pathogen-triggered immunity (PTI), effector-triggered immunity (ETI) and effector-triggered

susceptibility (ETS) (21). Briefly, upon infection the host recognizes hallmarks of the pathogen known as pathogen-associated molecular patterns (PAMPs) or microbe-associated molecular patterns (MAMPs) and initiates signal cascades leading to the horizontal resistance seen in PTI. Pathogens can utilize effectors to interfere with PTI leading to ETS. Should the host have the appropriate resistance proteins for recognition of specific pathogen effectors then the vertical resistance of ETI is observed. A common hallmark of ETI is programmed cell death or the hypersensitive response (HR). Here, pathogens can again utilize effectors to disrupt ETI or suppress HR. This coevolutionary ebb and flow between compatible and incompatible host-microbe interactions has led to the hypthosis of the plant-pathogen arms race (36).

**Introduction to *Clavibacter michiganensis***

*Clavibacter michiganensis* is a gram-positive plant pathogenic species belonging to the *Microbacteriaceae* of the *Actinobacteria* (35). *Clavibacter michiganensis* is the only species in the genus *Clavibacter*. It is divided into five subspecies based on host specificity as follows: subsp. *michiganensis* (*Cmm*, tomato canker), subsp. *sepedonicus* (*Cms*, potato ring rot), subsp. *insidiosus* (*Cmi*, wilt of alfalfa), subsp. *nebraskensis* (*Cmn*, wilt and blight of maize) and subsp. *tessellarius* (*Cmt*, leaf freckle and leaf spot of wheat) (13). Subspecies of *C. michiganensis* display a mucoid colony morphology in culture and are generally pigmented yellow to orange, with the exception of *Cms* which is typically white to pale yellow (Figure 1.1) (5). Other important plant pathogenic genera of bacteria closely related to *Clavibacter*, and in the same family, include *Curtobacterium*, *Rathayibacter* and *Leifsonia* (34).

**Symptoms and control of disease caused by *Clavibacter michiganensis* subsp. *sepedonicus***

As the causal agent of bacterial ring rot of potato (*Solanum tuberosum*), *Cms* is a vascular system-infecting bacterium of both above and belowground tissue of the host. Symptoms of the ring rot disease include wilting and discoloration of the foliage, a characteristic light brown rotting of the vascular ring as well as a cracked and sunken outer surface of the potato tuber (37). This pathogen is highly infectious and can survive for long periods of time as dried slime on field equipment and storage facilities. *Cms* exhibits an endophytic lifestyle and survives poorly in soil, although occurrence in plant debris is possible (16). The disease is controlled primarily through a "zero tolerance" policy for *Cms* in production of certified potato seed (15). *Cms* grows slowly in culture making isolation from plant material difficult. Therefore detection and quantification of *Cms* from infected plants is generally achieved using indirect fluorescent antibody staining (IFAS) (6), ELISA (8), and polymerase chain reaction (PCR) assays (28). Regular sanitation of field debris, equipment and storage facilities is also applied to disease management. The use of host resistance against bacterial ring rot is avoided given that resistant varieties can harbor significant pathogen populations and serve as sources of inoculum (25). Despite differences in symptom expression, all currently available cultivated potato varieties are susceptible to colonization by *Cms* (7).

**Genome structure of *Clavibacter michiganensis***

The full genome sequence of three *C. michiganensis* subspecies, *C. m.* subsp. *michiganensis* (NCPPB382), *C. m.* subsp. *sepedonicus* (ATCC33113), and *C. m.* subsp. *nebraskensis* (NCPPB2581) are now available (Table 1.1) (2, 11, 12). For *Cmm*, the genome consists of a single circular chromosome (3.30 Mb) and two circular plasmids, pCM1 (27 kb) and pCM2 (70 kb), totaling approximately 3.4 Mb. The G+C content of the genome is high, ranging from 72.7% in the chromosome to 66.5-67.5% in the plasmids. In total, there are 3080 coding sequences (CDSs) predicted in the genome (2984 CDSs on the chromosome, 28 on pCM1 and 68 on pCM2). Twenty-six of the predicted CDSs in *Cmm* were found to be pseudogenes (24 on the chromosome, and 2 on pCM2). For *Cms*, the genome consists of a single circular chromosome (3.26 Mb), a circular plasmid pCS1 (50 kb) and a linear plasmid pCSL1 (95 kb) totaling 3.35 Mb. The G+C content is also high, ranging from 72.5% in the chromosome to 67-68% in the plasmids. Approximately 85% of the genome is predicted coding sequence with a total of 3242 CDSs present in the genome (3058 CDSs on the chromosome, 67 on pCS1 and 117 on pCSL1). In contrast to *Cmm*, many more pseudogenes are found in *Cms* with 110 CDSs classified as pseudogenes (106 on the chromosome, 3 on pCS1 and 1 on pCSL1). Additionally, a number of IS elements (106) are present in the *Cms* genome, whereas these elements are rare in the genome of *Cmm*. The genome of *Cmn* consists of a single circular chromosome of 3.06 Mbps in size and lacks native plasmids. As was observed in the genomes of *Cmm* and *Cms*, The G+C content of *Cmn* is high at 73%. Roughly 3000 CDSs are predicted in the genome, of which about 50 are thought to be pseudogenes.

**Genomic comparisons of subspecies of *Clavibacter michiganensis***

Genomic comparisons between *Cmm*, *Cms* and *Cmn* reveal a high degree of similarity among the subspecies with nearly 90% DNA identity among shared genes. Furthermore, the genomes of *Cmm* and *Cmn* are highly collinear. In contrast, rearrangements are found in the genome of *Cms* (2). These rearrangements occur frequently and are typically bordered by IS elements, which are the presumed mechanism of the observed genomic shuffling. An example of such genomic reorganizations can be seen through examination of genome locations of pathogenesis-associated genes in *C. michiganensis*. In *Cmm*, many genes involved in pathogenesis are clustered within a pathogenicity island (PI) on the chromosome including the *chp*/*php* and the *ppa* gene families. Homologues of these genes in *Cms*, on the other hand, are scattered across the genome, and moreover, there is no evidence of the presence of a PI in the genome of *Cms* (2, 12). Additionally, the genome of *Cmn* lacks homologues to pathogenesis-associated genes found in *Cmm* and *Cms* (11). The expansion of IS elements and the increased presence of pseudogenes in association with loss of function for genes involved in nutrient utilization, regulation, transport and pathogenesis-related functions is evidence for niche adaptation of *Cms* since divergence from a presumed free-living ancestor. The completion of genome sequences of the three *C. michiganensis* subspecies affords researchers numerous opportunities for functional analyses of genes involved in important aspects of the molecular biology of this species. Such studies could facilitate a more comprehensive understanding of molecular plant-microbe interactions of this and related plant pathogenic bacteria.

**Genetics of pathogenicity of *Clavibacter michiganensis***

Overall the molecular interactions of *C. michiganensis* with its hosts are not clearly understood. Yet, recent discoveries in regards to pathogenesis of *C. michiganensis* are beginning to shed light on molecular mechanisms of this species. Two distinct pathogenicity determinants have been identified in the tomato pathogen, *Cmm*. *celA*, a cellulase gene, and *pat-1*, a putative serine protease gene, are encoded on pCM1 and pCM2, respectively, and have been demonstrated to be important in virulence of *Cmm* (10, 20). Nine additional genes sharing homology with *pat-1* (*phpA-B* and *chpA-G*) have been identified in *Cmm*, all of which are also predicted to encode for serine proteases. These homologues are located both on the chromosome and pCM2 of *Cmm* and are referred to as chromosome-encoded homologues of *pat-1* (*chp*) and plasmid-encoded homologues of *pat-1* (*php*) genes, repectively (3). A second gene family of related putative serine proteases, designated the *ppa* family consists of 11 members in the *Cmm* genome (12). Functional characterizations of members of the *chp* and *php* as well as the *ppa* gene families have demonstrated that some are involved in pathogenesis of *Cmm*. Mutation of *chpC* resulted in an impaired ability to colonize tomato and thus a reduction in disease severity (38). Inactivation of another homologue, *chpG*, led to the loss of the non-host HR in *Mirabilis jalapa* (38). Additionally, disruption of *ppaA* and *ppaC* resulted in reduction of both virulence and the relative ability to colonize tomato (11). Homologues of these genes exist in the genome of *Cms*. A homologue of *celA* is present on the plasmid pCS1 of *Cms* and also is associated with virulence of *Cms* (24, 30). Both plasmid and chromosome encoded homologues of *pat-1* have been identified in *Cms* (*php1-3* and *chp1-8*) (2, 3). The chromosomal homologue, *chp7*, of *Cms* most

closely resembles *pat-1* of *Cmm* and recently has been shown to be involved in HR elicitation in tobacco and virulence of *Cms* (31). Ten additional members of the *chp* and *php* gene family are known in *Cms*, yet neither the functions of these genes nor their contribution to pathogenesis of *Cms* have been examined.

**Genetic manipulation of *Clavibacter michiganensis***

With the completion of the genome sequences, characterization of gene function in *C. michiganensis* depends largely on the availability of technologies for genetic manipulation of this species. The greatest advances to date have been made with *Cmm* for which efficient transformation protocols and a system for generating targeted gene knockouts were developed (23, 38). Some of these tools have been adapted for use in *Cms*. Various strains of *Cms* have been demonstrated to be amenable to transformation (24). Additionally, a transposon mutant library of *Cms* consisting of 2100 mutants was developed and applied for functional analyses of the chromosomally-encoded serine protease *chp7* (31). This library was created with the insertion element Tn*1409*Cβ isolated from *Arthrobacter* sp. strain TM1 (14). Sequence analyses at the sites of insertion for a subset of about 200 mutants indicated a bias of Tn*1490*Cβ towards regions of low G+C content (77% of chromosomal insertions) limiting the utility of this library for future work. In fact, within the 200 mutant subset, insertion into chromosomal CDSs occurred in only 1% of the predicted 3058 CDSs present (31). The *Cms* strain selected for mutagenesis, R10, was not the same as was used for genome sequencing. Thus results from the R10 library might differ due to possible sequence divergence between R10 and the sequenced strain. Library utility in further functional genomic studies could

be enhanced through the construction of an alternative transposon mutant library made with the sequenced strain and a different transposable element. In addition to forward genetic approaches, a reverse genetic approach based on the development of a targeted gene replacement system for *Cms* would greatly facilitate future gene characterizations. Thus far, all technologies adapted from those developed for *Cmm* have been successfully applied in *Cms*, so the development of a gene replacement system for *Cms* is likely.

**The role of biofilms in pathogenesis**

Given that *Cms* is a vascular system-inhabiting plant pathogen and its propensity to survive long periods of time as dried slime, it is possible that biofilms play an important role in the lifestyle of this organism. Biofilms consist of aggregated bacteria which are held together by a network of polysaccharides and proteins referred to as extracellular polysaccharides (EPS) produced and secreted by the individual bacterium (39). The phenomenon of biofilm formation is quite complex and recent breakthroughs have provided insight into the underlying mechanisms involved in biofilm formation. It involves a number of actions by bacteria including surface adhesion, development of communication networks such as quorum sensing, aggregation of individuals, activation of necessary gene cascades and specialization of individuals within the microcommunity (17). Life in such a microcommunity is advantageous in that it provides a structure that protects memebers from the changing environment, predation, other competing microorganisms and also facilitates the uptake of nutrients and the exchange of genetic material (29).

It is now becoming evident that biofilms are an important component of many diseases caused by bacteria. Research in medical microbiology has more recently focused on the role of biofilms in pathogenicity and is finding that these structures are often important in oral and other chronic infections (32). This connection seems to make sense given that the bacteria can benefit from biofilm formation by increasing their ability to uptake nutrients and spread through the host while also decreasing their sensitivity to antibiotics. Additionally, the importance of biofilms formed by some plant pathogenic bacteria in host-microbe interactions is becoming more evident (33). Biofilm formation plays an important role in plant diseases caused by various vascular system-inhabiting bacterial pathogens including *Xylella fastidiosa* (26), *Xanthomonas campestris* pv. *campestris* (9), *Pantoea stewartii* (40), and *Ralstonia solanacearum* (22). *Clavibacter michiganensis* subsp. *michiganensis* was observed to form biofilms upon infection of tomato. A mutant of NCPPB382 lacking the PI lost the ability to form biofilms (4). These observations indicate that genetic control of biofilm formation is located in the PI of *Cmm* and that biofilms may be important to the plant-microbe interactions of *Cmm*. The formation of biofilms has been demonstrated in *Cms* both *in vitro*, using growth medium containing balsa wood as a substrate for biofilm formation, and *in planta* (27). Based on this observation the question of the importance of biofilms in the development of bacterial ring rot arises.

**Research direction**

Given its current status as a national and international quarantine pest, *Cms* has important implications in potato production. The primary means of control for *Cms* is

through the process of exclusion, but limitations of detection techniques, inapplicability of host resistance and the occurrence of latent infections have prevented eradication of *Cms* from production systems. Functional analyses of genes or phenotypes with putative functions in pathogenicity of *Cms* may lead to a better understanding of those mechanisms underlying host-pathogen interactions of *Cms* and could provide insight to improve detection and management of disease. The development and improvement of methodology for gene manipulation in *Cms* and its application towards functional characterization of *chp* and *php* genes is of high priority. Such studies are a necessary first step towards piecing together the broader contexts of the molecular host-microbe interactions of this pathosystem. Additionally, better understanding of mechanisms underlying host-pathogen interactions of *Cms* could lead to the identification of conserved mechanisms of pathogenicity of *C. michiganensis* and among other related Gram-positive pathogenic bacteria facilitating advancement of research in both animal and plant pathology.

The objectives of this work were the following: first, to develop a targeted mutagenesis system for *Cms* ATCC33113 and apply this strategy to the functional characterization of *php3*; second, to generate a new transposon mutant library in ATCC33113 using the *EzTn5* Transposome and mine this library for a mutant of *chp8* for subsequent functional analysis; finally, to evaluate scalable assays of biofilm formation by *Cms*.

**Table 1.1.** Genome content of three *Clavibacter michiganensis* subspecies (adapted from Eichenlaub and Gartemann, 2011)

| | *Clavibacter michiganensis* subspecies | | |
|---|---|---|---|
| | *Cmm* NCPPB382 | *Cms* ATCC33113 | *Cmn* NCPPB2581 |
| **Chromosome Size (Mbp)** | 3.3 | 3.26 | 3.06 |
| G+C Content | 72.7 | 72.6 | 73 |
| CDSs | 2984 | 3058 | ~3000 |
| Pseudogenes | 24 | 102 | ~50 |
| IS elements | 3 | 106 | 0 |
| **Plasmids** | pCM1 (27 kb)<br>pCM2 (70 kb) | pCS1 (50 kb)<br>pCSL1 (95 kb) | None |

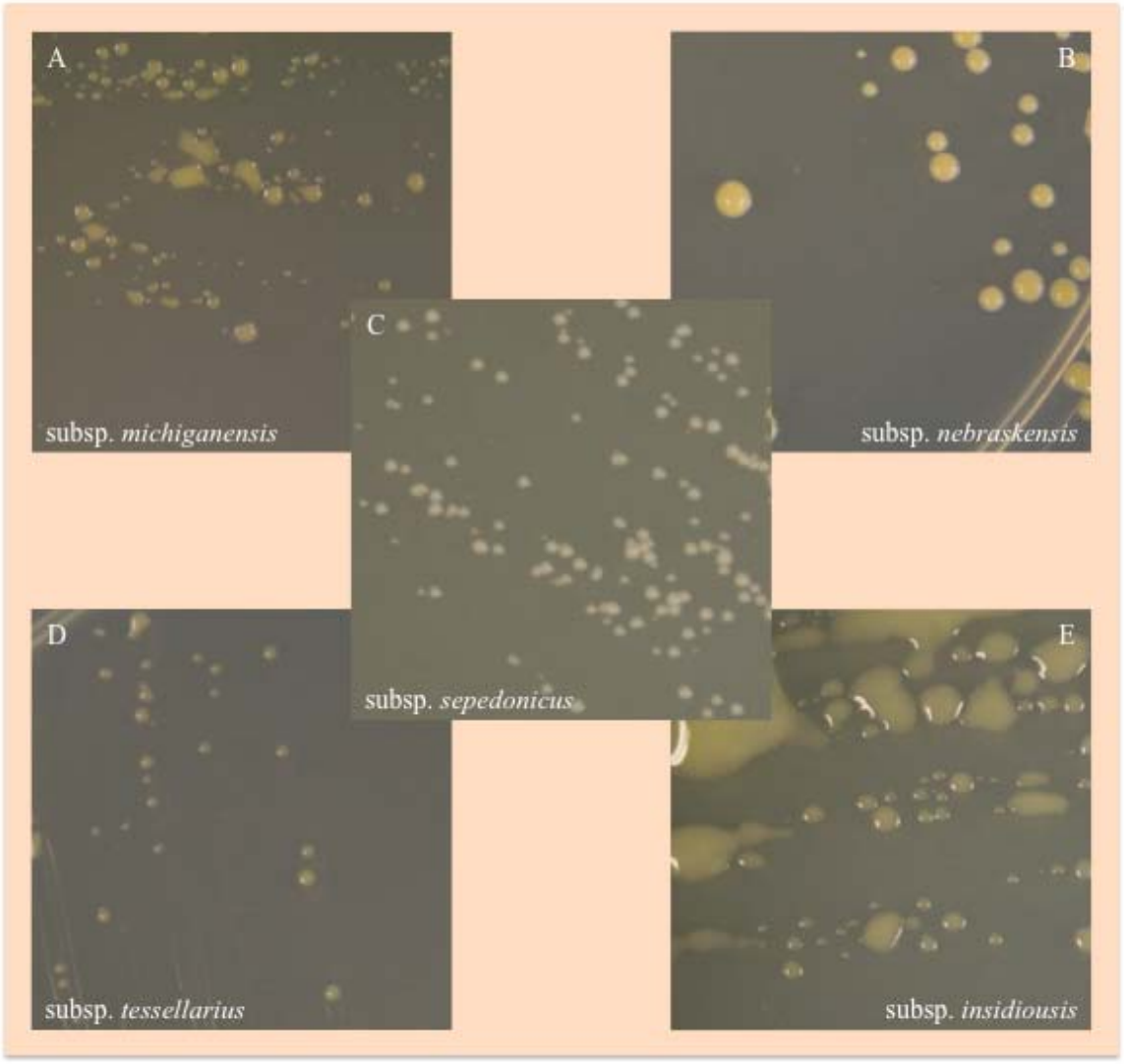


**Figure 1.1. Images of *Clavibacter michiganensis* subspecies in culture.** Cell cultures of the five *C. michiganensis* subspecies are shown. Bacteria were grown on solid Yeast Glucose Medium (YGM) at room temperature for 5-7 days prior to imaging. The following subspecies is shown in each panel: A.) *C. michiganensis* subsp. *michiganensis*, B.) *C. michiganensis* subsp. *nebraskensis*, C.) *C. michiganensis* subsp. *sepedonicus*, D.) *C. michiganensis* subsp. *tessellarius*, and E.) *C. michiganensis* subsp. *insidiosus*.

## References


1. **Alfano, J. R., and A. Collmer.** 2004. Type III secretion system effector proteins: Double agents in bacterial disease and plant defense. Annual Review of Phytopathology **42:**385-414.
2. **Bentley, S. D., C. Corton, S. E. Brown, A. Barron, L. Clark, J. Doggett, B. Harris, D. Ormond, M. A. Quail, G. May, D. Francis, D. Knudson, J. Parkhill, and C. A. Ishimaru.** 2008. Genome of the Actinomycete plant pathogen *Clavibacter michiganensis* subspecies *sepedonicus* suggests recent niche adaptation. Journal of Bacteriology **190:**2150-2160.
3. **Burger, A., I. Grafen, J. Engemann, E. Niermann, M. Pieper, O. Kirchner, K. H. Gartemann, and R. Eichenlaub.** 2005. Identification of homologues to the pathogenicity factor *pat-1*, a putative serine protease of *Clavibacter michiganensis* subsp. *michiganensis*. Microbiological Research **160:**417-27.
4. **Chalupowicz, L., E.-M. Zellermann, M. Fluegel, O. Dror, R. Eichenlaub, K.-H. Gartemann, A. Savidor, G. Sessa, N. Iraki, I. Barash, and S. Manulis.** 2010. Colonization and movement of GFP-labeled *Clavibacter michiganensis* subsp. *michiganensis* during tomato infection. Phytopathology **100:**252-261.
5. **Davis, M. J., and A. K. Vidaver.** 2001. Coryneform plant pathogens, p. 218-235. *In* N. W. Schaad, J. B. Jones, and W. Chun (ed.), Plant Pathogenic Bacteria, Third ed. APS Press, St. Paul, MN.
6. **De Boer, S. H., and R. J. Copeman.** 1980. Bacterial ring rot testing with the indirect fluorescent antibody staining procedure. American Journal of Potato Research **57:**457-465.
7. **De Boer, S. H., and M. McCann.** 1990. Detection of *Corynebacterium sepedonicum* in potato cultivars with different propensities to express ring rot symptoms. American Potato Journal **67:**685-695.
8. **De Boer, S. H., A. Wieczorek, and A. Kummer.** 1988. An ELISA test for bacterial ring rot of potato with a new monoclonal antibody. Plant Disease **72:**874-878.
9. **Dow, J. M., L. Crossman, K. Findlay, Y. Q. He, J. X. Feng, and J. L. Tang.** 2003. Biofilm dispersal in *Xanthomonas campestris* is controlled by cell-cell signaling and is required for full virulence to plants. Proceedings of the National Academy of Sciences of the United States of America **100:**10995-11000.
10. **Dreier, J., D. Meletzus, and R. Eichenlaub.** 1997. Characterization of the plasmid encoded virulence region *pat*-1 of phytopathogenic *Clavibacter michiganensis* subsp. *michiganensis*. Molecular Plant-Microbe Interactions **10:**195-206.
11. **Eichenlaub, R., and K. H. Gartemann.** 2011. The *Clavibacter michiganensis* subspecies: molecular investigation of Gram-positive bacterial plant pathogens. Annual Review of Phytopathology, Vol 49 **49:**445-464.
12. **Eichenlaub, R., K. H. Gartemann, B. Abt, T. Bekel, A. Burger, J. Engemann, M. Flugel, L. Gaigalat, A. Goesmann, I. Grafen, J. Kalinowski, O. Kaup, O. Kirchner, L. Krause, B. Linke, A. McHardy, F. Meyer, S. Pohle, C. Ruckert, S. Schneiker, E. M. Zellermann, A. Puhler, O. Kaiser, and D. Bartels.** 2008. The genome sequence of the tomato-pathogenic actinomycete *Clavibacter*

*michiganensis* subsp *michiganensis* NCPPB382 reveals a large island involved in pathogenicity. Journal of Bacteriology **190:**2138-2149.

13. **Eichenlaub, R., K. H. Gartemann, and A. Burger.** 2006. *Clavibacter michiganensis*, a group of Gram-positive phytopathogenic bacteria, p. 385-421, Plant-Associated Bacteria. Springer, Netherlands.
14. **Gartemann, K.-H., and R. Eichenlaub.** 2001. Isolation and characterization of IS*1409*, an insertion element of 4-chlorobenzoate-degrading *Arthrobacter* sp. strain TM1, and development of a system for transposon mutagenesis. Journal of Bacteriology **183:**3729-3736.
15. **Gudmestad, N. C.** 1987. Recommendations of the national task force for the eradication of bacterial ring rot. American Potato Journal **64:**695-697.
16. **Gudmestad, N. C., and G. A. Secor.** 1984. Bacterial ring rot- the changing scene. Valley Potato Grower **49:**18-21.
17. **Harrison, J. J., R. J. Turner, L. L. R. Marques, and H. Ceri.** 2005. Biofilms. American Scientist **93:**508-515.
18. **Hogenhout, S. A., and R. Loria.** 2008. Virulence mechanisms of Gram-positive plant pathogenic bacteria. Current Opinion in Plant Biology **11:**449-456.
19. **Hogenhout, S. A., R. A. L. Van der Hoorn, R. Terauchi, and S. Kamoun.** 2009. Emerging concepts in effector biology of plant-associated organisms. Molecular Plant-Microbe Interactions **22:**115-122.
20. **Jahr, H., J. Dreier, D. Meletzus, R. Bahro, and R. Eichenlaub.** 2000. The endo-B-1, 4-glucanase *CelA* of *Clavibacter michiganensis* subsp. *michiganensis* is a pathogenicity determinant required for induction of bacterial wilt of tomato. Molecular Plant-Microbe Interactions **13:**703-714.
21. **Jones, J. D. G., and J. L. Dangl.** 2006. The plant immune system. Nature **444:**323-329.
22. **Kang, Y. W., H. L. Liu, S. Genin, M. A. Schell, and T. P. Denny.** 2002. *Ralstonia solanacearum* requires type 4 pili to adhere to multiple surfaces and for natural transformation and virulence. Molecular Microbiology **46:**427-437.
23. **Kirchner, O., K. H. Gartemann, E. M. Zellermann, R. Eichenlaub, and A. Burger.** 2001. A highly efficient transposon mutagenesis system for the tomato pathogen *Clavibacter michiganensis* subsp. *michiganensis*. Molecular Plant-Microbe Interactions **14:**1312-8.
24. **Laine, M. J., H. Nakhei, J. Dreier, K. Lehtila, D. Meletzus, R. Eichenlaub, and M. C. Metzler.** 1996. Stable transformation of the Gram-positive phytopathogenic bacterium *Clavibacter michiganensis* subsp. *sepedonicus* with several cloning vectors. Applied and Environmental Microbiology **62:**1500-1506.
25. **Manzer, F. E., and C. J. Kurowski.** 1992. Bacterial ring rot disease development in resistant and susceptible cultivars. American Potato Journal **69:**363-370.
26. **Marques, L. L. R., H. Ceri, G. P. Manfio, D. M. Reid, and M. E. Olson.** 2002. Characterization of biofilm formation by *Xylella fastidiosa in vitro*. Plant Disease **86:**633-638.
27. **Marques, L. L. R., S. H. De Boer, H. Ceri, and M. E. Olson.** 2003. Evaluation of biofilms formed by *Clavibacter michiganesis* subsp. *sepedonicus*. Phytopathology **93:**S57.

28. **Mills, D., B. W. Russell, and J. W. Hanus.** 1997. Specific detection of *Clavibacter michiganensis* subsp. *sepedonicus* by amplification of three unique DNA sequences isolated by subtraction hybridization. Phytopathology **87:**853-861.
29. **Morris, C. E., and J. M. Monier.** 2003. The ecological significance of biofilm formation by plant-associated bacteria. Annual Review of Phytopathology **41:**429-53.
30. **Nissinen, R., S. Kassuwi, R. Peltola, and M. C. Metzler.** 2001. *In planta* - complementation of *Clavibacter michiganensis* subsp. *sepedonicus* strains deficient in cellulase production or HR induction restores virulence. European Journal of Plant Pathology **107:**175-182.
31. **Nissinen, R., Y. Xia, L. Mattinen, C. A. Ishimaru, D. Knudson, S. E. Brown, M. Metzler, and M. Pirhonen.** 2009. The putative secreted serine protease Chp-7 is required for full virulence and induction of a nonhost hypersensitive response by *Clavibacter michiganensis* subsp. *sepedonicus*. Molecular Plant-Microbe Interactions **22:**809-819.
32. **Parsek, M. R., and P. K. Singh.** 2003. Bacterial biofilms: an emerging link to disease pathogenesis. Annual Review of Microbiology **57:**677-701.
33. **Ramey, B. E., M. Koutsoudis, S. B. von Bodman, and C. Fuqua.** 2004. Biofilm formation in plant-microbe associations. Current Opinion in Microbiology **7:**602-609.
34. **Stackebrandt, E., E. Brambilla, and K. Richert.** 2007. Gene sequence phylogenies of the family *Mircobacteriaceae*. Current Microbiology **55:**42-46.
35. **Stackebrandt, E., and P. Schumann.** 2006. Introduction to the taxonomy of Actinobacteria, p. 297-321, The Prokaryotes. Springer, New York, NY.
36. **Stahl, E. A., and J. G. Bishop.** 2000. Plant-pathogen arms races at the molecular level. Current Opinion in Plant Biology **3:**299-304.
37. **Stevenson, W. R., R. Loria, G. D. Franc, and D. P. Weingartner (ed.).** 2001. Compendium of potato diseases, Second ed. APS Press, St. Paul, MN.
38. **Stork, I., K.-H. Gartemann, A. Burger, and R. Eichenlaub.** 2008. A family of serine proteases of *Clavibacter michiganensis* subsp. *michiganensis*: *chpC* plays a role in colonization of the host plant tomato. Molecular Plant Pathology **9:**599-608.
39. **Sutherland, I. W.** 2001. Biofilm exopolysaccharides: a strong and sticky framework. Microbiology **147:**3-9.
40. **von Bodman, S. B., W. D. Bauer, and D. L. Coplin.** 2003. Quorum sensing in plant-pathogenic bacteria. Annual Review of Phytopathology **41:**455-482.
41. **Woese, C. R.** 1987. Bacterial evolution. Microbiological Reviews **51:**221-271.

# Chapter 2

# Targeted mutagenesis of the serine protease, *php3*, reveals a minor role in virulence of *Clavibacter michiganensis* subsp. *sepedonicus*

## Introduction

Bacterial plant pathogens utilize a variety of strategies to induce disease. One of the best understood example of such a strategy is the essential role of the Type III secretion system (TTSS) and its associated effectors employed during interactions of most gram-negative bacterial pathogens and their hosts (1). In contrast, gram-positive bacterial plant pathogens lack the TTSS cellular machinery and thus have evolved alternative and diverse mechanisms to induce disease. Utilization of phytotoxins and manipulation of plant hormones are strategies that are known among gram-positive plant pathogenic genera *Streptomyces* and *Rhodococcus*, respectively (10).

*Clavibacter michiganensis* subsp. *sepedonicus* (*Cms*) is a gram-positive plant pathogen that causes bacterial ring rot of potato (*Solanum tuberosum*)(21). Recent discoveries in regards to pathogenesis of *C. michiganensis* are beginning to shed light on disease mechanisms of this species. Two distinct pathogenicity determinants have been identified in the closely related pathogen of tomato, *Clavibacter michiganensis* subsp. *michiganensis* (*Cmm*). *celA*, a cellulase gene, and pathogenicity-1 (*pat-1*), a putative serine protease gene, are encoded on plasmids pCM1 and pCM2, respectively, and are known to be important in virulence of *Cmm* (6, 12). A homologue of *celA* is present on the plasmid pCS1 of *Cms* and also is associated with virulence of *Cms* (14, 17). The chromosomal homologue of *pat-1*, *chp7* (CMS2989), of *Cms* most closely resembles *pat-1* of *Cmm* and recently was found to be necessary in HR elicitation in tobacco and virulence of *Cms* in eggplant and potato (18). Multiple chromosomal and plasmid-encoded homologues of *pat-1* (*chp* and *php* genes, respectively) are present in both *Cmm*

and *Cms* (2, 4). Of the 11 *pat-1* homologues that exist in the genome of *Cms*, only the function of *chp7* has been evaluated. Evidence from the functional characterization of Chp7 suggests that this protein may act as an effector. Yet, how this effector-like serine protease interacts within the host and the relative importance of other Chp and Php proteins is not understood.

The full genome sequence of the type strain of *Cms* (ATCC33113) has recently been completed (2). The 3.35 Mbps genome consists of a single circular chromosome (3,258,645 bp), a circular plasmid pCS1 (50,350 bp) and a linear plasmid pCSL1 (94,751 bp). The G+C content of the genome is high, and 88.4% of the genome is predicted coding sequence with a total of 3242 coding sequences (CDSs) present in the genome (3058 CDSs on the chromosome, 67 on pCS1 and 117 on pCSL1). Of the predicted CDSs, 110 CDSs were found to be pseudogenes (106 on the chromosome, 3 on pCS1 and 1 on pCSL1). A number of psuedogenes (110) and of IS elements (106) are present in the *Cms* genome, whereas these IS elements are rare in the genome of *Cmm* (8). Based on whole genome comparisons between *Cms* and *Cmm*, the expansion of IS elements and the increased presence of pseudogenes in association with loss of function for genes involved in nutrient utilization, regulation, transport and pathogenesis-related functions is evidence for niche adaptation of *Cms*.

The development of genetic resources and techniques for genetic manipulation of *Cms* are needed to exploit the genomic sequence and to facilitate a more comprehensive understanding of the role of *pat-1* homologues during molecular plant-microbe interactions of *C. michiganensis*. Critical breakthroughs in technologies are now available for *Cmm*, including efficient transformation protocols and a targeted gene

replacement system. Various strains of *Cms* have also been demonstrated to be amenable to transformation using methods developed in *Cmm* (14). Based on these findings and the fact that all technologies adapted from those developed for *Cmm* have been successfully applied in *Cms*, the development of a gene replacement system for *Cms* based on methods developed for *Cmm* would seem a viable strategy.

Further functional characterization of *chp* and *php* genes in *Cms* will build on the current understanding of the importance of this gene family in pathogenicity of *C. michiganensis* and could provide new focus to future studies. Priorities for functional characterization of *chp* and *php* genes could be facilitated by first identifying which of these are conserved across *Cms*. Here, a polymerase chain reaction (PCR)-based survey of *Cms* strains was conducted to examine the distribution of *chp* and *php* genes within the subspecies.

To support functional characterization, a targeted mutagenesis system for *Cms* was developed using *chp7* as a target for proof of concept. The targeted mutagenesis strategy was then used to generate a knockout mutant of *php3* for functional analysis. The *php3* gene was chosen for functional characterization because it is the closest homologue to *chpC* of *Cmm*, which has been shown to play a role in host colonization (22). Given the relatedness of these genes, it is possible that they could have similar functions in regards to colonization. Additionally, *php3* is encoded on a linear plasmid (pCSL1), which is common in *Cms*, but for which the importance to the lifestyle of *Cms* remains unknown.

## Materials and Methods

### *Bacterial strains and growth conditions*

Bacterial strains and plasmids used in this study are listed in Table 2.1. All bacteria were stored in nutrient broth/glycerol stocks at -80 C. *Clavibacter michiganensis* strains were grown on solid yeast glucose medium (YGM) for approximately seven days at room temperature (22-24 C)(5). Growth media were supplemented with chloramphenicol (5 μg/ml) or kanamycin (25 μg/ml) as needed for selection of transformants. *Escherichia coli* JM109 (Promega, Madison, WI) was grown on Luria-Bertani (LB) medium at 37 C for 18-22 hours. Growth media were supplemented with ampicillin (100 μg/ml), X-gal (80 μg/ml), isopropyl-β-D-thiogalactoside (IPTG, 0.5M), chloramphenicol (25 μg/ml), or kanamycin (50 μg/ml) as needed for selection of transformants. *Xanthomonas translucens* was grown on Wilbrink's agar (20) for approximately three days at 28-30 C.

### *Genomic DNA isolation and PCR amplification*

Genomic DNA (gDNA) was isolated according to Wilson (1997) with the following modifications (24). For *Cms*, gDNA was isolated from cells grown on YGM as a lawn for approximately three days at room temperature. Cells were harvested and suspended in one milliliter of Tris EDTA (TE) to which lysozyme (40 μg/ml) was added, and the suspension was incubated at 37 C for 20 min prior to the addition of 10% SDS

and proteinase K. Concentrations of gDNA were estimated by gel electrophoresis with ethidium bromide staining.

PCR experiments were done using a Gene Amp ® PCR System 2700 (Applied Biosystems, Life Technologies Corp., Carlsbad, CA) with the following parameters: an intial hold at 94 C for 10 minutes followed by 35 cycles of 94 C for 30 seconds, 58 C for 30 seconds, and 72 for one minute, then a final hold at 72 C for seven minutes. PCRs were run in a final reaction volume of 50 µl containing 0.5-1 ng gDNA, 10X PCR buffer (Applied Biosystems), dNTP mixture (10 mM each, Promega), 10% of 1:1 DMSO:1M betaine, 25 pmoles of each primer (Table 2.2), and 1.25 units of Amplitaq (Applied Biosystems). PCR primers were designed from the ATCC33113 genome sequence using the online software Primer3 (19). Primers were synthesized by Integrated DNA Technologies (IDT, Coralville, IA).

*Mutagenesis and complementation*

An antibiotic resistance cassette for use in targeted mutagenesis was constructed by excising a 2 kb *BamH*I/*Sph*I fragment containing the chloramphenicol resistance gene, *cmx*, from the plasmid pKGT452Cβ (9). The fragment was subsequently cloned into pGEM-3Z (Promega) to form pRLS3ZX1 (Figure 2.4A). The cloned antibiotic resistance cassette was amplified by PCR using a high-fidelity DNA polymerase, *Pfx50* (Invitrogen, Life Technologies Corp., Carlsbad, CA). The resulting blunt-ended 2 kb amplicon, which was gel purified using the QIAquick Gel Extraction Kit (Qiagen, Valencia, CA) according to manufacturer's protocol, served as the antibiotic resistance cassette for mutagenesis strategies.

A construct for targeted mutagenesis of *chp7* was developed via amplification by PCR using cloning primer pairs Pat1CmsF (5'-CGTATCCGATGAGCTGTCCTG-3') and Pat1CmsR (5'-AAATATTTCACACCATCCGCTGAG-3') (18) . The full-length *chp7* amplicon was cloned into pGEM-T Easy (Promega) resulting in pRLSTC7 (Figure 2.4B). The *cmx* antibiotic resistance cassette was inserted at a unique *Sma*I restriction site within *chp7*, resulting in the gene replacement vector, pRLSTC7X2 (Figure 2.4B). For complementation studies, the full-length *chp7* insert was excised from pRLSTC7 using *Eco*RI and cloned into compatible sites within pHN216 (14), replacing the gentamycin resistance gene and resulting in the complementation vector pRLS216C7.

A similar approach was taken for the development of targeted mutagenesis and complementation of *php3*. Here, *php3* was amplified using primers rlsPhp3f (5'-CCGACTGGTCTGGTGGTG-3') and rlsPhp3r (5'-GCATGTGAGCTCTGGACGTA-3') and cloned in pGEM-T Easy to form pRLSTP3A (Figure 2.4C). The antibiotic resistance cassette was inserted into a unique *Bal*I restriction site within *php3* to form pRLSTP3AX5 (Figure 2.4C). For complementation experiments, the full-length *php3* gene insert was excised from pRLSTP3A using *Hind*III/*Eco*RI and then cloned into pHN216 (14) resulting in pRLS216P3 (Figure 2.4C). In all cases, plasmids were transformed into and maintained in *E. coli* JM109. Plasmid DNA was isolated using the Wizard SV Miniprep Kit (Promega) and plasmids were verified by PCR and sequence analysis. Plasmid DNA for transformation of *Cms* was isolated using Midi Plasmid Kit (Qiagen).

*Transformation of* Clavibacter michiganensis *subsp.* sepedonicus

The strain ATCC33113 (Table 2.1) of *Cms* was used in all targeted mutagenesis experiments. *Cms* ATCC33113 is the type strain of the subspecies *sepedonicus* and it was also the strain used for sequencing the *Cms* genome (2). Preparation of transformation competent *Cms* cells was adapted from that described by Laine *et al*. (14). *Cms* cells were taken from a single colony and spread with a sterile swab on the surface of solid YGM. After 2-3 days of growth at room temperature, cells were harvested and suspended in 150 ml YGM broth to an optical density at 540 nm ($OD_{540}$) of approximately 0.05 and then grown for 22-24 hours ($OD_{540}$ of 0.6-0.9). Unless noted otherwise, all broth cultures were grown at room temperature with orbital shaking at 180 rpm. The liquid culture was then diluted by addition of 120 ml YGM broth and grown another 4-5 hours ($OD_{540}$ of 0.6-0.7). Glycine was added to a final concentration of 1%, and the culture was incubated for an additional 2 hours. Cells were harvested by centrifugation at 4000 rpm for 30 minutes in a 5810 R Centrifuge (Eppendorf, Hauppauge, NY). Cell pellets were washed in sterile 10% glycerol, resuspended in 10% glycerol with lysozyme (40 μg/ml) and incubated at 37 C for 10 minutes. Lysozyme-treated cells were harvest by centrifugation at 4000 rpm for 30 minutes and washed twice in 10% glycerol. The final cell pellet was resuspended in 250 μl 10% glycerol and either used immediately for transformation or stored at -80 C. Competent cells of *Cms* were transformed via electroporation using a MicroPulsar Electroporation Apparatus (BioRad, Hercules, CA). An electroporation mix containing 20 μl competent cells, 20 μl polyethylene glycol (PEG) 8000 (Sigma, St. Louis, MO), and 2 μl plasmid DNA (1 μg total) in TE was added to a 0.1 cm Gene Pulsar cuvette (BioRad) and exposed to two

pulses of 15 kV/cm at a 20 second interval with a resistance of 600 Ω and a capacitance of 10 μFD. Cells were immediately washed from the cuvette with 1 ml of SB medium (per 1 liter: 10 g tryptone, 5 g yeast extract, 4 g NaCl, 83.8 g sorbitol, 2.9 g $CaCl_2$ and 4 g $MgCl_2$) and allowed to recover for 4 hours at room temperature with orbital shaking at 180 rpm. Following recovery, cells were plated on YGM agar supplemented with the appropriate antibiotics for selection and grown for 7-10 days at room temperature.

*Plant disease assays*

Mutants of *Cms* containing alterations in *chp7* or *php3* were assayed for virulence on eggplant and potato. Inoculum for all virulence assays was prepared from a lawn of *Cms* cells grown on solid YGM for 2-3 days. Cells were harvested and suspended in 0.02 M potassium phosphate buffer (PPB) to an $OD_{540}$ of 0.1 (corresponding to approximately $1x10^8$ CFU/ml). For eggplant assays, seeds of *Solanum melongena* ('Black Beauty') were sown in germination mix. After germination, seedlings were transplanted to 4-inch pots and grown to the second leaf stage. To inoculate plants, the first true leaf was removed with a sterile scalpel and the petiole stump was split lengthwise. Plants were inoculated by placing 20 μl of a bacterial suspension on the split stump. For virulence assays in potato, six-week-old *in vitro* potato plantlets (*S. tuberosum* cv. Sangre) were removed from tissue culture, a few root tips were removed with sterile scissors and roots were soaked in a bacterial suspension for 10 minutes prior to being transplanted to soil in 6-inch pots. All plants were grown in Sunshine MVP Professional Growing Mix (Sun Gro Horticulture, Bellevue, WA) and maintained under greenhouse conditions (20-23 C with supplemental lighting to a day length of 16 hours) in the Plant Growth Facilities at

the University of Minnesota (St. Paul, MN). Pots were supplemented with Marathon (1% granular, OHP, Mainland, PA) and Osmocote Classic (14-14-14, Scotts, Marysville, OH) at transplanting according to manufacturer's recommendations.

Disease assessments in eggplant consisted of 8 inoculated plants per strain tested under a completely randomized design. Two to three independent assessments were completed for each strain. Inoculated plants were maintained for 21 days post-inoculation (dpi). Disease severity was rated daily from 8 to 21 dpi according to the Horsfall-Barratt scale which ranges from 1 to 12 where 1 is 0% and 12 is 100% disease (11). Disease assessments in potato consisted of 6 plants per strain tested in a completely randomized design and two independent assessments were carried out for each strain examined. Disease severity was rated daily from 35 to 50 dpi according to the Horsfall-Barratt scale. Data were analyzed by ANOVA using R (23) and mean separations were performed using Least Square Difference (LSD) Tests.

Mutants of *Cms* were also assayed for induction of a non-host hypersensitive response (HR) in tobacco, *Nicotiana tabacum* cv. Samsun. Tobacco seeds were sown in germination mix and seedlings were transplanted to 6-inch pots 1-2 weeks after germination. Tobacco plants were grown and maintained as described above in the Plant Growth Facilities at the University of Minnesota (St. Paul, MN). Roughly 3-6 weeks after transplanting, tobacco leaves were infiltrated with a bacterial cell suspension. Inoculum for all HR assays was prepared from a lawn of *Cms* cells grown on solid YGM for 2-3 days. Cells were harvested and suspended in 0.02 M PPB to an $OD_{540}$ of 0.8 (corresponding to approximately $8x10^8$ CFU/ml). Infiltrated leaves were monitored for

the appearance of HR for 72 hours. Each treatment was repeated three times per experiment and three independent experiments were completed.

*Immunofluorescence antibody staining*

Population densities of *Cms* in infected plant tissues were measured using immunofluorescence antibody staining (IFAS). Sample preparation for IFAS was carried out according to the manufacturer's protocol using the Immunofluorescence Assay (Cms IFA) Kit (Agdia, Elkhart, IN). Briefly, 1-2 inches of stem tissue was harvested at the crown from infected plants, and stored at -80 C until processing. Stem sections were macerated in phosphate-buffered 0.8% saline (PBS), and bacterial cells were harvested by centrifugation at 13,000 rpm for 15 minutes. Bacterial cell pellets were resuspended in PBS buffer, serially diluted, and spotted onto toxoplasmosis slides (Bellco Glass, Inc., Vineland, NJ). Slides were stained according to the manufactorers' protocol and stored at -20 C until viewed. Cells were viewed using an Eclipse E600 microscope equiped with a super high pressure mercury lamp attachment (Nikon, Tokyo, Japan) and filters set for fluorescein epi-fluorescence. Images were captured with an attached DMX1200F digital camera (Nikon) and ACT 1 imaging software (Nikon). Four tissue samples were processed for each treatment within an experiment and this was done for all experiments conducted. For each sample, 10 viewing frames were imaged and counted to obtain an estimate of the number of cells in that sample according to the following formula: IFAS units/g = $948.7x \bullet df \bullet g^{-1}$, where x = the average cell count per view, df = the dilution factor (i.e. a $10^{-2}$ dilution has a df = 1000), and g = the tissue sample weight (g). IFAS data were log transformed and analyzed by ANOVA using R (23).

## Results

### *Survey of* chp *and* php *genes in* Clavibacter michiganensis *subsp.* sepedonicus

The presence or absence of *chp* and *php* genes in a collection of *C. michiganensis* strains was assessed by PCR amplification. Eleven strains of *Cms* and one representative strain from each of the other four subspecies were examined (Table 2.1). PCR primers specific for each of the 11 *chp* and *php* genes in ATCC33113 were designed (Table 2.2) and used to amplify targets from gDNA templates of the above strain collection. In all cases, *chp* and *php* genes were amplified only with gDNA from *Cms* strains while no amplification was observed with gDNA from any of the other four subspecies (Table 2.3). As expected, the two pCS1 plasmid-encoded homologues, *php1* and *php2*, were not detected in strains BC-P45 and P45, which are known to lack the pCS1 plasmid (16). Notably, *chp7* and *chp8* could not be amplified in CIC243, a non-pathogenic and non-mucoid derivative of Cs3NM, indicating that perhaps a deletion in this region has resulted in a loss of the genes and thus a loss of pathogenicity. Additionally, three *Cms* strains [Cs7, Cs9 and mucoid Cs3NM (CIC242)] appear to lack *chp6*.

### *Targeted mutagenesis of* Clavibacter michiganensis *subsp.* sepedonicus

The feasibility of creating targeted mutations within the genome of *Cms* was tested by generating a knockout mutant of *chp7* via gene replacement. The *chp7* gene was chosen as a target for proof of concept because it is known to affect virulence in eggplant and potato, as well as HR induction in tobacco (18). Strain ATCC33113 was transformed with pRLSTC7X2, which carries *chp7* disrupted by the chloramphenicol

resistance cassette. From one transformation, 48 antibiotic resistant colonies were obtained per microgram DNA. Roughly 10% of these carried the predicted gene disruption within the *chp7* CDS, based on preliminary PCR screening with detection primers Pat1F (5'-CGTGCATCGCTCCCTGTG-3') and Pat1R (5'-TGACGACAGGTCCCCCAG-3') (18). Mutants exhibited colony morphology and growth similar to that of wildtype *Cms* (data not shown). One putative mutant, designated CIC254, was selected for further examination.

Disruption of *chp7* was verified by PCR with three different primer combinations. First, the *chp7* detection primers Pat1F and Pat1R were used to produce products with known size polymorphisms between wildtype (595 bp) and mutant templates (2624 bp) (Figure 2.2A). Additionally, the up- and downstream genomic regions flanking the antibiotic resistance cassette insertion site were amplified using primers CMSchp7+F (5'-GCTTCGTGACCACGAGTGT-3') with ISPcmxR (5'-TTTGACCATGTCCTGCAGTC-3'), and CMSchp7+R (5'-GGGTGATGAGCTACCAGCA-3') with ISPcmxL (5'-GTGAGTTTGGGATGCAGGAT-3'), respectively (Figure 2.2A). Genomic locations of primers CMSchp7+F and CMSchp7+R are up- and downstream, respectively, of the homologous region of pRLSTC7X2. Also, primer ISPcmxR and ISPcmxL are specific to the antibiotic resistance cassette and thus products of 1234 bp (upstream) and 828 bp (downstream) should only be observed with mutated DNA templates. PCR amplicons of the appropriate size were obtained with all templates, verifying that *chp7* was successfully mutated (Figure 2.2B). Results were further confirmed by sequence analysis (data not shown).

A complemented mutant of *chp7* was obtained by transforming CIC254 with pRLS216C7. Maximum transformation efficiencies for complementation reached approximately $2x10^6$ transformants/μg DNA. One putative complemented mutant, designated CIC255, was selected for further examination. Complementation of CIC254 was verified by PCR using the same three primer pairs as described for verifying mutation within *chp7*. PCR amplicons of the predicted sizes were observed for all templates, verifying that complementation of the *chp7* mutation was successful (Figure 2.2B). The 2624 bp product expected in *chp7* mutant templates when amplified with primers Pat1F and Pat1R was not observed for CIC255. This observation is likely attributed to PCR amplification bias towards the shorter 595 bp product from pRLS216C7 carried by CIC255. The fact that both up- and downstream genomic regions flanking the *cmx* antibiotic resistance cassette insertion site were amplified in CIC255 confirmed that it retained the *chp7* disruption. Results were further confirmed by sequence analysis (data not shown). These results demonstrated that targeted mutagenesis of *Cms* can be achieved via the gene replacement methodology described.

The targeted mutagenesis methodologies described for *chp7* were extended to the generation of a knockout mutant of *php3*. *Cms* ATCC33113 was transformed with pRLSTP3AX5. Transformants were selected on chloramphenicol and 39 resistant colonies per microgram DNA were obtained. Roughly 14% of these carried the predicted gene disruption within the *php3* CDS based on preliminary PCR screening with detection primers CMSphp3f (5'-ATCTCCCGGAAGCAAAAAGT-3') with CMSphp3r (5'-GCCTTCTCGCCGTCTTTACT-3'). Mutants exhibited similar morphology and growth

to that of wildtype *Cms* (data not shown). One putative mutant, designated CIC256, was selected for further examination.

Mutation of *php3* was verified by PCR using the same approach as described for verification of *chp7* mutation. Again, three different primer combinations were used for verification. *Php3* detection primers, CMSphp3f and CMSphp3r, produce amplicons with known size polymorphisms between wildtype (674 bp) and mutant templates (2723 bp) (Figure 2.3A). The up- and downstream genomic regions flanking the insertion site of the antibiotic resistance cassette were amplified using primers CMSphp3+F (TGCTCGTGTTCTGTGTCGAG) and ISPcmxR, yielding a 751 bp product, and CMSphp3+R (GCCGCAACATCCTCAAGA) and ISPcmxL, resulting in a 1000 bp product, respectively (Figure 2.3A). For all templates tested, PCR amplicons of the correct sizes were observed, indicating that successful mutation of *php3* had been accomplished through gene replacement (Figure 2.3B). Confirmation of these results was supported by sequence analysis (data not shown).

A complemented mutant of *php3* was obtained by transforming CIC256 with pRLS216P3. Transformation efficiencies for complementation were as high as $1.5x10^5$ transformants/μg DNA. One putative complemented mutant, designated CIC257, was selected for further examination. Complementation of CIC256 was verified by PCR using the same three primer pairs described above to verify mutation of *php3*. PCR amplicons of the appropriate sizes were observed for all templates, verifying that complementation of the *php3* mutation was successful (Figure 2.3B). The 2723 bp product expected in *php3* mutant templates amplified with primers CMSphp3f and CMSphp3r was not observed for CIC257. Again, this was likely attributed to PCR

amplification bias. Results were further confirmed by sequence analysis (data not shown).

*Role of* chp7 *and* php3 *in virulence and host colonization*

The virulence of *chp7* and *php3* mutants of *Cms* relative to ATCC33113 was evaluated in eggplant and potato. A representative set of inoculated eggplants is shown in Figures 1.4A and 1.6A. At 21 dpi, a highly significant reduction ($p$-value=$6.1 \times 10^{-9}$) in disease symptoms in eggplant was observed with the *chp7* mutant, CIC254, relative to wildtype *Cms* (Figure 2.4B). In fact, almost no disease symptoms were observed in eggplants inoculated with CIC254, with only 2 of 16 (12.5%) plants exhibiting disease symptoms at 21 dpi. Full virulence was restored by complementation with pRLS216C7 (strain CIC255) (Figure 2.4B). Additionally, a highly significant reduction ($p$-value=$5.8 \times 10^{-6}$) in AUDPC was observed in eggplants inoculated with CIC254, which was also restored through complementation (Figure 2.4C). A less dramatic yet significant reduction ($p$-value=0.03) in disease symptoms was also observed in plants inoculated with the *php3* mutant, CIC256 (Figure 2.6B). Here, 21 of 24 (87.5%) inoculated eggplants showed symptoms. The reduction in disease rating between plants inoculated with CIC256 and wildtype corresponds to an approximate reduction in disease severity of 12.5%. Full virulence of CIC256 was restored by complementation with pRLS216P3 (strain CIC257) (Figure 2.6B). However, statistically significant differences in AUDPC were not observed for plants inoculated with CIC256 or its complement, CIC257 (Figure 2.6C).

Differences observed in virulence between mutants and wildtype *Cms* in eggplant assays were corroborated by potato disease assessments. A representative set of inoculated potatoes is shown in Figures 1.5A and 1.7A. A highly significant reduction ($p$-value=$1.9x10^{-7}$) in disease symptoms was seen at 50 dpi in potatoes inoculated with CIC254. Virulence was rescued by complementation with pRLS216C7 (Figure 2.5B). Here, all plants inoculated with CIC254 showed disease symptoms but to a much lesser extent than those infected by wildtype *Cms* or the complemented strain, CIC255. A highly significant reduction ($p$-value=$3.0x10^{-6}$) in AUDPC was also observed in potatoes inoculated with CIC254, which was restored by complementation (Figure 2.5C). As was observed in eggplant, disruption of *php3* produced a significant reduction ($p$-value=0.04) in disease in potatoes inoculated with CIC256 (Figure 2.7B). An overall reduction in disease severity of 28.9% was observed. Additionally, an increase in disease symptoms was observed with potatoes inoculated with the *php3* complement, CIC257, relative to those inoculated with CIC256, yet this difference could not be separated statistically (Figure 2.7B). As for eggplant, statistically significant differences in AUDPC were not observed in potato (Figure 2.7C).

Mutants carrying disruptions in *chp7* and *php3* were further evaluated for their ability to induce a non-hostHR in tobacco. As predicted, CIC254 failed to induce HR in all tests and the ability to induce HR was restored by complementation. Mutation of *php3* had no affect on HR induction of *Cms* in tobacco (Figure 2.8).

Estimates of population densities of *Cms* were obtained by counting the number of IFAS units present in infected plant tissues. Sample images from the IFAS procedure are shown in Figures 1.9A and 1.10A. For CIC254, a significant reduction ($p$-

value=0.004) in population density was observed relative to wildtype *Cms*. Population densities of the *chp7* mutant, CIC254, were reduced about one log from wildtype levels of $2.7x10^9$ IFAS units/g tissue to $2.3x10^8$ IFAS units/g tissue (Figure 2.9B). Population densities were restored to wildtype levels by complementation ($6.3x10^9$ cells/g tissue). The same trend was found in potato tissues infected with these strains, where the numbers of CIC254 ($1.7x10^7$ cells/g tissue) were reduced relative to that of wildtype *Cms* and the complemented strain ($1.5x10^{10}$ and $1.7x10^9$ cells/g tissue, respectively) (Figure 2.9C). No significant differences in population densities were found in eggplant infected with CIC256 relative to wildtype *Cms* or CIC257 (Figure 2.10B). Yet, a significant reduction (*p*-value=0.03) was observed in potato. The population size of CIC256 in potato was about 10-fold lower than either wildtype *Cms* or CIC257 (Figure 2.10C).

**Discussion**

Overall, *chp* and *php* genes appear to be highly conserved within *Cms*. Based on PCR experiments conducted with *Cms* specific primers, the majority of strains contain the full suite of *pat-1* homologues. Previous reports showed *C. michiganensis* is a highly homogeneous subspecies and thus these results were not unexpected (3, 15). Furthermore, Brown *et al*. (3) observed differences in genetic fingerprints between virulent and avirulent strains of *Cms* and postulated that a genomic deletion in the avirulent strain, CIC243, may have resulted in the loss of virulence in potato and eggplant and an inability to induce non-host HR in tobacco. The inability to amplify *chp7*, a known pathogenicity determinant, as well as *chp8*, which is located in close proximity to

*chp7*, from the avirulent strain CIC243 supports these previous findings. In addition, the apparent loss of *chp6* from three pathogenic *Cms* strains may suggest that *chp6* plays a minor or no role in virulence of *Cms*.

Our results demonstrate for the first time that targeted mutagenesis by gene replacement is possible in *Cms*. A targeted gene knockout mutant of *chp7*, CIC254, was successfully generated using the gene replacement method described in our study. Plant disease assays reported here with CIC254 supported previous findings from studies of a *Cms* transposon mutant of *chp7* that demonstrated that *chp7* is needed for virulence of *Cms* in eggplant and potato as well as HR induction in tobacco (18). Since the complete genome sequence of ATCC33113 is available, targeted mutagenesis will greatly facilitate future functional characterization of genes of interest in this subspecies.

Through functional characterization of *php3*, it appears that this *pat-1* homolog is only of minor significance to virulence of *Cms* (Table 2.4). Additionally, *php3* does not appear to contribute to host colonization whereas, its closely related homologue in *Cmm*, *chpC* was shown to be important in host colonization (22). In *Cmm*, *pat-1* is required for virulence and *chpG* is responsible for induction of non-hostHR, where as in *Cms*, both of the functions are accomplished by *chp7* (6, 18, 22). Given this and the evidence for niche adaptation of *Cms* based on genome comparisons between these subspecies (2), it is likely that *chp* and *php* genes have evolved independent functions within their respective hosts.

When considering plant-microbe interactions, host responses to the presence of microbes can generally by classified into three categories: pathogen-triggered immunity (PTI), effector-triggered immunity (ETI) and effector-triggered susceptibility (ETS) (13).

Briefly, upon infection the host recognizes hallmarks of the pathogen known as pathogen-associated molecular patterns (PAMPs) or microbe-associated molecular patterns (MAMPs) and initiates signal cascades leading to the horizontal resistance seen in PTI. Pathogens can then utilize effectors to interfere with PTI leading to ETS. Should the host have the appropriate resistance proteins for recognition of specific pathogen effectors then ETI is observed. Overall the results obtained here suggest that *chp7* is the major driver of virulence for *Cms* and that the remaining *chp* and *php* genes examined within this gene family likely provide minor contributions to virulence. Furthermore, these results may suggest that Chp and Php proteins function as effectors. Given the reduction in virulence observed for *chp7* and *php3* mutant of *Cms*, it is possible that these effector-like serine proteases are acting to disrupt PTI within the host leading to ETS. Yet, the mechanism by which such disruption occurs requires further examination.

Identifying the role of *chp* and *php* genes in regards to pathogenicity is a necessary step towards understanding pathogenesis. The knowledge that Chp7 and Php3 may have effector-like functions within the host will allow for focused studies to better understand the mode of action of these proteins. Expression and isolation of Chp7 and Php3 followed by analysis of the protein structure could provide insights towards the function of these proteins and may facilitate identification of potential host targets. In addition, comparisons of gene expression profiles of wildtype and *chp* and *php* mutants as well as *Cms* and mock-inoculated host tissues could begin to describe the genes and pathways initiated during pathogenesis.

The targeted mutagenesis strategy described here resulted in specifically marked mutants. Recently, a novel approach towards the generation of specific unmarked

deletion mutants of members of the *Actinobacteria* was reported (7). The strategy uses cytosine deaminase for negative selection and relies on natural resistance to 5-fluorcytosine (5FC) and sensitivity to 5-fluorouracil (5FU). Preliminary assays demonstrate that *Cms* is indeed resistant to 5FC and sensitive to 5FU, indicating that this technique may be applicable to mutagenesis of *Cms*. The ability to generate unmarked deletion mutants of *Cms* could allow for stacking of multiple gene knockouts within a single strain and could enhance future studies of gene expression and functional characterization of putative pathogenicity genes.

**Table 2.1.** Bacterial strains and plasmids used in this study.

| Strain ID | Strain | Description | Source/Reference |
|---|---|---|---|
| ***Clavibacter michiganenesis* subsp. *sepedonicus*** | | | |
| CIC31 | CIC2 rif50r | Spontaneous rifampicin-resistant mutant of CSU #2539-69 | C. Ishimaru (12) |
| CIC194 | BC-P45 | Spontaneous spectinomycin-resistant mutant of P45 | C. Orser (22) |
| CIC209 | P45 | Lacks the native plasmid, pCS1 | A. Oleson (17) |
| CIC238 | Cs7 | | M. Metzler |
| CIC240 | Cs9 | | M. Metzler |
| CIC242 | Cs3NM | Mucoid derivative of Cs3NM, pathogenic | S. H. DeBoer (3) |
| CIC243 | Cs3NM | Non-mucoid derivative of Cs3NM, non-pathogenic | S. H. DeBoer (3) |
| CIC244 | ATCC9850 | Wildtype | ATCC (17) |
| CIC245 | ATCC33111 | Wildtype | ATCC (17) |
| CIC250 | ATCC33113 | Type strain | ATCC (17) |
| CIC253 | R10 | | R. Nissinen (19) |
| CIC254 | CmsC7X20 | ATCC33113 transformed with pRLSTC7X2 | This study |
| CIC255 | CmsC7X20c.1 | CmsC7X20 transformed with pRLS216C7 | This study |
| CIC256 | CmsP3X50 | ATCC33113 transformed with pRLSTP3AX5 | This study |
| CIC257 | CmsP3X50c.1 | CmsP3X50 transformed with pRLS216P3 | This study |
| CIC258 | Cms216A | ATCC33113 transformed with pHN216 | This study |
| ***Clavibacter michiganenesis* subsp. *michiganensis*** | | | |
| CIC14 | 15-20 smr | | A. Vidaver |
| ***Clavibacter michiganenesis* subsp. *nebraskensis*** | | | |
| CIC16 | 313.0 smr | | A. Vidaver |
| ***Clavibacter michiganenesis* subsp. *tessellarius*** | | | |
| CIC21 | 82055.9 | | A. Vidaver |
| ***Clavibacter michiganenesis* subsp. *insidiosis*** | | | |
| CIC261 | R1-1 | Isolated from alfalfa from Minnesota | D. Samac |
| ***Escherichia coli*** | | | |
| JM109 | *E. coli* JM109 | Transformation competent *E. coli* | Promega |
| ***Xanthomonas translucens*** | | | |
| CIX32 | TS4-10A | *X. translucens* isolated from barley in MN | R. Curland |

| Plasmid ID | Resistance[1] | Description | Source |
|---|---|---|---|
| pGEM-T Easy | Amp | *E. coli* cloning vector | Promega |
| pGEM-3Z | Amp | *E. coli* cloning vector | Promega |
| pKGT452Cβ | Amp, Cmx | Tn*1409*Cβ delivery vector | Gartemann and Eichenlaub (9) |
| pHN216 | Neo, Gn | *Clavibacter-E. coli* shuttle vector | Laine (15) |
| pRLS3ZX1 | Cmx | pGEM-3Z carrying *Bam*HI/*Sph*I fragment of pKGT452Cβ | This study |
| pRLSTC7 | Amp | *chp7* cloned in pGEM-T Easy | This study |
| pRLSTC7X2 | Amp, Cmx | pRLSTC7 carrying the antibiotic resistance cassette within *chp7* | This study |
| pRLS216C7 | Neo | *chp7* cloned in pHN216 | This study |
| pRLSTP3A | Amp | *php3* cloned in pGEM-T Easy | This study |
| pRLSTP3AX5 | Amp, Cmx | pRLSTP3A carrying the antibiotic resistance cassette within *php3* | This study |
| pRLS216P3 | Neo | *php3* cloned in pHN216 | This study |

[1] Amp=Ampicilin, Cmx=Chloramphenicol, Neo=Neomycin, Gn=Gentamycin

**Table 2.2.** PCR primers used in this study.

| Primer Name | Target | Usage | Tm | Product Size | Sequence (5'-3') |
|---|---|---|---|---|---|
| CMSchp1f | *chp1* | Detection | 57 | 894 bp | GCTCTCCTTCCCGTCCTC |
| CMSchp1r | *chp1* | Detection | 57 | | GGGGATGTACGCTGTGTAGG |
| CMSchp2f | *chp2* | Detection | 57 | 620 bp | CGGTAGACCATCACTGCACA |
| CMSchp2r | *chp2* | Detection | 56 | | GGAGATGGGGATGTAGGTCA |
| CMSchp3f | *chp3* | Detection | 54 | 848 bp | ATCGTCCGGTAATCGAACAG |
| CMSchp3r | *chp3* | Detection | 57 | | CGGGAGGTACGTCATCTTGT |
| CMSchp4f | *chp4* | Detection | 58 | 607 bp | CTCAAGTACGACCGCTGGAC |
| CMSchp4r | *chp4* | Detection | 56 | | CGTAGTTCGGCTGAAGATGG |
| CMSchp5f | *chp5* | Detection | 54 | 607 bp | TCATGAAGTACTCCGGCATC |
| CMSchp5r | *chp5* | Detection | 55 | | TTGGCGATCGTGATGTAGTG |
| CMSchp6f | *chp6* | Detection | 57 | 723 bp | GTCTCCGCACTCATCCTCTC |
| CMSchp6r | *chp6* | Detection | 55 | | GGAGAAGGGCACGTAAAACA |
| CMSchp8f | *chp8* | Detection | 55 | 636 bp | CGTGAGGCGTACAAGTCAAA |
| CMSchp8r | *chp8* | Detection | 55 | | TACGGTGCTGATGCTTCTTG |
| CMSphp1f | *php1* | Detection | 55 | 790 bp | GTGCATAATTGGGCTGCTCT |
| CMSphp1r | *php1* | Detection | 59 | | ACACTGACCTGCCTGACTCC |
| CMSphp2f | *php2* | Detection | 57 | 606 bp | ACAGGAACTGGCATCCTGTC |
| CMSphp2r | *php2* | Detection | 56 | | ATACGGTTGCTCTCGGAAGA |
| CMSphp3f | *php3* | Detection | 55 | 694 bp | ATCTCCCGGAAGCAAAAAGT |
| CMSphp3r | *php3* | Detection | 57 | | GCCTTCTCGCCGTCTTTACT |
| Pat1F[1] | *chp7* | Detection | 59 | 595 bp | CGTGCATCGCTCCCTGTG |
| Pat1R[1] | *chp7* | Detection | 59 | | TGACGACAGGTCCCCCAG |
| rlsPhp3f | *php3* | Cloning | 58 | 1306 bp | CCGACTGGTCTGGTGGTG |
| rlsPhp3r | *php3* | Cloning | 57 | | GCATGTGAGCTCTGGACGTA |
| Pat1CmsF[1] | *chp7* | Cloning | 57 | 1418 bp | CGTATCCGATGAGCTGTCCTG |
| Pat1CmsR[1] | *chp7* | Cloning | 56 | | AAATATTTCACACCATCCGCTGAG |
| CMSChp7+F | *chp7* upstream | Verification | 57 | 1887 bp | GCTTCGTGACCACGAGTGT |
| CMSChp7+R | *chp7* downstream | Verification | 57 | | GGGTGATGAGCTACCAGCA |
| CMSphp3+F | *php3* upstream | Verification | 57 | 1576 bp | TGCTCGTGTTCTGTGTCGAG |
| CMSphp3+R | *php3* downstream | Verification | 56 | | GCCGCAACATCCTCAAGA |
| ISPcmxL | antibiotic cassette | Sequence | 55 | N/A | GTGAGTTTGGGATGCAGGAT |
| ISPcmxR | antibiotic cassette | Sequence | 55 | N/A | TTTGACCATGTCCTGCAGTC |
| ISPchp7L | *chp7* | Sequence | 55 | N/A | CATCCCCATCGCTGTACTTT |
| ISPchp7R | *chp7* | Sequence | 54 | N/A | AGGAGGGCGAATATGCTTTT |
| ISPphp3L | *php3* | Sequence | 55 | N/A | GAGCCCGAGAGTGATGAAAA |
| ISPphp3R | *php3* | Sequence | 53 | N/A | CGGGATAATGACCGATCAAG |
| T7 | pGEM-vectors | Sequence | 48 | N/A | TAATACGACTCACTATAGGG |
| SP6 | pGEM-vectors | Sequence | 42 | N/A | TATTTAGGTGACACTATAG |

[1]Primers from Nissinen et al. 2009 (18)

**Table 2.3.** Survey of *pat-1* homologues detectable with PCR primers specific for *chp* and *php* sequences in *Clavibacter michiganensis* subsp. *sepedonicus*.[1]

| Strain ID | Species[2] | chp1 | chp2 | chp3 | chp4 | chp5 | chp6 | chp7 | chp8 | php1 | php2 | php3 |
|---|---|---|---|---|---|---|---|---|---|---|---|---|
| CIC31 | *Cms* | + | + | + | + | + | + | + | + | + | + | + |
| CIC194 | *Cms* | + | + | + | + | + | + | + | + | - | - | + |
| CIC209 | *Cms* | + | + | + | + | + | + | + | + | - | - | + |
| CIC238 | *Cms* | + | + | + | + | + | - | + | + | + | + | + |
| CIC240 | *Cms* | + | + | + | + | + | - | + | + | + | + | + |
| CIC242 | *Cms* | + | + | + | + | + | - | + | + | + | + | + |
| CIC243 | *Cms* | + | + | + | + | + | + | - | - | + | + | + |
| CIC244 | *Cms* | + | + | + | + | + | + | + | + | + | + | + |
| CIC245 | *Cms* | + | + | + | + | + | + | + | + | + | + | + |
| CIC250 | *Cms* | + | + | + | + | + | + | + | + | + | + | + |
| Cms R10 | *Cms* | + | + | + | + | + | + | + | + | + | + | + |
| CIC14 | *Cmm* | - | - | - | - | - | - | - | - | - | - | - |
| CIC16 | *Cmn* | - | - | - | - | - | - | - | - | - | - | - |
| CIC21 | *Cmt* | - | - | - | - | - | - | - | - | - | - | - |
| Cmi R1-1 | *Cmi* | - | - | - | - | - | - | - | - | - | - | - |

[1]Primer pairs and predicted product sizes as shown in Table 2.2. (+)=product of the predicted size is present and (-)=product of the predicted size is not present
[2]*Cms=C. michiganensis* subsp. *sepedonicus*, *Cmm=C. michiganensis* subsp. *michiganensis*, *Cmn=C. michiganensis* subsp. *nebraskensis*, *Cmt=C. michiganensis* subsp. *tessellarius*, and *Cmi=C. michiganensis* subsp. *insidiosus*

**Table 2.4.** Summary of known functions associated with *chp* and *php* genes in *Clavibacter michiganensis* subsp. *sepedonicus* ATCC33113 and their closest homologues in *C. michiganensis* subsp. *michiganensis* NCPPB382.

| | | | **Closest *Cmm* Homologue**[a] | | |
|---|---|---|---|---|---|
| **Gene** | **Name** | **Function** | **Gene** | **Name** | **Function** |
| CMS0980 | *chp1* | Unknown | pCM2_0053 | *phpB* | Unknown |
| CMS0981 | *chp2* | Unknown | pCM2_0053 | *phpB* | Unknown |
| CMS1260 | *chp3* | Unknown | CMM_PS_05 | *chpE* | Unknown |
| CMS1262 | *chp4* | Unknown | CMM_PS_05 | *chpE* | Unknown |
| CMS2837 | *chp5* | Unknown | CMM_PS_05 | *chpE* | Unknown |
| CMS2909 | *chp6* | Unknown | CMM_0059 | *chpG* | Required for HR in *Mirabilis jalapa* (22) |
| CMS2989 | *chp7* | Required for full virulence and non-hostHR induction (18)(This study) | pCM2_0054 | *pat-1* | Required for full virulence (6) |
| CMS2991 | *chp8* | Unknown | CMM_PS_04 | *chpD* | Unknown |
| pCS0022 | *php1* | Unknown | CMM_PS_10 | *chpB* | Unknown |
| pCS0037 | *php2* | Unknown | pCM2_0054 | *pat-1* | Required for full virulence (6) |
| PCSL0017 | *php3* | Involved in virulence (This study) | CMM_0053 | *chpC* | Required for host colonization (22) |

[a]Eichenlaub, R. *et al*. 2008. Journal of Bacteriology. 190:2138-2149

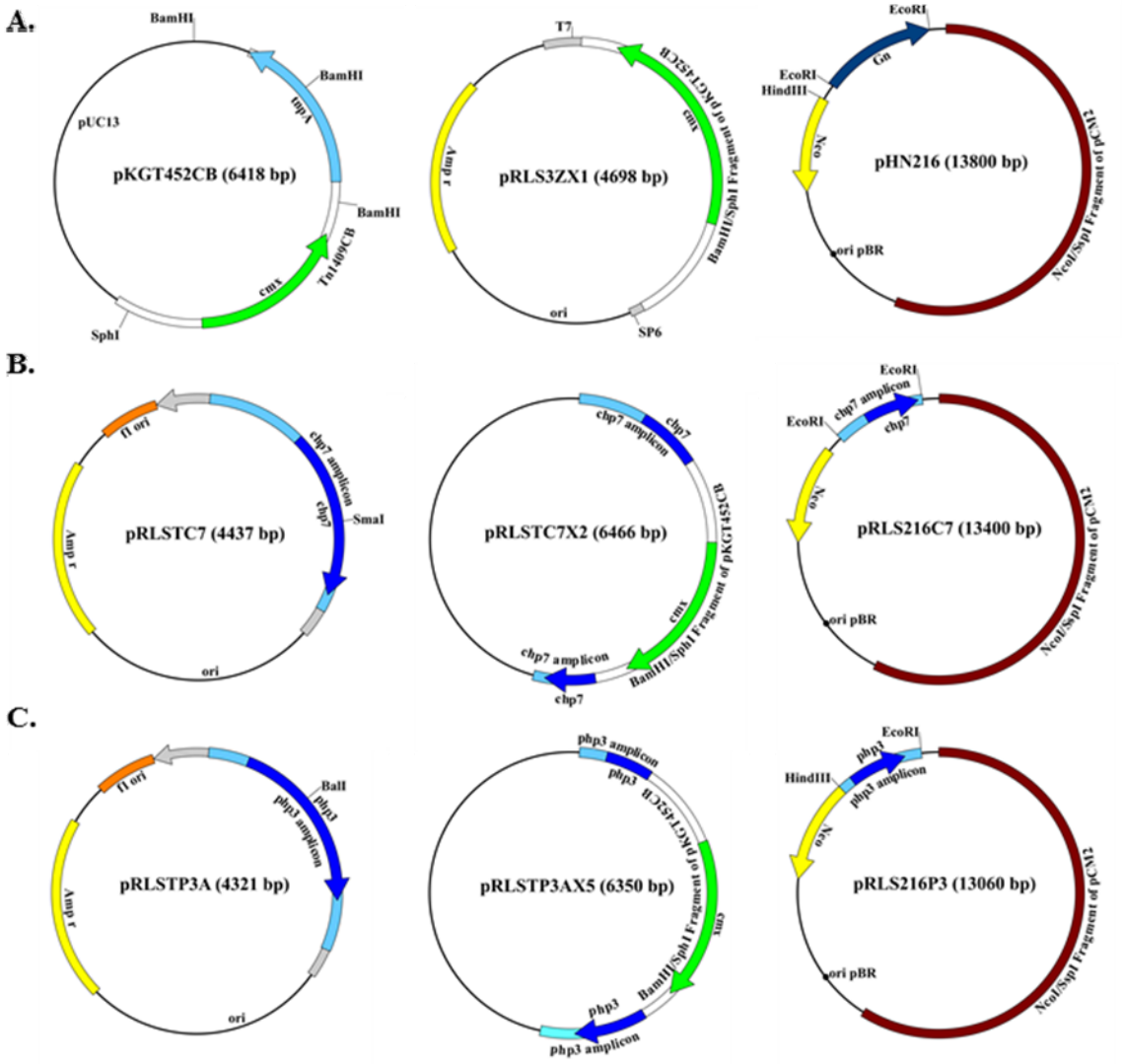


**Figure 2.1. Plasmid maps.** Maps of the plasmids constructed for use in this study are shown. A) Plasmid sources of the antibiotic cassette used for targeted gene disruption: pKGT452Cβ (antibiotic resistance cassette source, *cmx*) (9), pRLS3ZX1 carrying the cloned antibiotic resistance cassette from pKGT452Cβ and *E. coli-Clavibacter* shuttle vector pHN216 (14). B) Plasmids for targeted mutagenesis and complementation of *chp7*: pRLSTC7, full-length *chp7* clone; pRLSTC7X2, *chp7* targeted mutation vector; and pRLS216C7, *chp7* complementation vector. C) Plasmids for targeted mutagenesis and complementation of *php3*: pRLSTP3A, full-length *php3* clone; pRLSTP3AX5, *php3* targeted mutation vector; and pRLS216P3, *php3* complementation vector.

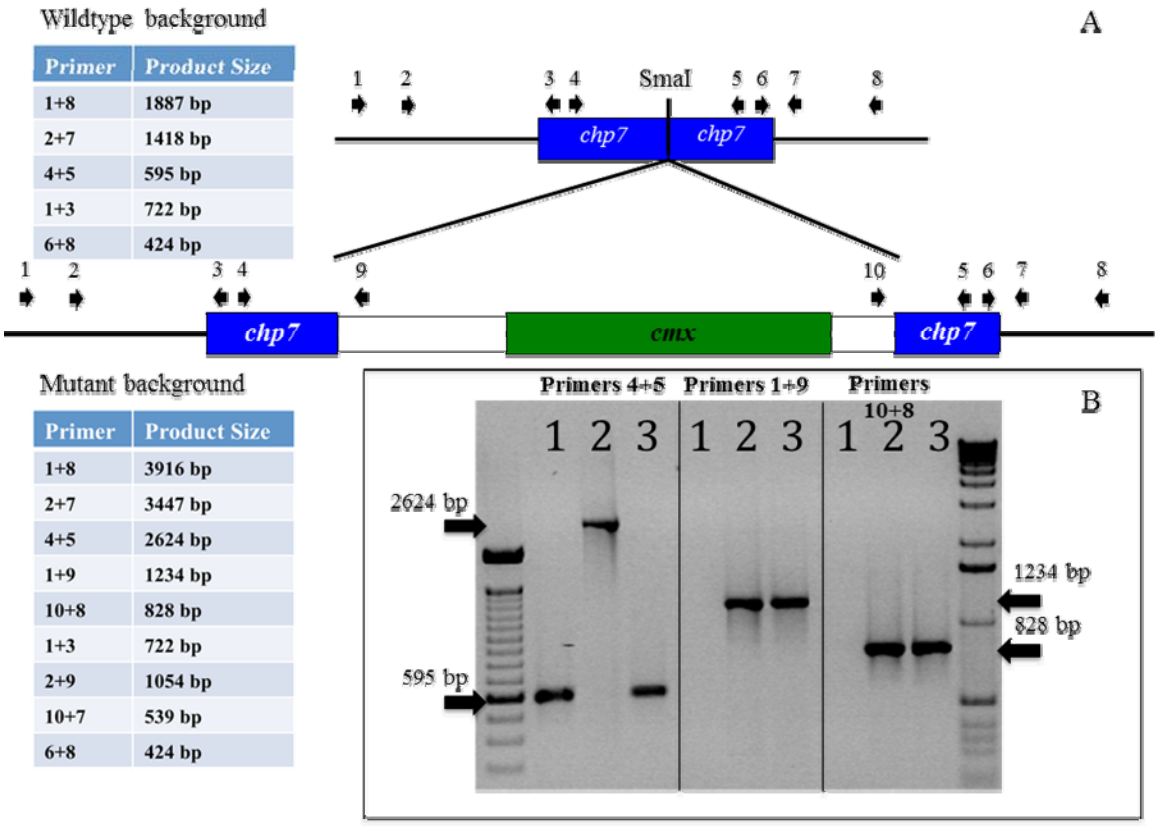


**Figure 2.2: Physical map of *chp7* in ATCC33113 and its derivatives CIC254 and CIC255.** Genome region of *chp7* showing the site of mutation and primer locations as well as the results of PCR verification of mutation and complementation of *chp7* are depicted. A) Primer locations are indicated by numbered arrows, where 1=CMSchp7+F, 2=Pat1CmsF, 3=ISPchp7R , 4=Pat1F , 5=Pat1R , 6=ISPchp7R , 7=Pat1CmsR , 8=CMSchp7+R , 9=ISPcmxR , and 10=ISPcmxL. Predicted PCR product sizes from wildtype templates are shown for various primer pairs in the table in the upper left while the product sizes for pairs from mutated templates are in the table at the lower left. B) Here, an agarose gel image shows the PCR verification of mutation and complementation of *chp7*. Gel lanes are numbered based on template where 1=ATCC33113, 2=CIC254 and 3=CIC255. Numbers at the top of the gel image indicate the three primer sets used. Arrows on the right and left sides of the gel mark product sizes.

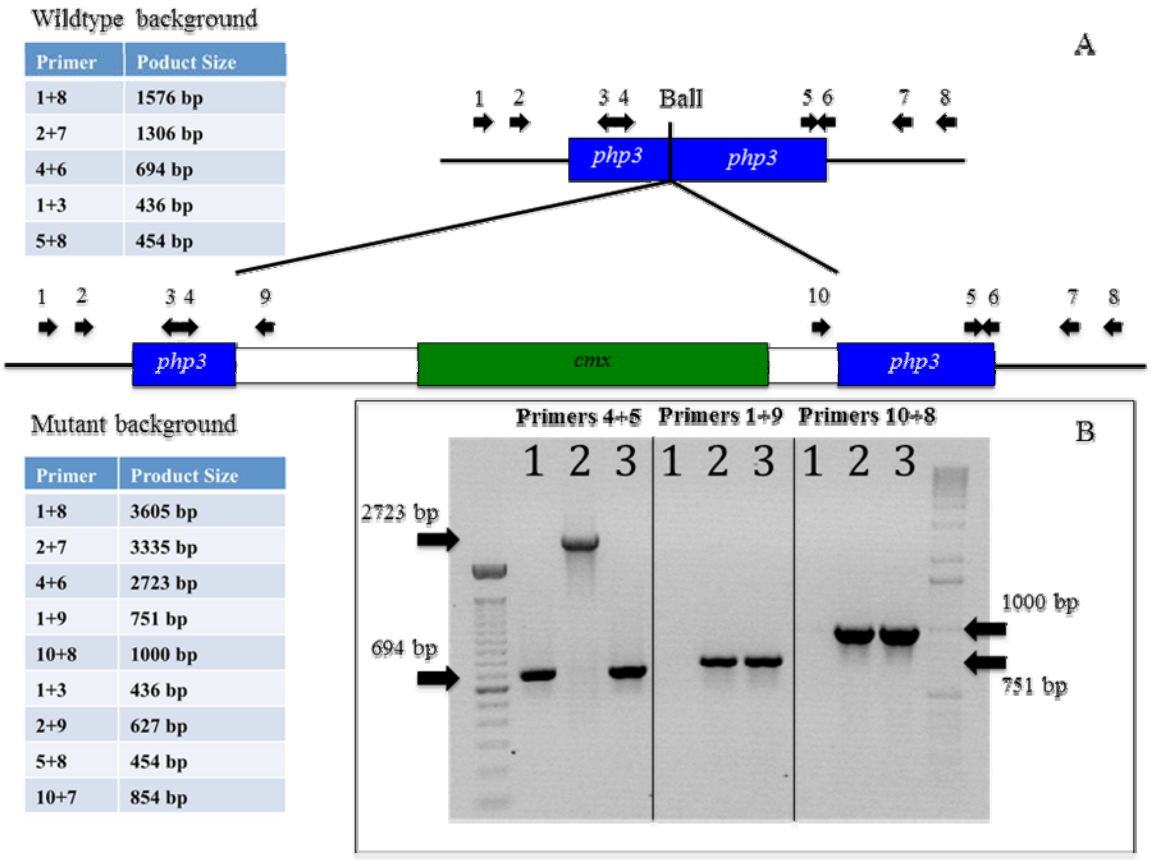


**Figure 2.3: Physical map of *php3* in ATCC33113 and its derivatives CIC256 and CIC257.** Genome region of *php3* showing the site of mutation and primer locations as well as the results of PCR verification of mutation and complementation of *php3* are depicted. A) Primer locations are indicated by numbered arrows, where 1=CMSphp3+F, 2=rlsPhp3F, 3=ISPphp3R , 4=CMSphp3F , 5=ISPphp3R , 6=CMSphp3R , 7=rlsPhp3R , 8=CMSphp3+R , 9=ISPcmxR , and 10=ISPcmxL. Predicted PCR product sizes from wildtype templates are shown for various primer pairs in the table in the upper left while the product sizes for pairs from mutated templates are in the table at the lower left. B) Here, an agarose gel image shows the PCR verification of mutation and complementation of *php3*. Gel lanes are numbered based on template where 1=ATCC33113, 2=CIC256 and 3=CIC257. Numbers at the top of the gel image indicate the three primer sets used. Arrows on the right and left sides of the gel mark product sizes.

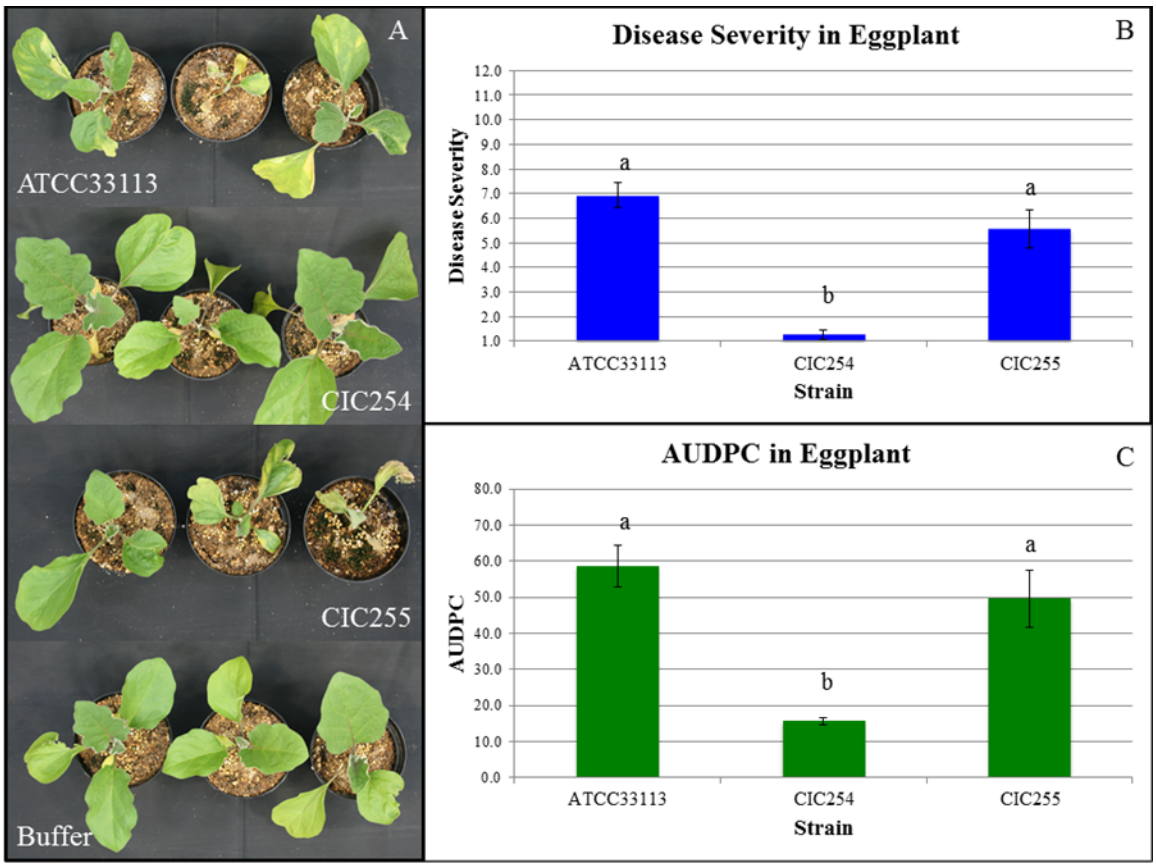


**Figure 2.4. Contribution of *chp7* to virulence of *Cms* in eggplant.** A summary of disease assays of wildtype, *chp7* mutant, and the complemented *chp7* mutant of *Cms* are shown (strains ATCC33113, CIC254 and CIC255, respectively). For graphical summaries, standard errors of the means are represented with error bars and letters above the bars indicate significance classes based on LSD tests. A) Images of a representative subset of eggplants inoculated with ATCC33113, CIC254 and CIC255 and buffer at 21 dpi. B) Graphical representation of mean disease rating at 21 dpi of eggplants infected with ATCC33113, CIC254 and CIC255 for all trials. C) Graphical representation of mean area under disease progress curve (AUDPC) of eggplants infected with ATCC33113, CIC254 and CIC255 for all trials.

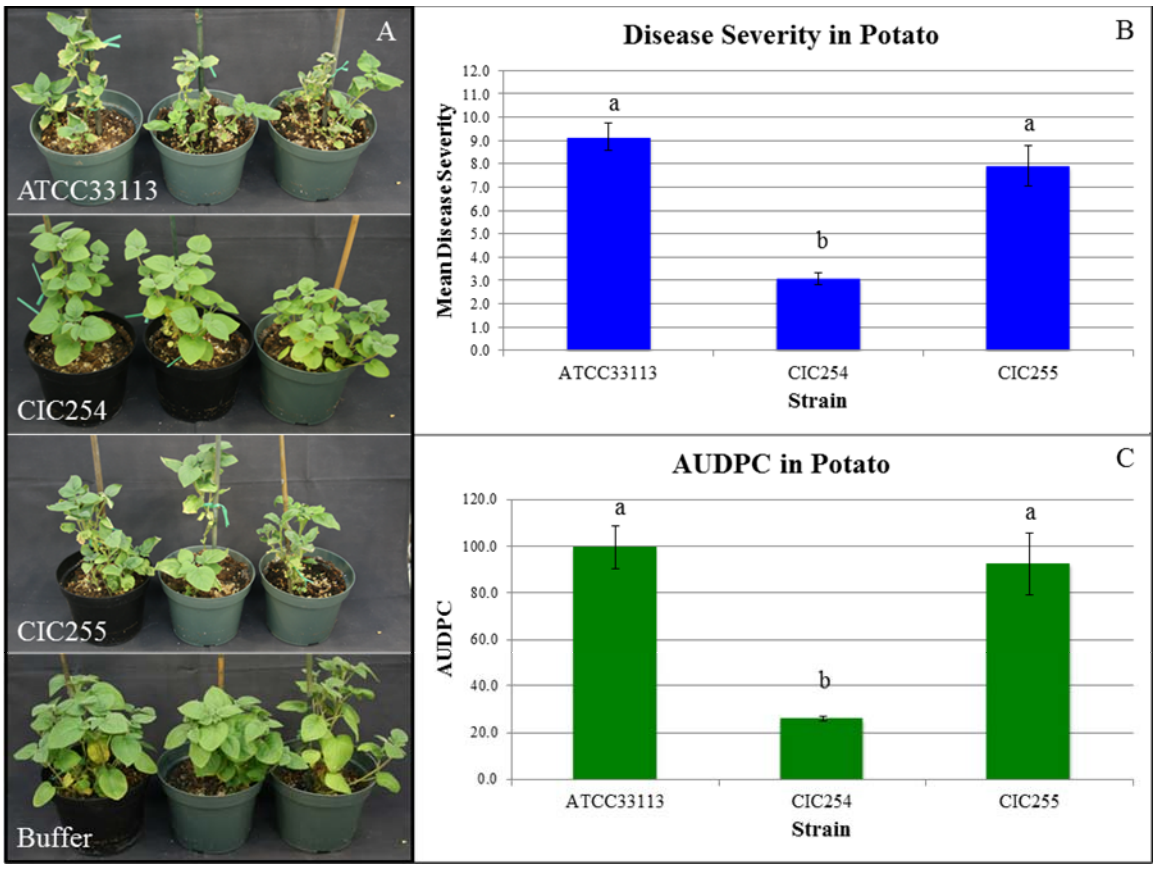


**Figure 2.5. Contribution of *chp7* to virulence of *Cms* in potato.** A summary of disease assays of wildtype, *chp7* mutant, and the complemented *chp7* mutant of *Cms* are shown (strains ATCC33113, CIC254 and CIC255, respectively). For graphical summaries, standard errors of the means are represented with error bars and letters above the bars indicate significance classes based on LSD tests. A) Images of a representative subset of potatoes inoculated with ATCC33113, CIC254 and CIC255 and buffer at 50 dpi. B) Graphical representation of mean disease rating at 50 dpi of potatoes infected with ATCC33113, CIC254 and CIC255 for all trials. C) Graphical representation of mean AUDPC of potatoes infected with ATCC33113, CIC254 and CIC255 for all trials.

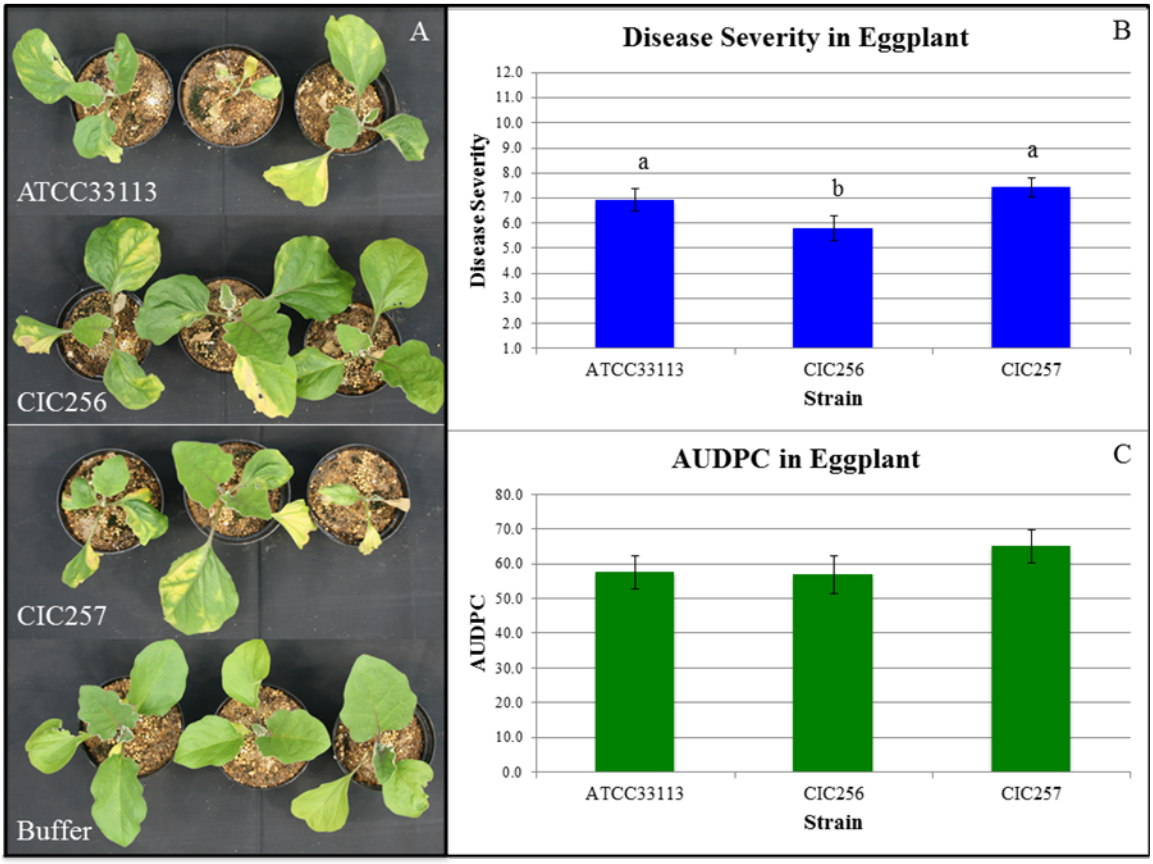


**Figure 2.6. Contribution of *php3* to virulence of *Cms* in eggplant.** A summary of disease assays of wildtype, *php3* mutant, and the complemented *php3* mutant of *Cms* are shown (strains ATCC33113, CIC256 and CIC257, respectively). For graphical summaries, standard errors of the means are represented with error bars and letters above the bars indicate significance classes based on LSD tests and the lack of letter indicates no significant differences observed. A) Images of a representative subset of eggplants inoculated with ATCC33113, CIC256 and CIC257 and buffer at 21 dpi. B) Graphical representation of mean disease rating at 21 dpi of eggplants infected with ATCC33113, CIC256 and CIC257 for all trials. C) Graphical representation of mean AUDPC of eggplants infected with ATCC33113, CIC256 and CIC257 for all trials.

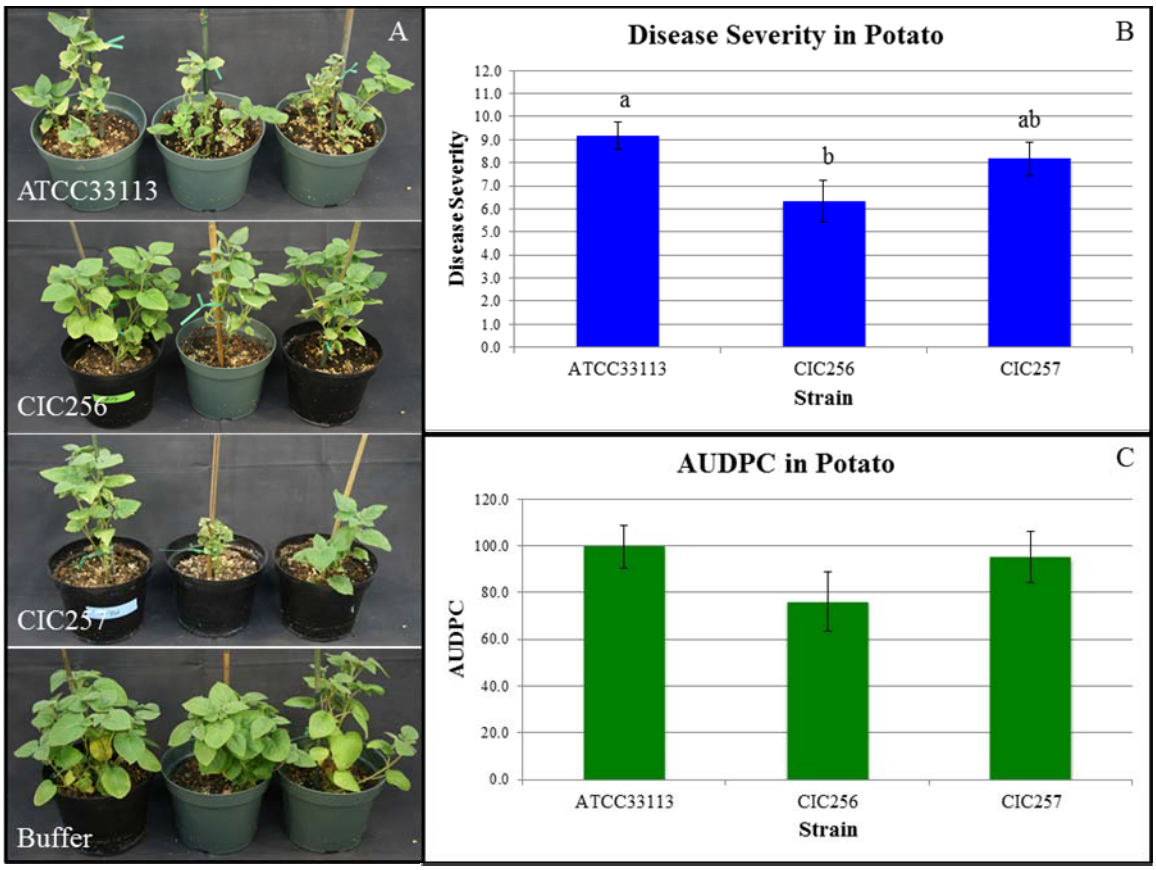


**Figure 2.7. Contribution of *php3* to virulence of *Cms* in potato.** A summary of disease assays of wildtype, *php3* mutant, and the complemented *php3* mutant of *Cms* are shown (strains ATCC33113, CIC256 and CIC257, respectively). For graphical summaries, standard errors of the means are represented with error bars and letters above the bars indicate significance classes based on LSD tests and the lack of letter indicates no significant differences observed. A) Images of a representative subset of potatoes inoculated with *Cms* ATCC33113, CIC256 and CIC257 strains and buffer at 50 dpi. B) Graphical representation of mean disease rating at 50 dpi of potatoes infected with ATCC33113, CIC256 and CIC257 for all trials. C) Graphical representation of mean AUDPC of potatoes infected with ATCC33113, CIC256 and CIC257 for all trials.

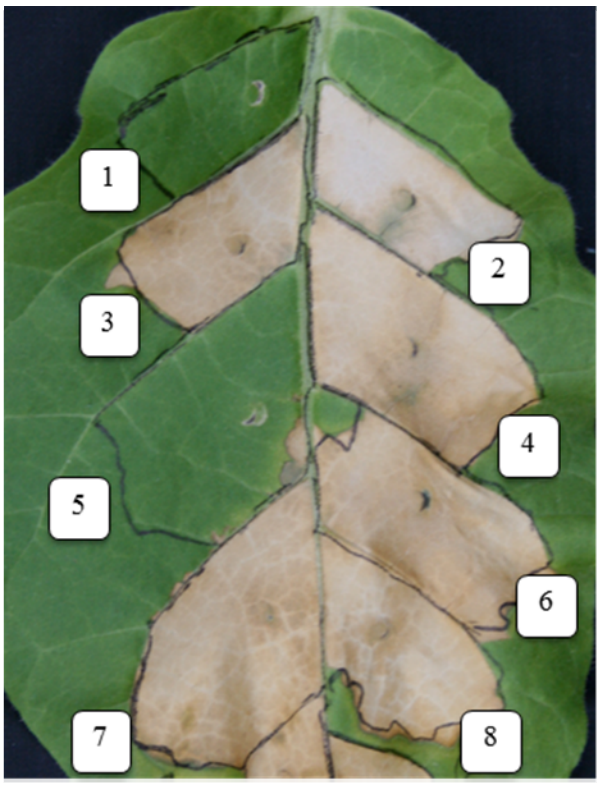


| Strain | HR |
|---|---|
| 1. Mock | - |
| 2. CIX32 | + |
| 3. ATCC33113 | + |
| 4. CIC260 | + |
| 5. CIC254 | - |
| 6. CIC255 | + |
| 7. CIC256 | + |
| 8. CIC257 | + |

**Figure 2.8. HR induction by *Clavibacter michiganensis* subsp. *sepedonicus* ATCC33113 and its *chp7* and *php3* mutants.** A representative image of an HR assay in tobacco can be seen on the left. A legend showing the particular strain infiltrated at each leaf spot and its corresponding HR reaction is at the right. CIX32=*Xanthomonas translucens* (positive control), ATCC33113=*Cms* wildtype, CIC260=ATCC33113 carrying the empty shuttle vector pHN216, CIC254=*Cms chp7* mutant, CIC255=*Cms* complemented *chp7* mutant, CIC256=*Cms php3* mutant, and CIC257=*Cms* complemented *php3* mutant. A positive HR response is indicated by '+' and a negative HR by '-'.

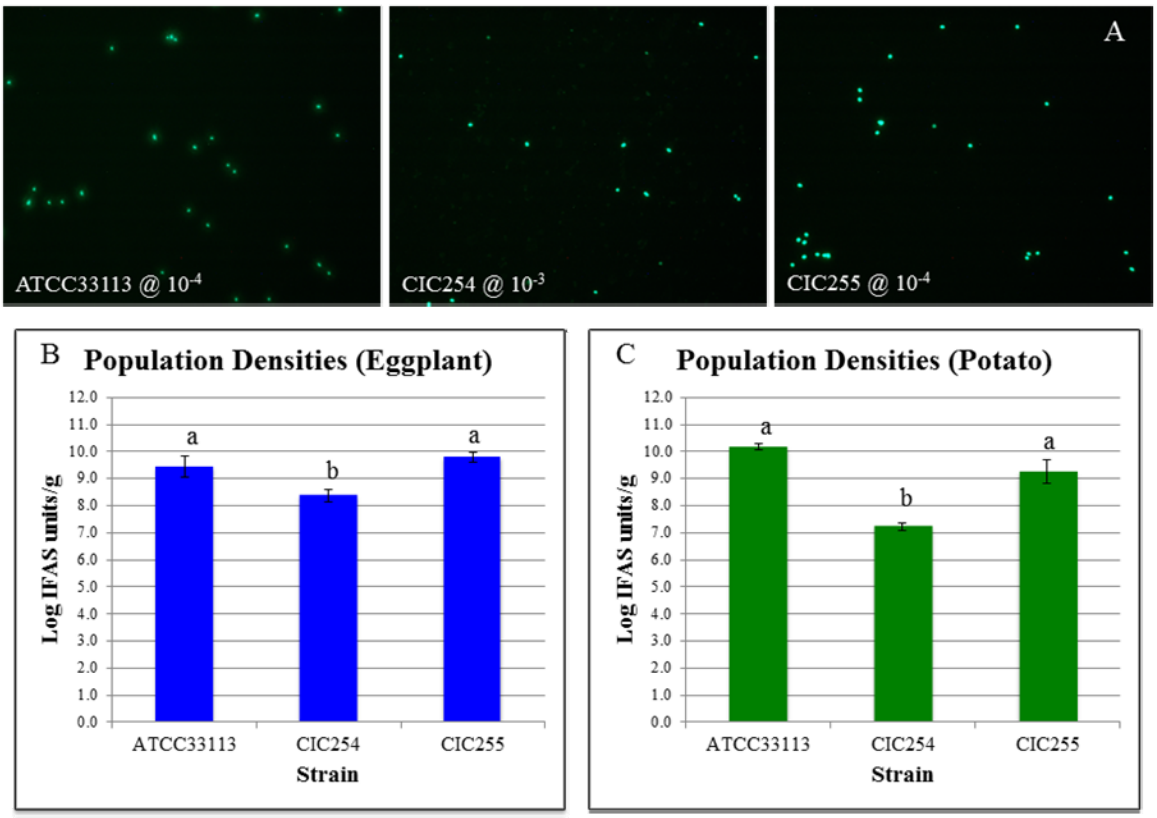


**Figure 2.9. Contribution of *chp7* to host colonization of eggplant and potato.** Representative IFAS images and a summary of bacterial cell populations in eggplants and potatoes infected with wildtype, *chp7* mutant, and the complemented *chp7* mutant of *Cms* are shown (strains ATCC33113, CIC254 and CIC255, respectively). A) Sample IFAS images of diluted cells suspensions of *Cms* isolated from plant tissue infected with ATCC33113 (at a $10^{-4}$ dilution), CIC256 (at a $10^{-3}$ dilution), and CIC257 (at a $10^{-4}$ dilution). B) Graphical summary of the mean population density estimates (log IFAS units/g) at 21 dpi of eggplants infected with ATCC33113, CIC254 and CIC255. C) Graphical summary of the mean population density estimates (log IFAS units/g) at 50 dpi of potatoes infected with ATCC33113, CIC254 and CIC255.

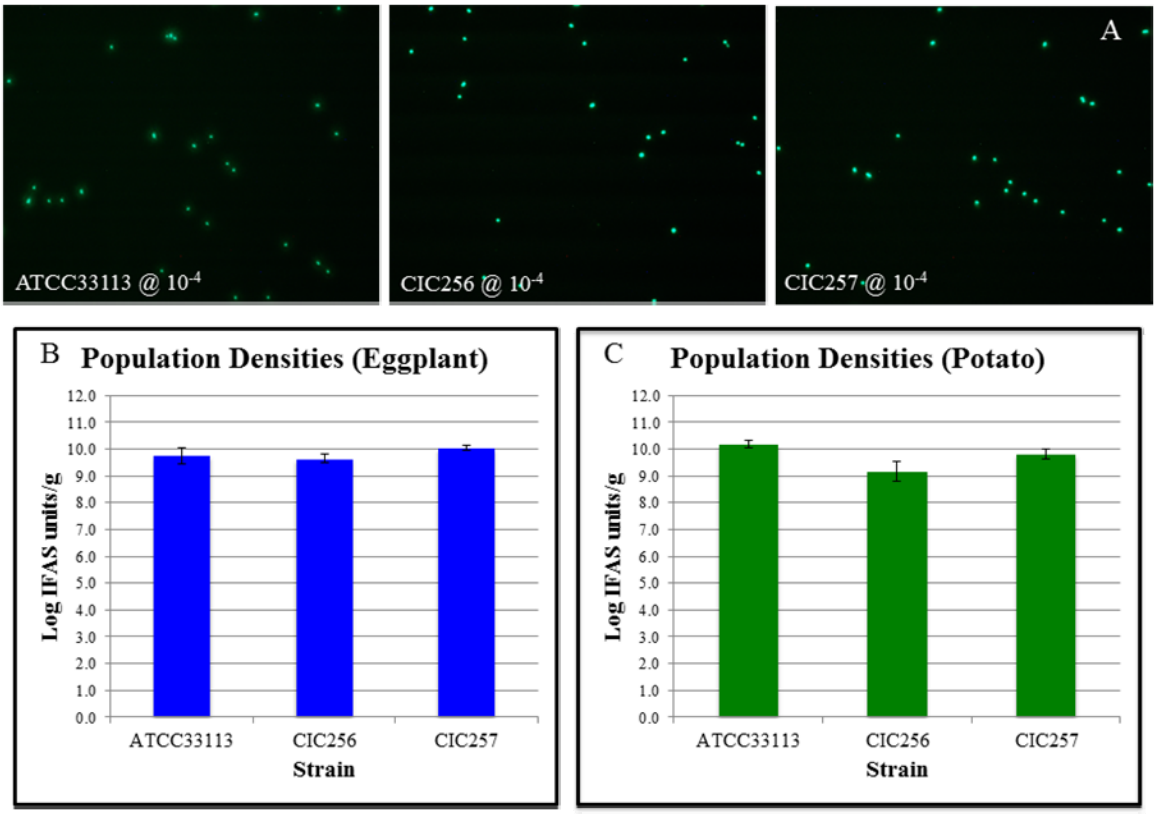


**Figure 2.10. Contribution of *php3* to host colonization of eggplant and potato.** Representative IFAS images and a summary of bacterial cell populations in eggplant and potatoes infected with wildtype, *php3* mutant, and the complemented *php3* mutant of *Cms* are shown (strains ATCC33113, CIC256 and CIC257, respectively). A) Sample IFAS images of diluted cells suspensions of *Cms* isolated from plant tissue infected with ATCC33113 (at a $10^{-4}$ dilution), CIC256 (at a $10^{-4}$ dilution), and CIC257 (at a $10^{-4}$ dilution). B) Graphical summary of the mean population density estimates (log IFAS units/g) at 21 dpi of eggplants infected with ATCC33113, CIC256 and CIC257. C) Graphical summary of the mean population density estimates (log IFAS units/g) at 50 dpi of potatoes infected with ATCC33113, CIC256 and CIC257.

## References


1. **Alfano, J. R., and A. Collmer.** 2004. Type III secretion system effector proteins: Double agents in bacterial disease and plant defense. Annual Reviews of Phytopathology **42:**385-414.
2. **Bentley, S. D., C. Corton, S. E. Brown, A. Barron, L. Clark, J. Doggett, B. Harris, D. Ormond, M. A. Quail, G. May, D. Francis, D. Knudson, J. Parkhill, and C. A. Ishimaru.** 2008. Genome of the Actinomycete plant pathogen *Clavibacter michiganensis* subspecies *sepedonicus* suggests recent niche adaptation. Journal of Bacteriology **190:**2150-2160.
3. **Brown, S. E., A. A. Reilley, D. L. Knudson, and C. A. Ishimaru.** 2002. Genomic fingerprinting of virulent and avirulent strains of *Clavibacter michiganensis* subspecies *sepedonicus*. Current Microbiology **44:**112-119.
4. **Burger, A., I. Grafen, J. Engemann, E. Niermann, M. Pieper, O. Kirchner, K. H. Gartemann, and R. Eichenlaub.** 2005. Identification of homologues to the pathogenicity factor *pat-1*, a putative serine protease of *Clavibacter michiganensis* subsp. *michiganensis*. Microbiological Research **160:**417-27.
5. **De Boer, S. H., and R. J. Copeman.** 1980. Bacterial ring rot testing with the indirect fluorescent antibody staining procedure. American Journal of Potato Research **57:**457-465.
6. **Dreier, J., D. Meletzus, and R. Eichenlaub.** 1997. Characterization of the plasmid encoded virulence region *pat*-1 of phytopathogenic *Clavibacter michiganensis* subsp. *michiganensis*. Molecular Plant-Microbe Interactions **10:**195-206.
7. **Dubeau, M.-P., M. G. Ghinet, P.-E. Jacques, N. Clermont, C. Beaulieu, and R. Brzezinski.** 2009. Cytosine deaminase as a negative selection marker for gene disruption and replacement in the genus *Streptomyces* and other Actinobacteria. Applied Environmental Microbiology **75:**1211-1214.
8. **Eichenlaub, R., K. H. Gartemann, B. Abt, T. Bekel, A. Burger, J. Engemann, M. Flugel, L. Gaigalat, A. Goesmann, I. Grafen, J. Kalinowski, O. Kaup, O. Kirchner, L. Krause, B. Linke, A. McHardy, F. Meyer, S. Pohle, C. Ruckert, S. Schneiker, E. M. Zellermann, A. Puhler, O. Kaiser, and D. Bartels.** 2008. The genome sequence of the tomato-pathogenic Actinomycete *Clavibacter michiganensis* subsp. *michiganensis* ncppb382 reveals a large island involved in pathogenicity. Journal of Bacteriology **190:**2138-2149.
9. **Gartemann, K.-H., and R. Eichenlaub.** 2001. Isolation and characterization of IS*1409*, an insertion element of 4-chlorobenzoate-degrading *Arthrobacter* sp. Strain TM1, and development of a system for transposon mutagenesis. Journal of Bacteriology **183:**3729-3736.
10. **Hogenhout, S. A., and R. Loria.** 2008. Virulence mechanisms of Gram-positive plant pathogenic bacteria. Current Opinion in Plant Biology **11:**449-456.
11. **Horsfall, J. G., and R. W. Barratt.** 1945. An improved grading system for measuring plant disease. Phytopathology **35:**655.

12. **Ishimaru, C. A., N. L. V. Lapitan, A. VanBuren, A. Fenwick, and K. Pedas.** 1994. Identification of parents suitable for molecular mapping of immunity and resistance genes in *Solanum* species. American Potato Journal **71:**517-533.
13. **Jahr, H., J. Dreier, D. Meletzus, R. Bahro, and R. Eichenlaub.** 2000. The endo-b-1, 4-glucanase *celA* of *Clavibacter michiganensis* subsp. *michiganensis* is a pathogenicity determinant required for induction of bacterial wilt of tomato. Molecular Plant-Microbe Interactions **13:**703-714.
14. **Jones, J. D. G., and J. L. Dangl.** 2006. The plant immune system. Nature **444:**323-329.
15. **Laine, M. J., H. Nakhei, J. Dreier, K. Lehtila, D. Meletzus, R. Eichenlaub, and M. C. Metzler.** 1996. Stable transformation of the Gram-positive phytopathogenic bacterium *Clavibacter michiganensis* subsp. *sepedonicus* with several cloning vectors. Applied and Environmental Microbiology **62:**1500-1506.
16. **Louws, F. J., J. Bell, C. M. Medina-Mora, C. D. Smart, D. Opgenorth, C. A. Ishimaru, M. K. Hausbeck, F. J. de Bruijn, and D. W. Fulbright.** 1998. Rep-PCR-mediated genomic fingerprinting: A rapid and effective method to identify *Clavibacter michiganensis*. Phytopathology **88:**862-868.
17. **Mogen, B. D., A. E. Oleson, R. B. Sparks, N. C. Gudmestad, and G. A. Secor.** 1988. Distribution and partial characterization of pCS1, a highly conserved plasmid present in *Clavibacter michiganense* subsp. *sepedonicum*. Phytopathology **78:**1381-1386.
18. **Nissinen, R., S. Kassuwi, R. Peltola, and M. C. Metzler.** 2001. *In planta* - complementation of *Clavibacter michiganensis* subsp. *sepedonicus* strains deficient in cellulase production or HR induction restores virulence. European Journal of Plant Pathology **107:**175-182.
19. **Nissinen, R., Xia Y., Mattinen L., Ishimaru C. A.,, and D. L. Knudson, Knudson S. E., Metzler M., Pirhonen M.** 2009. The putative secreted serine protease Chp-7 is required for full virulence and induction of a nonhost hypersensitive response by *Clavibacter michiganensis* subsp. *sepedonicus*. Molecular Plant-Microbe Interactions : MPMI **22:**809-819.
20. **Rozen, S., and H. J. Skaletsky.** 2000. Primer3 on the www for general users and for biologist programmers. *In* S. Krawetz and S. Misener (ed.), Bioinformatics methods and protocols: Methods in molecular biology. Humana Press, Totowa, NJ.
21. **Sands, D. C., G. Mizrak, V. N. Hall, H. K. Kim, H. E. Bockelman, and M. J. Golden.** 1986. Seed transmitted bacterial diseases of cereals: Epidemiology and control. Arab Journal of Plant Protection **4:**127-125.
22. **Schneider, J. B., J.-l. Zhao, and C. S. Orser.** 1993. Detection of *Clavibacter michiganensis* subsp. *sepedonicus* by DNA amplification. FEMS Microbiology Letters **109:**207-212.
23. **Stackebrandt, E., and P. Schumann.** 2006. Introduction to the taxonomy of Actinobacteria, p. 297-321, The prokaryotes. Springer, New York, NY.
24. **Stork, I., K.-H. Gartemann, A. Burger, and R. Eichenlaub.** 2008. A family of serine proteases of *Clavibacter michiganensis* subsp. *michiganensis*: *chpc* plays a role in colonization of the host plant tomato. Molecular Plant Pathology **9:**599-608.

25. **Team, R. D. C.** 2008. R: A language and environment for statistical computing. R Foundation for Statistical Computing, Vienna, Austria.
26. **Wilson, K.** 1997. Preparation of genomic DNA from bacteria. Current Protocols in Molecular Biology **27:**2.4.1-2.4.5.

# Chapter 3

# Transposon-mediated mutagenesis of *chp8* suggests a role in host colonization and virulence of *Clavibacter michiganensis* subsp. *sepedonicus*

## Introduction

*Clavibacter michiganensis* subsp. *sepedonicus* (*Cms*) is a gram-positive plant pathogen that causes bacterial ring rot of potato (*Solanum tuberosum*). Recent discoveries in regards to pathogenesis of *Cms* are beginning to shed light on disease mechanisms of this subspecies. Specific genes involved in pathogenicity have been identified. A cellulase gene, *celA*, is present on the plasmid pCS1 of *Cms* and is associated with virulence of *Cms* (10, 12). CMS2989 (*chp7*), a chromosomal homologue of *pat-1*, a known pathogenicity determinant of the closely related tomato pathogen *C. michiganensis* subsp. *michiganensis* (*Cmm*) (5), was found to be necessary in HR elicitation in tobacco and virulence of *Cms* in eggplant and potato (13). Multiple chromosomal and plasmid-encoded homologues of *pat-1* (*chp* and *php* genes, respectively) are present in both *Cmm* and *Cms* (1, 3). Of the 11 *pat-1* homologues that exist in the genome of *Cms*, we now know that both *chp7* and *php3* contribute to virulence (see Chapter 1). Yet, the relative importance of the remaining *chp* and *php* genes is unknown.

The full genome sequence of the type strain of *Cms* (ATCC33113) has recently been completed (1). The development of genetic resources and techniques for genetic manipulation of *Cms* are needed to exploit the genomic resources and to facilitate a more comprehensive understanding of molecular plant-microbe interactions in regards to *chp* and *php* genes in *Cms*. Critically important technologies are now available for functional genomic studies of *Cmm* including efficient transformation protocols and a targeted gene replacement system. Opportunely, methods developed for *Cmm* have been largly

adaptable to studying *Cms*. Various strains of *Cms* have been demonstrated to be amenable to transformation as well as transposon mutagenesis using methods developed in *Cmm* (10). A transposon mutant library of *Cms* R10 consisting of 2100 mutants was previously generated via electroporation with Tn*1409*Cβ (13). This library was instrumental in obtaining a mutant in R10 that was avirulent in both potato and eggplant. However, the utility of this library in future studies may be limited. First, the library was created in R10 (13) and not in the sequenced type strain, ATCC33113. There exists then the potential, although limited, that findings in R10 may not be directly applicable to ATCC33113 due to sequence divergence. Secondly, the observed insertional bias of Tn*1409*Cβ into genomic regions of abnormally low G+C content further limits the utility of the R10 library. Development of a more efficient transposon mutagenesis system in the type strain of *Cms* could facilitate future functional studies of *chp* and *php* genes, as well as other genes or phenotypes of interest in *Cms*.

Further functional characterization of *chp* and *php* genes will build on the current understanding of the importance of this gene family to pathogenicity of *Cms* and could provide new focus to future studies of disease mechanisms of this bacterium. Such studies require development and improvement of strategies for genetic manipulation in *Cms*. Here, a transposon mutant library was generated in the type strain ATCC33113 using the *EzTn5*™ Kan-2 Transposome (Epicentre, Madison, WI). This new library was constructed in an effort to achieve greater randomness of transposon insertion and to expand on existing genomic resources. The library was screened for insertions into *chp* and *php* genes using a combination of RATE PCR and sequence analysis to identify targets for further functional characterization. Specifically, *chp8* was targeted for

functional analysis, given that it is conserved among pathogenic strains of *Cms*, yet appears to be absent in the non pathogenic strain CIC243 (see Chapter 1).

## Materials and Methods

### *Bacterial strains and growth conditions*

Bacterial strains and plasmids used in this study are listed in Table 3.1. All bacteria were stored in nutrient broth/glycerol stocks at -80 C. *Clavibacter michiganensis* strains were grown on solid yeast glucose medium (YGM) for approximately seven days at room temperature (22-24 C)(4). Growth media were supplemented with chloramphenicol (5 μg/ml) or kanamycin (25 μg/ml) as needed for selection of transformants. *Escherichia coli* JM109 (Promega, Madison, WI) was grown on Luria-Bertani (LB) medium at 37 C for 18-22 hours. Growth media were supplemented with ampicillin (100 μg/ml), X-gal (80 μg/ml), isopropyl-β-D-thiogalactoside (IPTG, 0.5M), chloramphenicol (25 μg/ml), and/or kanamycin (50 μg/ml) as needed for selection of transformants.

### *Transformation of* Clavibacter michiganensis *subsp.* sepedonicus *and library construction*

The strain ATCC33113 (Table 3.1) of *Cms* was used in all mutagenesis experiments. *Cms* ATCC33113 is the type strain of the subspecies *sepedonicus* and it was also the strain used for sequencing the *Cms* genome (1). Preparation of *Cms* competent

cells and transformation were preformed as described previously in Chapter 2. Briefly, *Cms* competent cells were transformed via electroporation using a MicroPulsar Electroporation Apparatus (BioRad, Hercules, CA), and an electroporation mix containing 20 µl of a *Cms* competent cell suspension, 20 µl of polyethylene glycol (PEG) 8000 (Sigma, St. Louis, MO), and 2 µl plasmid DNA (1 µg total) in TE. Cells were exposed to two pulses of 15 kV/cm at a 20 second interval with a resistance of 600Ω and a capacitance of 10 µFD. Cells were immediately washed and allowed to recover for 4 hours. Following recovery, cells were plated onto YGM agar supplemented with the appropriate antibiotic selection and grown for 7-10 days at room temperature. Antibiotic resistant colonies were individually selected and arrayed into 96-well plates containing nutrient broth yeast extract (NBY) soft agar (0.6% agar) with kanamycin (25 µg/ml) (16). Library plates were grown for approximately 4 to 5 days at room temperature, and then replicated to fresh plates containing NBY with kanamycin (25 µg/ml) and grown for 3-4 days. Glycerol was added to a final concentration of 15% and plates were stored at -80 C for subsequent analyses.

*Characterization of the transposon library in ATCC33113*

Library plates were copied to fresh plates containing NBY with kanamycin (25 µg/ml) and grown 3-4 days. Genomic DNA (gDNA) isolation was performed in a 96-well format using the QuickExtract™ Bacterial DNA Extraction Kit (Epicentre) according to the manufacturer's protocol. Isolated gDNA served as template for a 90 cycle single primer polymerase chain reaction (PCR) called RATE PCR using either Inv-2 (5'-GAACTTTTGCTGAGTTGAAGGATCA-3') or RATE FP (5'-

GACAACGCAGACCGTTCC-3') to amplify genomic regions flanking the site of *EzTn5* insertion (Table 3.2) (6). RATE PCR experiments were run using a Gene Amp ® PCR System 2700 (Applied Biosystems, Life Technologies Corp., Carlsbad, CA) with the following parameters: an initial hold at 94 C for 10 minutes followed by 30 cycles of 94 C for 30 seconds, 62 C for 30 seconds, and 72 for three minutes, 30 cycles of 94 C for 30 seconds, 30 C for 30 seconds, and 72 for two minutes, 30 cycles of 94 C for 30 seconds, 62 C for 30 seconds, and 72 for two minutes, and then a final hold at 72 C for seven minutes. PCRs were run at a final reaction volume of 50 µl containing 3 µl of QuickExtract™ isolated gDNA, 10X PCR buffer (Applied Biosystems), dNTP mixture (10 mM each, Promega), 10% of 1:1 DMSO:1M betaine, 25 pmoles of primer, and 1.25 units of Amplitaq (Applied Biosystems). RATE PCR products were purified using either ethanol precipitation or ExoSAP enzymatic purification and were sent for sequencing by ACGT Inc. (Wheeling, IL) using Kan2 FP-1 sequence primer (5'-ACCTACAACAAAGCTCTCATCAACC-3', Epicentre) . Sequences were aligned with the genome of *Cms* ATCC33113 using BLAST to identify the sites of *EzTn5* insertion. Insertion sites were viewed in Artemis (The Welcome Trust Sager Institute, Hinxton, England) to determine transposon orientation and G+C content. A flowchart of library construction and characterization is depicted in Figure 3.1.

*Generation of a* chp8 *complemented mutant*

A 2 kb *Bam*HI/*Sph*I fragment containing the chloramphenicol resistance gene, *cmx*, was excised from the plasmid pKGT452Cβ (7) and cloned into pGEM-3Z (Promega) resulting in pRLS3ZX1. Full length coding sequence of *chp8* was amplified

by PCR and cloned into pGEM-T Easy (Promega) yielding pRLSTC85. The 2 kb *cmx* insert of pRLS3ZX1 was excised using *Sal*I and *Sac*I and inserted into pRLSTC85 upstream of the *chp8* coding sequence to form pRLSTC85X. The full insert of pRLSTC85X, including both the *cmx* and *chp8* genes, was amplified by PCR using the high fidelity DNA polymerase *Pfx50* (Invitrogen) and vector primer T7 and SP6. The resulting amplicon was cloned into pGEM-3Z (Promega) yielding pRLS3Z85X. The insert of pRLS3Z85X was excised using *Hind*III and *Eco*RI and cloned into pHN216 (10) giving the complete complementation construct pRLS216C85X1 (Figure 3.2). In all cases, plasmids were transformed into and maintained in *E. coli* JM109. Plasmid DNA was isolated using the Wizard SV Miniprep Kit (Promega) and plasmids were verified by PCR and sequence analysis. Plasmid DNA for transformation of *Cms* was isolated using the Midi Plasmid Kit (Qiagen).

*Verification of* chp8 *mutagenesis and complementation*

Mutation of *chp8* caused by *EzTn5* and subsequent complementation was verified by PCR. PCR experiments were done using a Gene Amp ® PCR System 2700 (Applied Biosystems) with the following parameters: an initial hold at 94 C for 10 minutes followed by 35 cycles of 94 C for 30 seconds, 58 C for 30 seconds, and 72 for one minute, and then a final hold at 72 C for seven minutes. PCRs were run at a final reaction volume of 50 µl containing 1 µl of *Cms* gDNA template (approximately 10 ng) , 10X PCR buffer (Applied Biosystems), dNTP mixture (10 mM each, Promega), 10% of 1:1 DMSO:1M betaine, 25 pmoles of primer (Table 3.2), and 1.25 units of Amplitaq (Applied Biosystems). PCR products were separated by agarose gel electrophoresis then

stained with ethidium bromide. PCR primers were designed from the ATCC33113 genome sequence using the online software Primer3 (14). Primers were synthesized by Integrated DNA Technologies (IDT, Coralville, IA).

*Plant disease assays*

Mutants of *Cms* ATCC33113 were assayed for virulence in eggplant. Disease assessments were performed as described previously in Chapter 2. Briefly, seedlings at the second leaf stage were inoculated at the petiole stump where the first true leaf was excised. Inoculum was prepared from *Cms* cells grown as a lawn on solid YGM for 2-3 days. Cells were harvested and suspended in 0.02 M potassium phosphate buffer (PPB) to an $OD_{540}$ of 0.1 (corresponding to approximately $1x10^8$ CFU/ml). Disease assessments in eggplant consisted of 8 inoculated plants per strain tested under a completely randomized design. Two to three independent assessments were completed for each strain. Inoculated plants were maintained for 21 days post-inoculation (dpi). Disease severity was rated daily from 8 to 21 dpi according to the Horsfall-Barratt scale which ranges from 1 to 12 where 1 is 0% and 12 is 100% disease (9). Data were analyzed by ANOVA using R (15) and mean separations were performed using Least Square Difference (LSD) Tests. All plants were maintained under greenhouse conditions (20-23 C with supplemental lighting to a day length of 16 hours) and pots were supplemented with Marathon (1% granular, OHP, Mainland, PA) and Osmocote Classic (14-14-14, Scotts, Marysville, OH) according to the manufacturer's recommendations.

Mutants of *Cms* were also assayed for induction of HR in tobacco, *Nicotiana tabacum* cv. Samsun. HR induction assays were conducted as described in Chapter 2.

Briefly, tobacco leaves were infiltrated with a bacterial cell suspension. Inoculum was prepared from *Cms* cells grown as a lawn on solid YGM for 2-3 days. Cells were harvested and suspended in PPB to an $OD_{540}$ of 0.8 (corresponding to approximately $8x10^8$ CFU/ml). Infiltrated leaves were monitored from the appearance of HR for 72 hours. Each treatment was repeated three times per experiment and three independent experiments were completed.

*Immunofluorescence antibody staining*

Population densities of *Cms* in infected plant tissues were measured using immunofluorescence antibody staining (IFAS). Sample preparation and visualization for IFAS were carried out as described in Chapter 2. Briefly, 1-2 inches of stem tissue was macerated in phosphate buffered saline (PBS) releasing bacterial cells. Serial dilutions of these cells were spotted onto toxoplasmosis slides (Bellco Glass, Inc., Vineland, NJ) and stained according to Cms IFA protocol (Agdia, Elkhart, IN). Cells were viewed under epi-fluorescence and images were captured. Four tissue samples were processed for each strain, and cells were counted in 10 viewing frames for each sample. IFAS data were log transformed and analyzed using ANOVA in R (15).

**Results**

*Random mutagenesis of* Clavibacter michiganensis *subsp.* sepedonicus

*Cms* type strain ATCC33113 was successfully transformed with the *EzTn5*™ Transposome (Epicentre). Kanamycin resistant transformants were selected and arrayed

into a 96-well format library. In total, over 5100 transformants were generated via ten transformations, which is an average efficiency of $5.1X10^2$ transformants/μg *EzTn5*. To address library quality, 60 individual library entries were selected and characterized by colony morphology. The majority of transformants had colony morphologies and growth rates similar to that of ATCC33113. Ten of the 60 entries (16.7%) appeared to be mixed entries. In each case these mixed entries displayed two colony morphologies and the same two colony morphologies were consistent among the potentially mixed entries. Additionally, two of the 60 (3.3%) entries did not grow and were likely dead.

The randomness of *EzTn5* insertion in *Cms* was assessed by a combination of RATE PCR and sequence analysis. Briefly, RATE PCR is a 90 cycle single primer PCR that is designed to amplify genomic regions that flank the insertion site of a transposon. A PCR primer that is specific to the transposon used for mutagenesis is used in PCR with the gDNA template of interest for 30 cycles at a stringent annealing temperature to generate transposon-flanking template by primer extension. Immediately after, a second set of 30 cycles at a reduced, non-stringent annealing temperature is run without adding reagents or reaction dilution to produce amplicons arbitrarily, some of which will include transposon-flanking regions. Finally, another 30 cycles at a stringent annealing temperature is run to amplify the amplicons produced in the second set of cycles. The final reaction products are purified and subjected to sequencing using a nested transposon-specific primer, ultimately excluding any non-specific amplicons produced during the RATE PCR. RATE PCR and sequence analysis was performed on template DNA isolated from nearly 400 transformants. Of these, 170 entries yielded sequence of high enough quality to unambiguously assign a genome location for the site of *EzTn5*

insertion. Locations of the *EzTn5* insertions are summarized in Table 3.3. For the 170 insertions identified, 140 occurred within the chromosome (82%), 22 occurred in pCS1 (13%) and 8 in pCSL1 (5%). After excluding insertions into IS elements, rRNA genes and redundant insertions, 81 unique coding sequences (CDSs) were disrupted in the chromosome, 7 in pCS1 and 5 in pCSL1 representing 3%, 15% and 6%, respectively, of the total predicted CDSs for these genomic regions. Overall, insertions occurred rather evenly across the genome with insertion frequencies ranging from 5-19% among various genomic segments (Figure 3.3A). The G+C content at the sites of insertion were also determined. The majority (53%) of insertions occurred in genome regions were the G+C content was near average (67.5-75% in the chromosome, 63-70% in pCS1 and 65-72% in pCSL1), while another 29% occurred in regions with low G+C content (Figure 3.3B).

*Mutagenesis and complementation of* chp8

RATE PCR identified one mutant, designated CIC258, containing an *EzTn5* insertion within the coding sequence of *chp8*. CIC258 demonstrated colony morphology and growth in culture similar to that of ATCC33113. The mutation within *chp8* was further verified by PCR using four different primer combinations. First, *chp8* detection primers CMSchp8f (5'-CGTGAGGCGTACAAGTCAAA-3') and CMSchp8r (5'-TACGGTGCTGATGCTTCTTG-3') were used to produce products with known size polymorphisms between wildtype (636 bp) and mutant templates (1857 bp) (Figure 3.4A). Additionally, two upstream genomic regions and downstream genomic regions flanking the *EzTn5* insertion site were amplified using primers CMSchp8r with Inv2 (407 bp), rlsChp8f (5'-CGGTACTTCGACCTCTCGAT-3') with Inv2 (882 bp), and

CMSchp8f with Inv1 (5'-ATGGCTCATAACACCCCTTGTATTA-3') (565 bp), respectively (Figure 3.4A). Given that a transposon-specific primer amplified the segments flanking transposon insertion, no amplification would be expected in wildtype *Cms* templates. In all cases, PCR analyses showed amplification only where expected and amplicons of the appropriate sizes were observed, confirming that mutation of *chp8* was achieved (Figure 3.4B).

A complemented *chp8* mutant strain was obtained by transforming CIC258 with pRLS216C85X1. One putatively complemented mutant, designated CIC259, was selected for further examination. CIC259 demonstrated colony morphology and growth similar to ATCC33113. Complementation of CIC258 was verified by PCR using the same four primer pairs described for the verification of *chp8* mutation. PCR amplicons of the appropriate sizes were observed for all templates tested verifying that complementation of the *chp8* mutation was successful (Figure 3.4B). The 1857 bp product expected in *chp8* mutant templates amplified by primers CMSchp8f and CMSchp8r was not observed for CIC259. This observation is likely attributed to PCR amplification bias towards the shorter 636 bp product from pRLS216C85X1 carried by CIC259. The observation that both up- and downstream genomic regions flanking the insertion site of *EzTn5* were amplified in CIC259 confirmed that the original transposon insertion was in place along with the complementing plasmid.

*Contributions of* chp8 *to virulence*

The contribution of *chp8* to virulence of *Cms* was evaluated in eggplant, which has been used extensively as an alternative host in research on bacterial ring rot (2). A

representative set of inoculated eggplants is shown in Figure 3.5A. At 21 dpi, a significant reduction (*p*-value=0.009) in disease severity in eggplant was observed with the *chp8* mutant, CIC258, relative to wildtype. Nearly all plants (23 of 24 plants = 95.8%) inoculated with CIC258 expressed symptoms of disease (Figure 3.5B). An increase in mean disease severity was observed in eggplants inoculated with the complemented strain CIC259, yet this difference could not be separated statistically from either wildtype or CIC258 (Figure 3.5B). Statistically significant differences in AUDPC were not observed for plants inoculated with CIC258 or its complement, CIC259 (Figure 3.5C). Additionally, CIC258 and CIC259 still retained the ability to induce a non-host HR in tobacco (data not shown).

*Population sizes of* Clavibacter michiganensis *subsp.* sepedonicus *in eggplant*

Population densities of *Cms* present in infected eggplants were measured using IFAS. Sample images from the IFAS procedure are shown in Figure 3.6A. For CIC258, a significant reduction (*p*-value=0.005) in population density was observed relative to wildtype *Cms* with density estimate of $4.1 \times 10^9$ cell/g tissue and $1.5 \times 10^{10}$ cells/g tissue, respectively (Figure 3.6B). The number of *Cms* cells present in eggplants inoculated with CIC259 was intermediate to that observed with CIC258 and ATCC33113, and could not be separated statistically (Figure 3.6B).

**Discussion**

Symptoms of bacterial ring rot are the result of a series of as yet incompletely understood interactions between *Cms* and its host. The results reported here indicate that *chp8* appears to play a minor yet measurable role in virulence of *Cms*, as was observed for *php3* (Chapter 1). Taken together with previous reports of the role of *chp7* in virulence of *Cms*, it would appear that *chp7* is the primary driver of pathogenicity and that other *chp* and *php* genes examined contribute to a lesser degree (13). *chp8* effects not only disease severity but also host colonization. Loss of *chp8* resulted in population densities that were reduced by nearly one order of magnitude, relative to wildtype. Evidence is now building that would suggest the Chp and Php proteins of *Cms* perhaps function as virulence effectors in the host. Under this hypothesis, a number of important questions in regards to their relative roles remain unanswered. It is possible that *Cms* employs a suite of effector-like serine proteases that could have different host targets or be spatially or temporally localized differently within the host. Holtsmark *et al.* (8) reported differences in the expression patterns of *chp* and *php* genes *in planta* and more specifically found that *chp7* was down-regulated while *chp8* was up-regulated *in planta* relative to *in vitro*. Given this, it is possible the utilization of these effector-like proteins is regulated based on timing of expression. Further examination of gene expression as well as fluorescent tagging of Chp and Php proteins to track their localization within in the host could provide useful insights regarding the role of Chp and Php proteins in interactions of *Cms* and its host.

In analyses of the contributions of *chp8* to both virulence and host colonization of *Cms*, significant reductions in disease severity and population density observed with CIC258 were not fully recovered by complementation. These observations could be explained by the fact that it was necessary to include an additional antibiotic resistance marker in the construct used for complementing *chp8*. It is possible that the presence of this marker had some effect on the expression of *chp8* by orientation of these genes on the plasmid or possibly by some type of inhibitory secondary structure of the plasmid.

The *EzTn5* KAN-2 Transposome successfully generated a transposon mutant library of over 5100 mutants in *Cms* type strain ATCC33113. This new library has addressed many of the shortcomings reported for the previously generated library, which was obtained with the *Arthrobacter* transposon Tn*1409*Cβ, in *Cms* wildtype strain R10 (13). First, as mentioned above, the new library was generated in the sequenced *Cms* type strain ATCC33113, which alleviates any concerns arising from sequence divergence between ATCC33113 and R10. In addition, *EzTn5* inserted randomly into the genome thus circumventing the insertion bias of Tn*1409*Cβ for regions of low G+C content. Overall, the gains accomplished in transposon mutagenesis of *Cms* should facilitate future functional genomic studies of *Cms*.

Although improvements were achieved in transposon mutagenesis of *Cms*, potential shortcomings still exist with this newly generated library. Approximately 55% of library entries are predicted to contain insertions into unique CDSs. Assuming that there are 3242 predicted CDSs in total and the library contains 5118 mutants, nearly 87% of the predicted CDSs in the *Cms* genome would be represented with insertions in this library. Thus the genome of *Cms* has not been saturated, leaving some CDSs

uninterrupted. Also, the potential of mixed entries might further reduce the number of CDSs disrupted in this library. As mentioned previously, 16.7% of entries examined in quality control experiments appeared to be mixed, based on the presence of two colony types in culture. For one entry, these colony types were isolated for further evaluation. Both colony types exhibit morphology that would not be considered atypical of wildtype *Cms* with the primary difference between these types being that one appeared to be slightly smaller and less mucoid. However, when RATE PCR was used to characterize subcultures representing these two colony types and their sequences compared, both yielded the same sequence indicating that these colony types do not arise from insertions into different genome regions. The different colony types could be artifacts of culture conditions or could be the result of insertions affecting the stability of colony morphology.

In summary, three *pat-1* homologues from *Cms* have now been evaluated for their relative contributions to virulence, non-hostHR induction and host colonization. Evidence from these evaluations indicates that the proteins encoded by these homologues may act as effectors within the host and that each are likely contributing differently to pathogenesis of *Cms*. Further examination into the expression and localization of Chp and Php proteins in the host would build on our current understanding of the role of these serine protease effector-like proteins in host-microbe interactions of *Cms*.

**Table 3.1.** Bacterial strains and plasmids used in this study.

| Strain ID | Strain | Description | Source/Reference |
|---|---|---|---|
| *Clavibacter michiganenesis* subsp. *sepedonicus* | | | |
| CIC250 | ATCC33113 | Type strain | ATCC (11) |
| CIC258 | Cms42.E2 | CIC250 with EzTn5 insertion into coding sequence of *chp8* | This study |
| CIC259 | Cms42.E2c.1 | Cms42.E2 transformed with pRLS216C85X1 - *chp8* mutation complement | This study |
| *Escherichia coli* | | | |
| JM109 | *E. coli* JM109 | Transformation competent *E. coli* | Promega |

| Plasmid ID | Resistance[1] | Description | Source |
|---|---|---|---|
| pGEM-T Easy | Amp | *E. coli* cloning vector | Promega |
| pGEM-3Z | Amp | *E. coli* cloning vector | Promega |
| pKGT452Cβ | Amp, Cmx | Tn*1409*Cβ delivery vector | Gartemann and Eichenlaub (7) |
| pHN216 | Neo, Gn | *Clavibacter-E. coli* shuttle vector | Laine (10) |
| pRLS3ZX1 | Cmx | pGEM-3Z carrying BamHI/SphI fragment of pKGT452Cβ | This study |
| pRLSTC85 | Amp | pGEM-T Easy carrying *chp8* clone | This study |
| pRLSTC85X | Amp, Cmx | pRLSTC85 with a SalI/SacI fragment of pRLS3ZX1 | This study |
| pRLS3ZC85X | Amp, Cmx | pGEM-3Z carrying cloned insert of pRLSTC85X | This study |
| pRLS216C85X1 | Amp, Cmx | pHN216 carrying cloned insert of pRLS3ZC85X | This study |

[1]Amp=Ampicillin, Cmx=Chloramphenicol, Neo=Neomycin, Gn=Gentamycin

**Table 3.2.** PCR primers used in this study.

| Primer Name | Usage | Tm | Product Size | Sequence (5'-3') |
|---|---|---|---|---|
| CMSchp8f | Detection | 55 | 636 bp | CGTGAGGCGTACAAGTCAAA |
| CMSchp8r | Detection | 55 | | TACGGTGCTGATGCTTCTTG |
| rlsChp8f | Cloning | 56 | 1471 bp | CGGTACTTCGACCTCTCGAT |
| rlsChp8r | Cloning | 57 | | GTCTTCCTGACAACCCCTGA |
| RATE FP | Sequence | 57 | N/A | GACAACGCAGACCGTTCC |
| RATE RP | Sequence | 58 | N/A | GGCCTCGAGCAAGACGTT |
| Inv-1[1] | Sequence | 56 | N/A | ATGGCTCATAACACCCCTTGTATTA |
| Inv-2[1] | Sequence | 56 | N/A | GAACTTTTGCTGAGTTGAAGGATCA |
| KAN-2 FP-1[2] | Sequence | 63 | N/A | ACCTACAACAAAGCTCTCATCAACC |
| T7 | Sequence | 48 | N/A | TAATACGACTCACTATAGGG |
| SP6 | Sequence | 42 | N/A | TATTTAGGTGACACTATAG |

[1]Primers from Ducey and Dyer 2002

[2]Primer included as part of the *EzTn5* KAN-2 Transposome Kit (Epicentre)

**Table 3.3.** Summary of representative sample of *EzTn5* insertions within *Clavibacter michiganensis* subsp. *sepedonicus* ATCC33113.

| **Category** | **Chromosome** | **pCS1** | **pCSL1** | **Total** |
|---|---|---|---|---|
| Number of insertions assigned unambiguously | 140 | 22 | 8 | 170 |
| Number in coding sequences (CDSs) | 124 | 13 | 7 | 144 |
| Number of redundant insertions (includes IS elements and rRNA) | 43 | 6 | 2 | 51 |
| Number in IS elements or rRNA | 35 | 0 | 0 | 35 |
| Number in low G+C regions (excludes IS elements and rRNA) | 29 | 3 | 5 | 37 |
| Number of intergenic insertions | 16 | 9 | 1 | 26 |
| Number of redundant insertions | 2 | 5 | 0 | 7 |
| Number in low G+C regions | 8 | 3 | 1 | 12 |
| Total insertions in low G+C regions | 37 | 6 | 6 | 49 |
| Percent of insertions in CDSs | 89 | 59 | 88 | 85 |
| Percent of insertions in low G+C regions | 26 | 27 | 75 | 29 |
| Total predicted CDSs | 3058 | 89 | 117 | 3264 |
| Percent of CDSs disrupted | 3 | 15 | 6 | 3 |

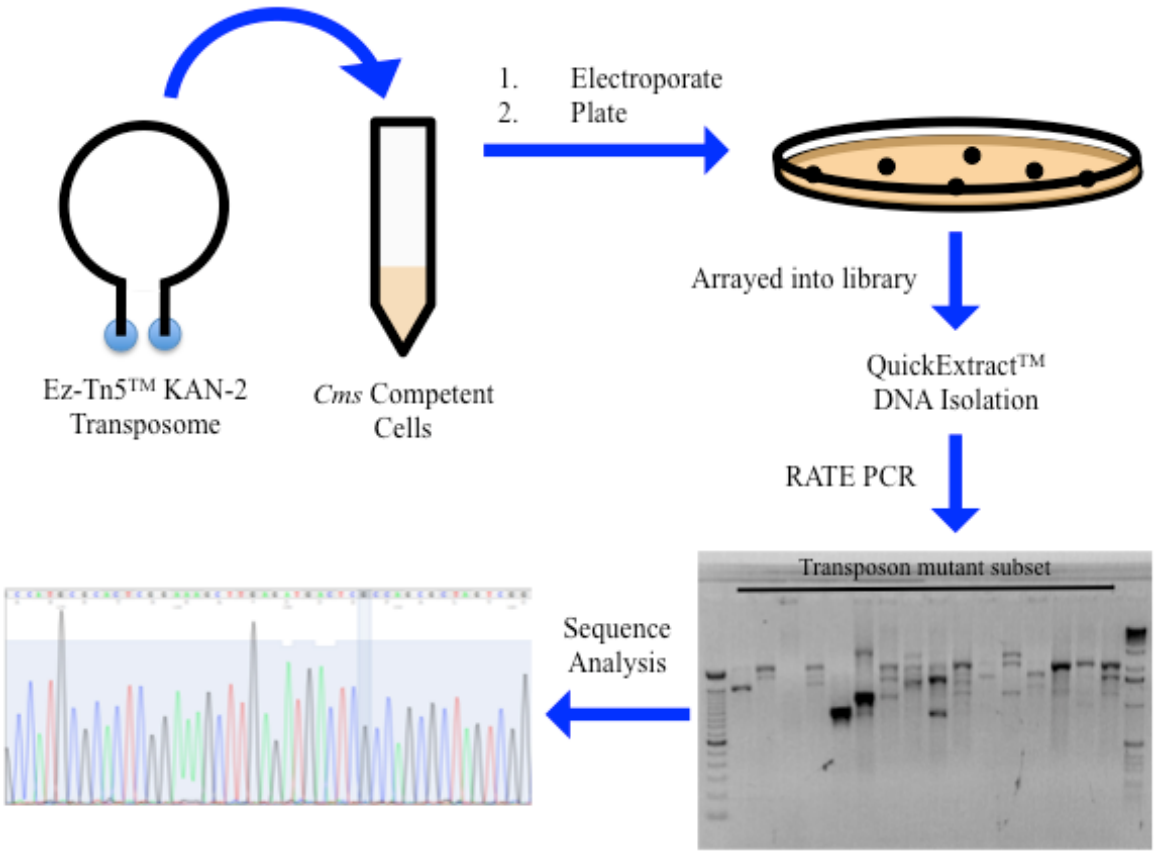


**Figure 3.1. Flowchart of transposon library construction and characterization.** The procedures for *Cms* transposon library construction and characterization are depicted. Briefly, *Cms* ATCC33113 was transformed with *EzTn5* Transposome, and transformants were arrayed into library plates. DNA was isolated from selected individuals and the insertion sites were identified by the combination of RATE PCR and sequence analysis.

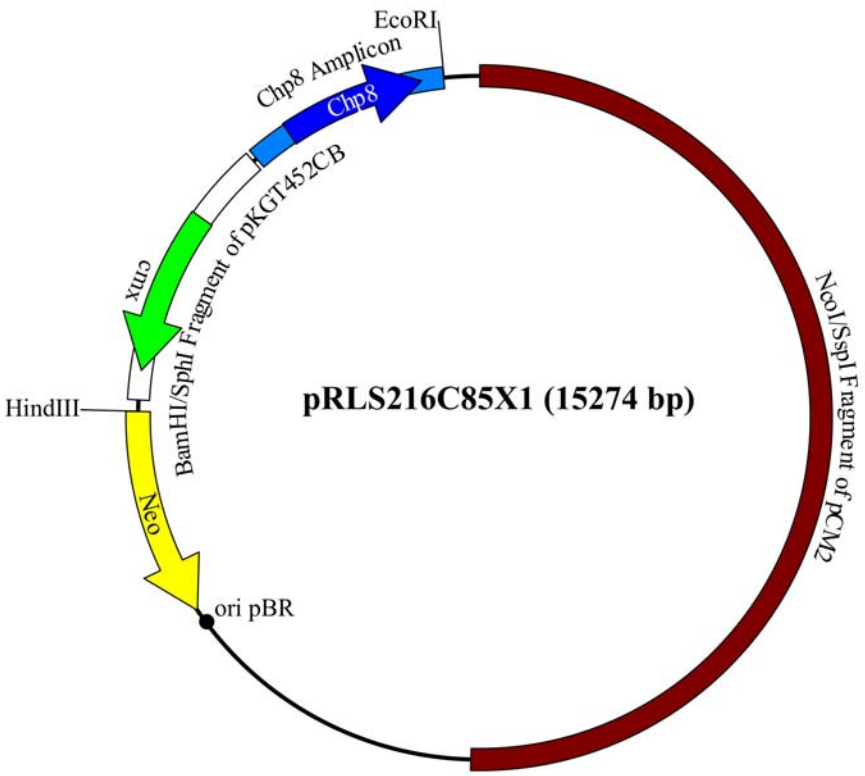


**Figure 3.2. Physical map of the complementation vector pRLS216C85X.** The plasmid used for complementation of the *EzTn5* mutation of *chp8* is shown. Here, a pHN216 backbone carries the cloned *chp8* region (coding sequence indicated by the arrow) and the *Bam*HI/*Sph*I fragment of pKGT452Cβ containing the chloramphenicol resistance gene, *cmx*.

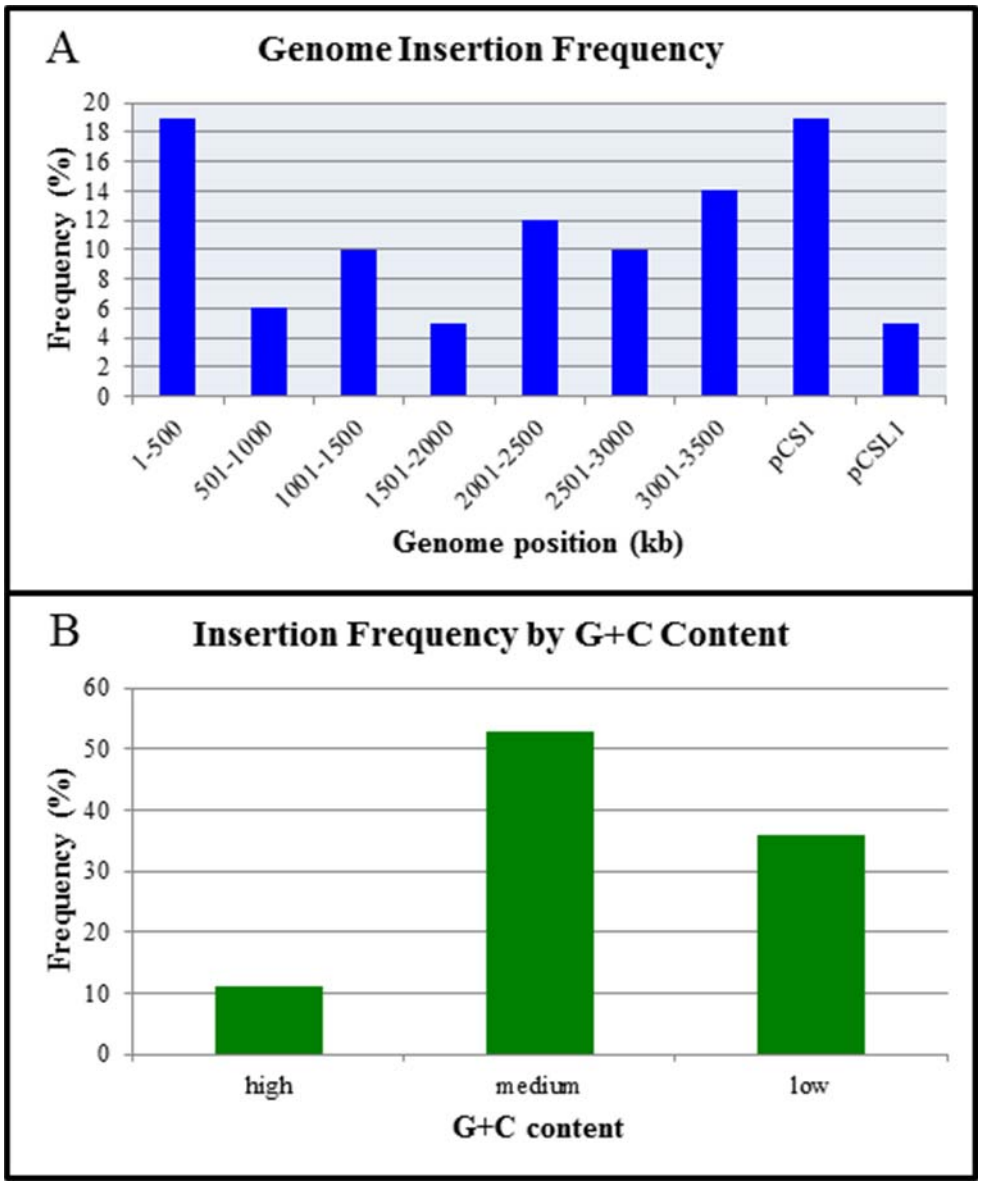


**Figure 3.3. Graphical summary of *EzTn5* insertions within ATCC33113.** Graphical representation of the location of inserts within 170 *EzTn5* transposon mutants of *Cms* is shown. A) Histogram showing insertion frequency within 500 kb segments of the *Cms* chromosome and the two native plasmids, pCS1 and pCSL1. B) Histogram showing the insertion frequency based on the G+C content at the site of insertion where low = under 67.5%, medium = 67.5-75% and high = over 75% in the chromosome, low = under 63%, medium = 63-70% and high = over 70% in pCS1 and low = under 65%, medium =65-72% and high = over 72% in pCSL1.

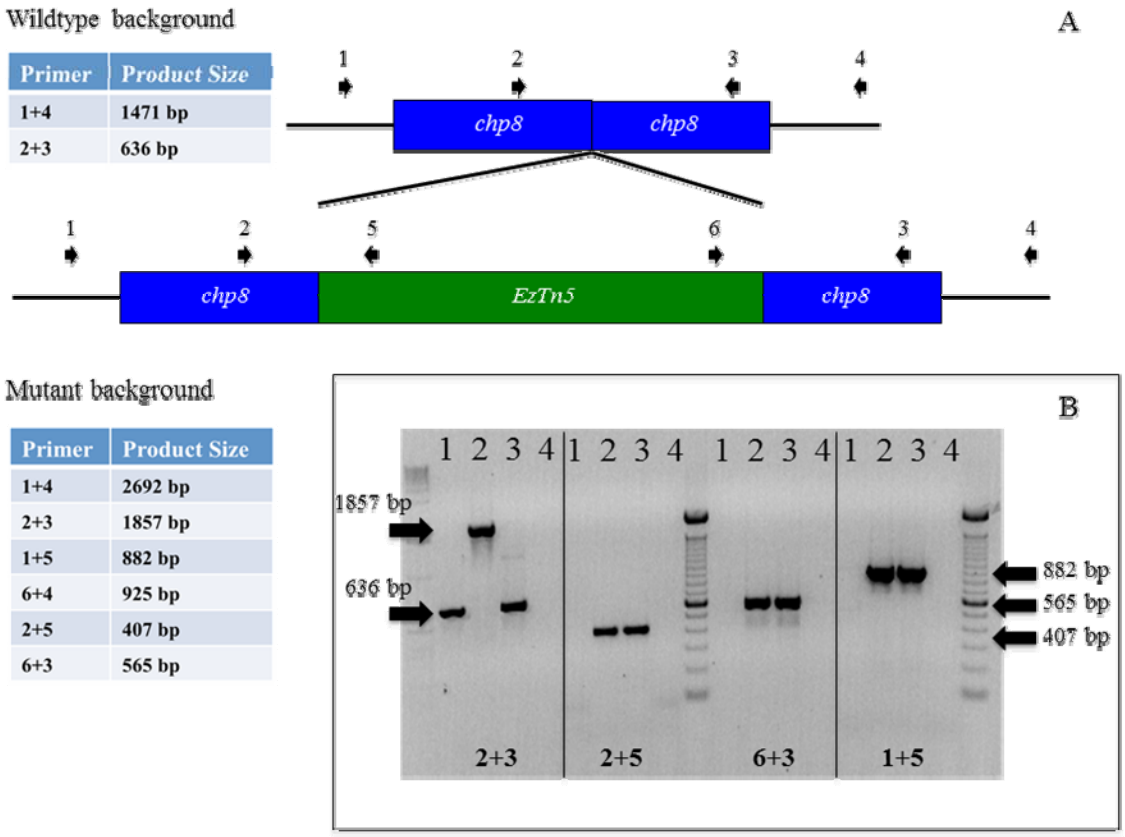


**Figure 3.4. Physical map of ATCC33113 and its derivatives CIC258 and CIC259.** Genomic region of *chp8* showing the site of *EzTn*5 insertion and primer locations as well as the results of PCR verification of mutation and complementation of *chp8* are depicted. A) Primer locations are indicated by numbered arrows where 1=rlsChp8f, 2=CMSchp8r, 3=CMSchp8f, 4=rlsChp8r, 5=Inv2, and 6=Inv1. Predicted PCR product sizes from wildtype templates are shown for various primer pairs in the table in the upper left while the product sizes for pairs from mutant templates are in the table at the lower left. B) Gel of PCR products of mutant and complemented *chp8*. Lanes are numbered by template where 1=ATCC33113, 2=CIC258, 3=CIC259 and 4=Water. Four primer sets are shown as indicated by the numbers at the bottom of the gel. Arrows on the right and left sides mark product sizes.

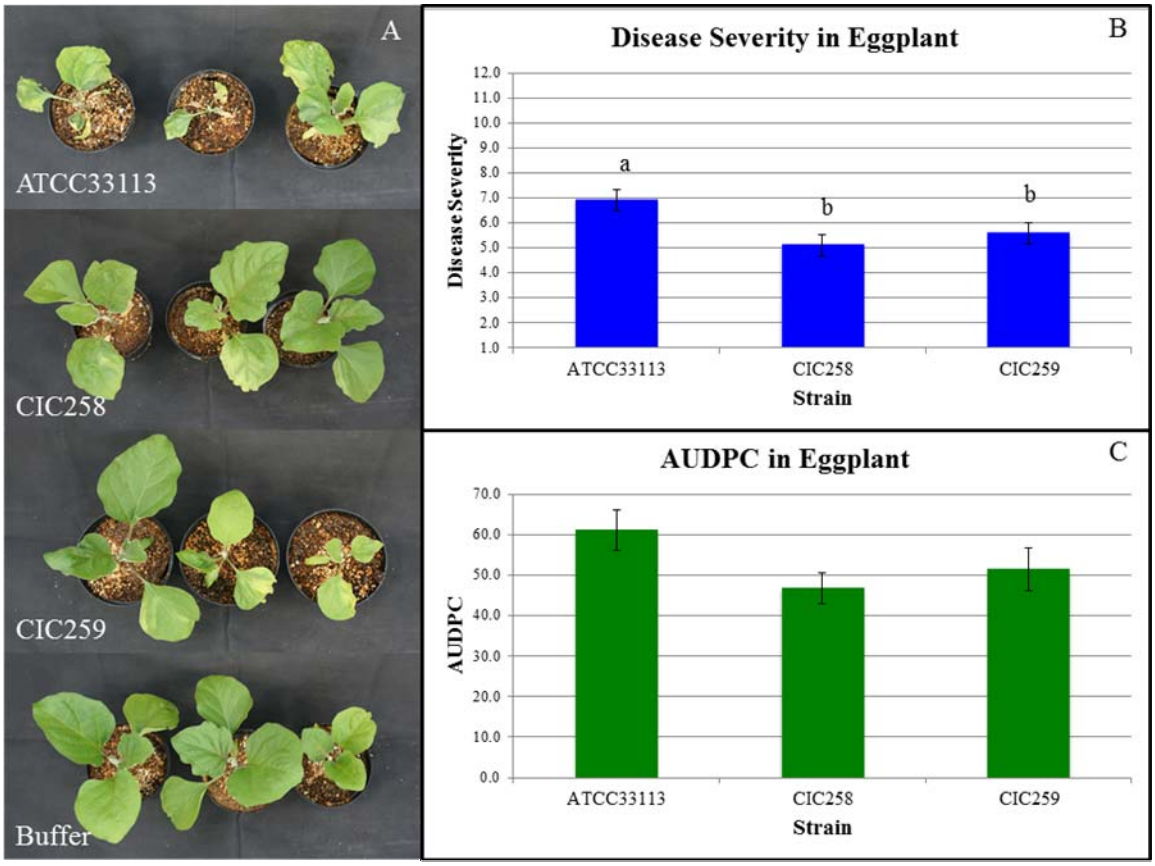


**Figure 3.5. Contributions of *chp8* to virulence of *Cms* in eggplant.** A summary of disease assays of wildtype, *chp8* mutant, and the complemented *chp8* mutant of *Cms* are shown (strains ATCC33113, CIC258 and CIC259, respectively). A) Images of a representative subset of eggplants inoculated with ATCC33113, CIC258 and CIC259 and buffer at 21 dpi. B) Mean disease rating at 21 dpi of eggplants infected with ATCC33113, CIC258 and CIC259 for all trials. C) Mean area under the disease progress curve (AUDPC) of eggplants infected with ATCC33113, CIC258 and CIC259 for all trials. For graphical summaries, standard errors of the means are represented with error bars and letters above the bars indicate significance classes based on LSD tests and the lack of letters indicates no significant differences observed.

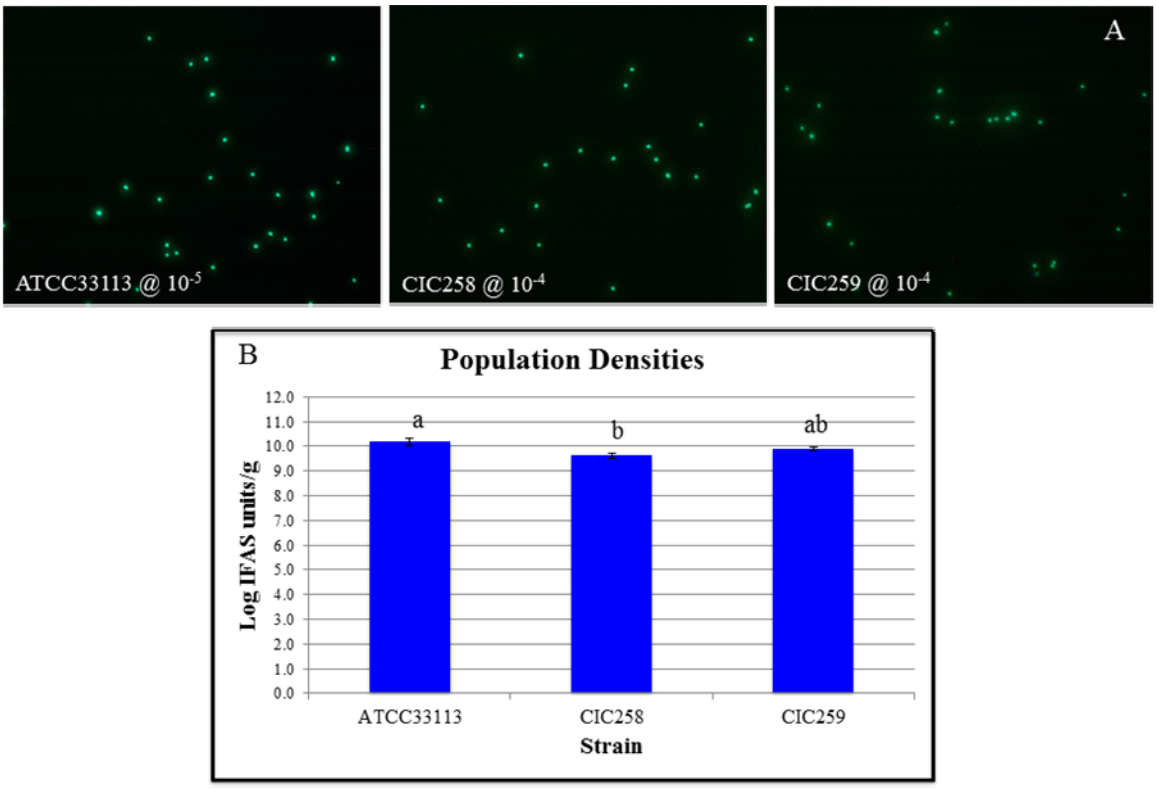


**Figure 3.6. Contributions of *chp8* to colonization of eggplant.** Representative images and a summary of bacterial cell population sizes in eggplants infected with wildtype, *chp8* mutant, and the complemented *chp8* mutant of *Cms* are shown (strains ATCC33113, CIC254 and CIC255, respectively). A) Sample IFAS images of diluted cell suspensions of *Cms* isolated from plant tissue infected with ATCC33113 (at a $10^{-5}$ dilution), CIC258 (at a $10^{-4}$ dilution), and CIC259 (at a $10^{-4}$ dilution) *Cms*. B) Mean population sizes (log IFAS units/g) at 21 dpi of infected eggplants.

## References


1. **Bentley, S. D., C. Corton, S. E. Brown, A. Barron, L. Clark, J. Doggett, B. Harris, D. Ormond, M. A. Quail, G. May, D. Francis, D. Knudson, J. Parkhill, and C. A. Ishimaru.** 2008. Genome of the Actinomycete plant pathogen *Clavibacter michiganensis* subspecies *sepedonicus* suggests recent niche adaptation. Journal of Bacteriology **190:**2150-2160.
2. **Bishop, A. L., and S. A. Slack.** 1987. Effect of innoculum dose and preparation, strain variation, and plant growth conditions on the eggplant assay for bacterial ring rot. American Potato Journal **64:**227-234.
3. **Burger, A., I. Grafen, J. Engemann, E. Niermann, M. Pieper, O. Kirchner, K. H. Gartemann, and R. Eichenlaub.** 2005. Identification of homologues to the pathogenicity factor *pat-1*, a putative serine protease of *Clavibacter michiganensis* subsp. *michiganensis*. Microbiological Research **160:**417-27.
4. **De Boer, S. H., and R. J. Copeman.** 1980. Bacterial ring rot testing with the indirect fluorescent antibody staining procedure. American Journal of Potato Research **57:**457-465.
5. **Dreier, J., D. Meletzus, and R. Eichenlaub.** 1997. Characterization of the plasmid encoded virulence region *pat*-1 of phytopathogenic *Clavibacter michiganensis* subsp. *michiganensis*. Molecular Plant-Microbe Interactions **10:**195-206.
6. **Ducey, T. F., Dyer D. W.** 2002. Rapid identification of Ez::Tn5$^{TM}$ transposon insertion sites in the genome of *Neisseria gonnorroeae*. EPICENTRE Forum **9:**6-7.
7. **Gartemann, K.-H., and R. Eichenlaub.** 2001. Isolation and characterization of IS*1409*, an insertion element of 4-chlorobenzoate-degrading *Arthrobacter* sp. Strain TM1, and development of a system for transposon mutagenesis. Journal of Bacteriology **183:**3729-3736.
8. **Holtsmark, I., G. Takle, and M. Brurberg.** 2008. Expression of putative virulence factors in the potato pathogen *Clavibacter michiganensis* subsp. *sepedonicus* during infection. Archives of Microbiology **189:**131-139.
9. **Horsfall, J. G., and R. W. Barratt.** 1945. An improved grading system for measuring plant disease. Phytopathology **35:**655.
10. **Laine, M. J., H. Nakhei, J. Dreier, K. Lehtila, D. Meletzus, R. Eichenlaub, and M. C. Metzler.** 1996. Stable transformation of the Gram-positive phytopathogenic bacterium *Clavibacter michiganensis* subsp. *sepedonicus* with several cloning vectors. Applied and Environmental Microbiology **62:**1500-1506.
11. **Mogen, B. D., A. E. Oleson, R. B. Sparks, N. C. Gudmestad, and G. A. Secor.** 1988. Distribution and partial characterization of pCS1, a highly conserved plasmid present in *Clavibacter michiganense* subsp. *sepedonicum*. Phytopathology **78:**1381-1386.
12. **Nissinen, R., S. Kassuwi, R. Peltola, and M. C. Metzler.** 2001. *In planta* - complementation of *Clavibacter michiganensis* subsp. *sepedonicus* strains deficient in cellulase production or HR induction restores virulence. Eur J Plant Pathol **107:**175-182.

13. **Nissinen, R., Xia Y., Mattinen L., Ishimaru C. A.,, and D. L. Knudson, Knudson S. E., Metzler M., Pirhonen M.** 2009. The putative secreted serine protease Chp-7 is required for full virulence and induction of a nonhost hypersensitive response by *Clavibacter michiganensis* subsp. *sepedonicus*. Molecular Plant-Microbe Interactions **22:**809-819.
14. **Rozen, S., and H. J. Skaletsky.** 2000. Primer3 on the www for general users and for biologist programmers. *In* S. Krawetz and S. Misener (ed.), Bioinformatics methods and protocols: Methods in Molecular Biology. Humana Press, Totowa, NJ.
15. **Team, R. D. C.** 2008. R: A language and environment for statistical computing. R Foundation for Statistical Computing, Vienna, Austria.
16. **Vidaver, A. K.** 1967. Synthetic and complex media for the rapid dection of fluorescence of phytopathogenic *Pseudomonads*: Effect of the carbon source. Applied Microbiology **15:**1523-1524.

# Chapter 4

# Evaluation of scalable assays of biofilm formation by *Clavibacter michiganensis* subsp. *sepedonicus*

## Introduction

Bacteria are generally thought of as independent, free-living organisms, yet more recently that view has shifted toward an appreciation that in nature bacteria live in microcommunities within biofilms. Biofilms consist of aggregated bacteria connected by a network of bacterially produced polysaccharides and proteins referred to as extracellular polysaccharide slime (EPS) (5). Bacterial infections involving biofilms are often problematic in hospitals, particularly in transplant surgeries, in oral health, and in many chronic infections. Biofilms have also been found to be an important component of bacterial diseases of plants including those caused by *Xylella fastidiosa* (8), *Xanthomonas campestris* pv. *campestris* (4), *Pantoea stewartii* (15), and *Ralstonia solanacearum* (6). *Clavibacter michiganensis* subsp. *michiganensis* (*Cmm*) was observed to form biofilms upon infection of tomato and a mutant of NCPPB382 lacking the pathogenicity island (PI) was found to have lost the ability to form biofilms (2). These observations indicate that genetic control of biofilm formation is likely located in the PI of *Cmm* and that biofilms may be important to the plant-microbe interactions of *Cmm*.

*Clavibacter michiganensis* subsp. *sepedonicus* (*Cms*) is a gram-positive, vascular system-inhabiting bacterium that causes bacterial ring rot of potato, *Solanum tuberosum*. *Cms* is highly infectious and can survive in seeds, tubers and plant debris, and on equipment and storage facilities for a number of years. Given its current status as a national and international quarantine pest, *Cms* has important implications in potato production. The formation of biofilms has been demonstrated in *Cms* both *in vitro* and *in planta* (9). Yet, how and why this process occurs is not clear. Given that biofilm

formation appears to affect the outcome of *Cmm* interactions in tomato and that *Cms* contains homologues to genes located within the PI of *Cmm*, the question arises as to the role of these homologues in biofilm formation and virulence of *Cms*.

Development of an appropriate assay for assessing biofilm formation by *Cms* is a necessary first step towards addressing a number of key questions regarding the role of biofilms in bacterial ring rot. In this study, three different assays were evaluated for their relative efficiency at measuring *in vitro* biofilm formation of *Cms*. Two assays, the minimum biofilm eradication concentration (MBEC) assay (Innovotech, Edmonton, AB Canada) and the biofilm staining assay, were quantitative and the third, the balsa wood biofilm assay, was qualitative. The MBEC has been used for high-throughput testing of biofilm sensitivity to antimicrobial compounds. Here, the MBEC system was adapted to test biofilm formation of *Cms*. The biofilm staining assay was adapted from an assay reported by Merritt *et al.* in 2005 (10). The balsa wood biofilm assay was developed for scalable qualitative evaluation of biofilm formation. These biofilm assays were used to screen a collection of more than 5100 *EzTn5*™ (Epicentre, Madison, WI) mutants of *Cms*.

## Materials and Methods

### *Bacterial strains and growth conditions*

Bacterial strains used in this study are listed in Table 4.1. All bacteria were stored in nutrient broth/glycerol stocks at -80 C. *Clavibacter michiganensis* strains were grown on solid yeast glucose medium (YGM) for approximately seven days at room

temperature (22-24 C)(3). Transposon library plates were replicated in nutrient broth yeast extract (NBY) medium and were grown at room temperature with orbital shaking at 150 rpm for 3-4 days prior to use in biofilm assays (14).

*MBEC biofilm assay*

The MBEC assay uses a 96-well microtiter plate format in which the plate lid is adapted with a series of pegs that extend into the plate wells and provide a surface for biofilm formation. The peg surfaces can be coated with different substrates that promote biofilm growth. To inoculate MBEC plates, *Cms* strains were grown from a single colony as lawns on solid YGM for 3-4 days. Cells were harvested and suspended in liquid YGM to an $OD_{590}$ of 0.8 (corresponding to approximately $8x10^8$ CFU/ml). Five microliters of a bacterial cell suspension was transferred to microtiter plate wells containing 145 μl of YGM. For assaying the mutant library, cells were grown in microtiter plates as described above and 5 μl from each well was transferred to MBEC plate wells containing 145 μl of YGM. MBEC plates were incubated at room temperature for 10 days. During that time, spent media was removed and replenished with fresh YGM every 2-3 days. After incubation, the MBEC pegs were rinsed briefly by dipping in sterile water and then placed in a new mircotiter plate containing 0.02 M potassium phosphate buffer (PPB). Plates were sonicated for 30-45 minutes to remove cells adhered to the surface and bacterial titers were measured either by direct colony counts on solid YGM, by spectrophotometery on a Labsystems Multiskan Plus plate reader (Fisher Scientific, Pittsburgh, PA) at a wavelength of 590 nm, or by a combination of colony counts and optical density readings.

*Biofilm staining assay*

The biofilm staining assay relies on crystal violet staining of bacterial cells adhering to a plastic or glass surface. The stain can be eluted from biofilms and quantified via optical density with a plate reader. The procedure used for this assay was adapted from that reported by Merritt *et al.* in 2005 (10) using a 24-well microtiter plate format. Briefly, *Cms* strains were grown and inoculated to assay plates as described for the MBEC biofilm assay with the exception that 500 µl (*Cms* strains) or 100 µl (*Cms* transposon mutants) of bacterial cell suspensions were transferred to 1500 µl of growth media. Plates were incubated at room temperature for 10 days. Growth media and planktonic bacteria were removed from the wells and wells were gently washed with sterile water. Cells adhering to the surface were stained with 0.1% crystal violet for 10 min., washed twice with sterile water and then allowed to air dry. The crystal violet stain was eluted with 95% ethanol and quantified spectrophotometerically at 500-600 nm.

*Balsa wood biofilm assay*

The balsa wood biofilm assay is a 24-well format assay developed for qualitative assessment of biofilm formation by *Cms* (9). Here, balsa wood fragments serve as a substrate for the growth of biofilms. Assay plates were inoculated as described for the biofilm staining assay. After inoculation, 2 cm long sterile balsa wood sections were placed into each well and plates were incubated for 10 days at room temperature. Following incubation, each well was inspected visually and was rated as either positive or negative for the presence of *Cms* biofilms.

## Results

*MBEC biofilm assay*

Measurement of bacterial titer using a plate reader was optimized by generating a set of bacterial suspensions of known optical density (OD) at 590 nm (1.0, 0.75, 0.5, 0.25, 0.1, 0.075, 0.05 and 0.025) with *Cms* test strains CIC250, CIC254, CIC255, CIC256 and CIC257. The bacterial suspensions were arrayed into a 96-well microtiter plate and were measured with the plate reader. Plate readings correlated very well ($R^2$=0.999) with the known $OD_{590}$ of the bacterial suspensions (Figure 4.1A). The same bacterial suspensions were also subjected to serial dilution and plating onto solid YGM for viable colony counts (VCC). Plate readings were transformed to $OD_{590}$ values and plotted against the log VCC. The correlation between transformed plate readings and log VCC was moderate ($R^2$=0.686) (Figure 4.1B). Unless otherwise noted the results reported here were used to transform subsequent plate readings to log VCC estimates for strains assayed. Additionally, it was observed that the detection limit of the plate reader was approximately $1x10^6$ CFU/ml (data not shown).

Various test conditions, including growth on an orbital shaker versus a plate rocker, hydroxyapatite versus cellulose as the coating on MBEC pegs, and plate position were evaluated to optimize the MBEC assay prior to application of the assay for screening the *Cms* transposon mutant library. The affect of orbital shaking at 150 rpm on biofilm formation of several strains of *Cms* was compared to that obtained with gentle shaking on a plate rocker. Bacterial growth in plates placed on the plate rocker generally

produced higher bacterial titers relative to plates placed on an orbital shaker (Figure 4.2A). Biofilms produced by CIC194, CIC242, CIC243, CIC250, CIC254, CIC255, CIC256, CIC257, CIC258 and CIC259 were evaluated on MBEC pegs coated with either hydroxyapatite or cellulose. A preference for the hydroxyapatite substrate was observed (Figure 4.2B). The affect of position within the microtiter plate was determined by inoculating wells at different positions with CIC194, CIC242, CIC243, CIC250 and CIC253. In general, bacterial titers were slightly higher for biofilms produce in wells around the periphery of the microtiter plate (Figure 4.2C). It was concluded that the optimal conditions for biofilm studies using the MBEC assay could be achieved with pegs that were coated with hydroxyapatite and by incubating plates on a plate rocker.

Strains of *Cms*, CIC250, CIC254, CIC255, CIC256 and CIC257, were evaluated under the optimized MBEC conditions and quantified as described above. Bacterial titers within biofilms were measured using the plate reader, and transformed plate readings were compared to actual VCC as determined by serial dilution plating. In both the actual VCC and the calculated VCC, significant differences (p-values=$1.76X10^{-5}$ and 0.008, respectively) by strain were observed (Figure 4.3). Although significant differences were observed, these differences were small; however, actual VCC did not agree well with calculated VCC. Ultimately, differences in biofilm formation among strains were detected, but the differences observed were not in agreement for the two quantification methods tested.

Approximately 500 *EzTn*5 mutants of ATCC33113, representing 9.25% of the library, were screened in duplicate for the ability to produce biofilms in the MBEC assay. From this initial screening, 6 mutants that failed to produce detectable biofilms were

identified (41.B10, 42.B9, 42.D5, 42.D6, 43.B2 and 43.F10). These strains were pulled from the library and rescreened with replication to verify their biofilm phenotype. For this secondary screening, optical density was measured by plate reading and actual VCC was determined. The secondary screening of the putative biofilm-deficient *Cms* mutants did not confirm impaired biofilm formation. Significant differences in actual bacterial titer were observed between wildtype and *Cms* mutants (Figure 4.4A). No significant differences due to strain were observed for the calculated VCC extrapolated from optical density readings (Figure 4.4B). Again, actual VCC and calculated VCC were not in agreement.

*Biofilm staining assay*

The biofilm staining assay for studying biofilm formation by *Cms* was tested with several *Cms* strains (CIC194, CIC242, CIC243, CIC250, CIC254, CIC255, CIC256 and CIC257). Treatments included cell culture-treated and untreated microtiter plates. In all cases, *Cms* failed to adhere sufficiently to the surface of the microtiter well. Therefore, this assay was abandoned as a strategy for studying biofilm formation by *Cms*.

*Balsa wood biofilm assay*

Various test conditions, including growth on an orbital shaker versus on a plate rocker and growth medium were evaluated as part of the assay optimization prior to application of the assay for screening the *Cms* transposon mutant library. Six different growth media were evaluated: nutrient broth, nutrient broth amended with glucose (2 g/l), NBY, Luria-Bertani (LB), yeast extract peptone glucose (YPG) (7) and YGM. Strains

grown in LB on the plate rocker produced the most robust biofilms under the conditions tested. These conditions were used for subsequent assays. Example images of positive and negative biofilms results are shown in Figure 4.5.

Approximately 200 mutants from the *EzTn*5 library, representing 3.7% of the library, of ATCC33113 were screened in duplicate. From this initial library screening, 3 mutants failed to produce biofilms (51.G3, 48.E8 and 48.F2). These were pulled from the library and rescreened with replication to verify their relative ability to produce biofilms under the test conditions. All of the putative biofilm-negative mutants tested positive for biofilm formation in 83-100% of the secondary screens (Figure 4.6).

**Discussion**

Two of the biofilm assays examined in this study could be considered as potential strategies for future assessment of biofilm formation by *Cms*. Currently, both of these assays are still diminished in their utility, given the observed inconsistencies between initial library screens and secondary screens of putative biofilm deficient mutants. The formation of biofilms is a complex trait that is likely influenced by a number of factors that are not understood in *Cms*. Given this, it is not unexpected to observe variation in biofilm formation leading to inconsistencies between screens. Of these, the MBEC remains the most promising given that it is more scalable, quantitative and even small differences in bacterial titers can be detected. To improve the utility of this assay, the optimization of quantification should be revisited with greater replication. Through the generation of additional data in regards to quantification it may be possible to improve

estimations of bacterial titer using optical density plate readings. Additionally, this could reduce the need to verify readings with serial dilution plating, which can be laborious when conducting high-throughput screens. It was observed that *Cmm* strains grown in xylem sap produced biofilm-like structures *in vitro* (2). Based on this observation, it is possible that use of xylem sap in assays of biofilm formation by *Cms* could improve consistency and reproducibility.

MBEC biofilm assays of the *Cms* transposon mutant library identified 6 mutants that were reduced in their ability to produce biofilms relative to the wildtype strain. Although these differences were less than one order of magnitude, they were measurable by serial dilutions. Given their reduced ability to form biofilms, these mutants may warrant further investigation.

**Table 4.1.** Bacterial strains used in this study.

| Strain ID | Strain | Description | Source |
|---|---|---|---|
| ***Clavibacter michiganenesis* subsp. *sepedonicus*** | | | |
| CIC194 | BC-P45 | Spontaneous spectinomycin-resistant mutant of P45 | C. Orser (13) |
| CIC242 | Cs3NM | Mucoid derivative of Cs3NM | S. H. DeBoer (1) |
| CIC243 | Cs3NM | Non-mucoid derivative of Cs3NM | S. H. DeBoer (1) |
| CIC250 | ATCC33113 | Type strain | ATCC (11) |
| CIC253 | R10 | | R. Nissinen (12) |
| CIC254 | CmsC7X20 | CIC250 transformed with pRLSTC7X2 | Chapter 1 |
| CIC255 | CmsC7X20c.1 | CmsC7X20 transformed with pRLS216C7 | Chapter 1 |
| CIC256 | CmsP3X50 | CIC250 transformed with pRLSTP3AX5 | Chapter 1 |
| CIC257 | CmsP3X50c.1 | CmsP3X50 transformed with pRLS216P3 | Chapter 1 |
| CIC258 | Cms42.E2 | CIC250 with *EzTn*5 insertion into coding sequence of *chp8* | Chapter 2 |
| CIC259 | Cms42.E2c.1 | Cms42.E2 transformed with pRLS216C85X1 - *chp8* mutation complement | Chapter 2 |
| 41.B10 | Cms41.B10 | CIC250 transformed with *EzTn*5 | This study |
| 42.B9 | Cms42.B9 | CIC250 transformed with *EzTn*5 | This study |
| 42.D5 | Cms42.D5 | CIC250 transformed with *EzTn*5 | This study |
| 42.D6 | Cms42.D6 | CIC250 transformed with *EzTn*5 | This study |
| 43.B2 | Cms43.B2 | CIC250 transformed with *EzTn*5 | This study |
| 43.F10 | Cms43.F10 | CIC250 transformed with *EzTn*5 | This study |
| 48.E2 | Cms48.E2 | CIC250 transformed with *EzTn*5 | This study |
| 48.F2 | Cms48.F2 | CIC250 transformed with *EzTn*5 | This study |
| 51.G3 | Cms51.G3 | CIC250 transformed with *EzTn*5 | This study |

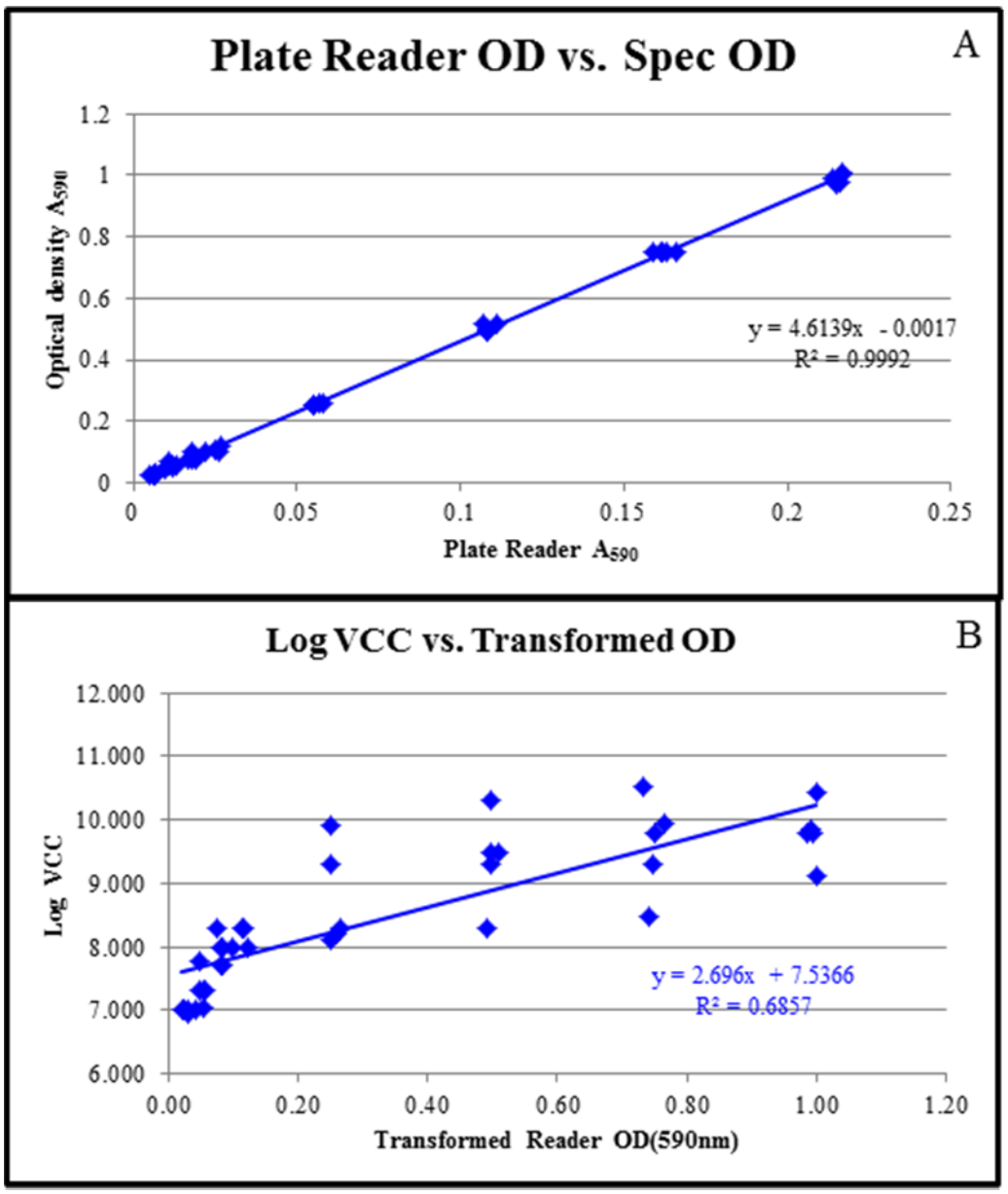


**Figure 4.1. Optimization of spectrophotometeric quantification of MBEC biofilms.** Linear relationships between plate readings and known optical densities ($OD_{590}$) of bacterial suspensions as well as viable colony counts (VCC) and transformed plate readings are shown. A) Graphical representation of the linear relationship between measurements of optical density obtained with the plate reader and known spectrophotometer $OD_{590}$ readings for a set of bacterial suspensions. Equation and $R^2$ value for the relationship is indicated on the graph. B) Graphical representation of the linear relationship between transformed plate readings and log VCC as determined by serial dilution plating of the same bacterial suspensions. Equation and $R^2$ value for the relationship is indicated on the graph.

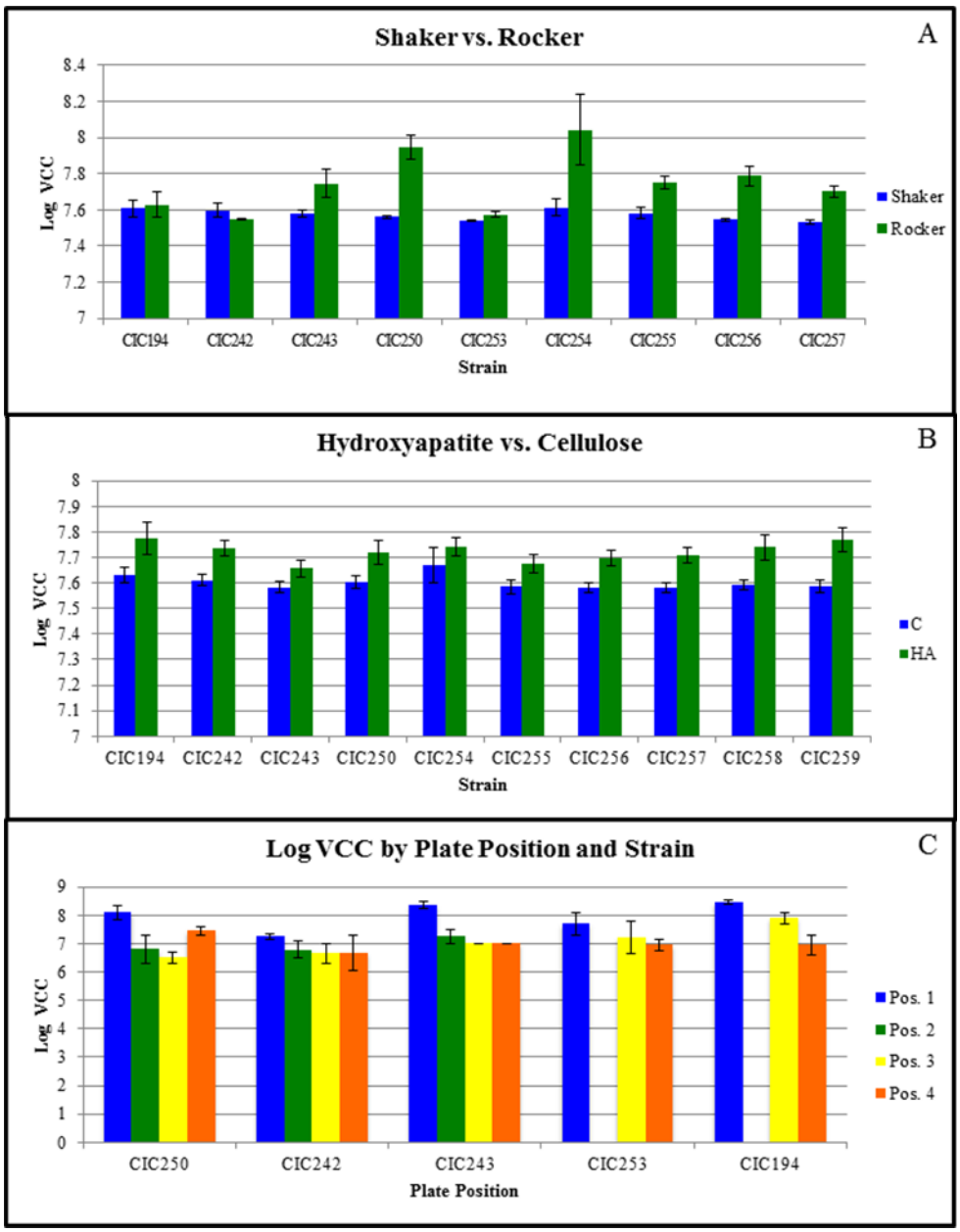


**Figure 4.2. Optimization of conditions for biofilms formation in the MBEC assay.** Graphical summaries of optimization of test conditions examined with several strains of *Cms*. A) Comparison of biofilm-associated bacterial titer (log VCC ) after incubation on either an orbital shaker (blue) or a plate rocker (green) is depicted graphically. Error bars indicate standard error. B) Comparison of bacterial titer (log VCC) after growth on either hydroxyapatite (blue) or cellulose (green) coated pegs. Error bars indicate standard error. C) Effect of plate position on bacterial titer (log VCC) where 1=outermost wells, 2=next wells inward, 3=next well inward and 4=innermost wells. Error bars indicate standard error.

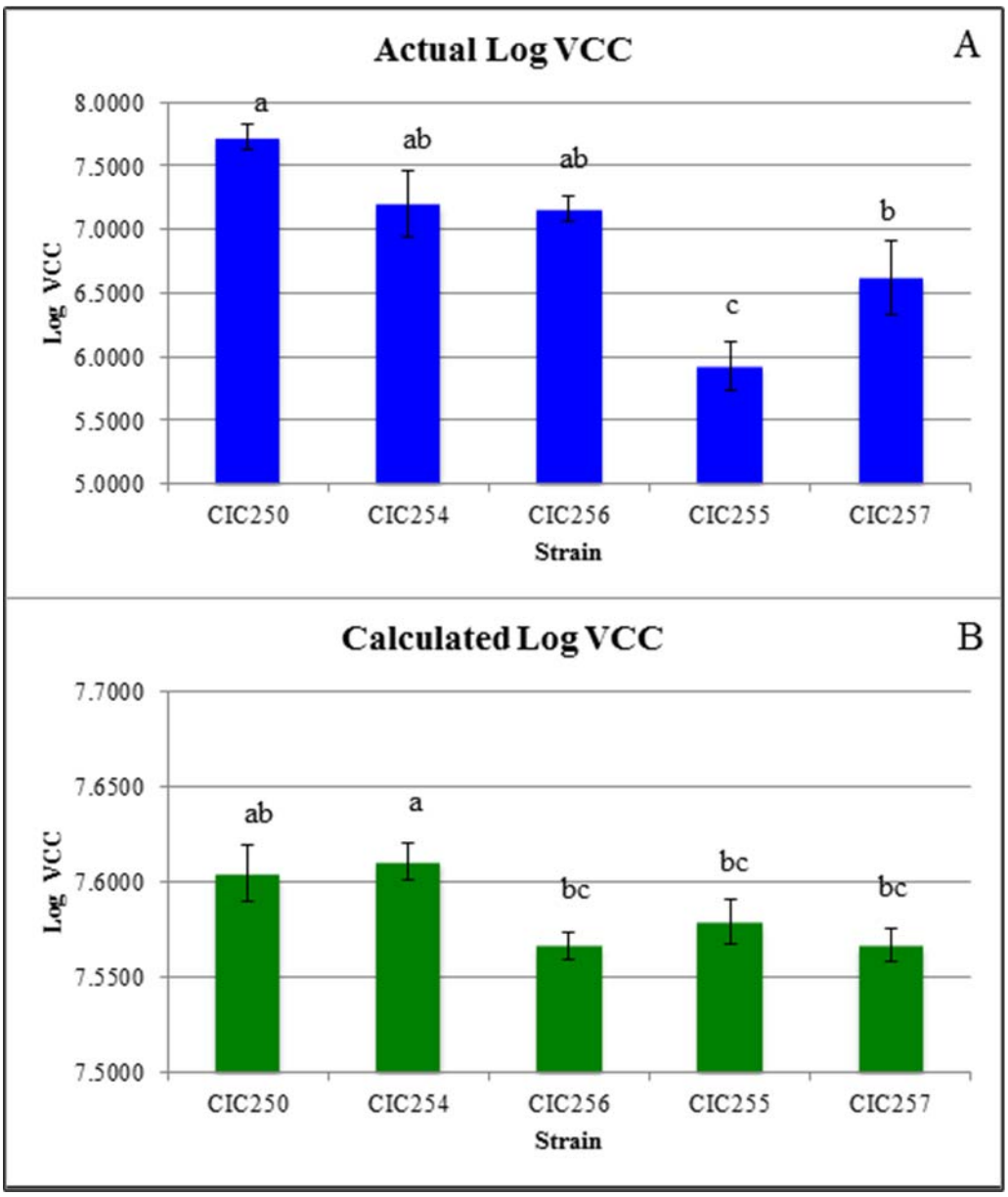


**Figure 4.3. Biofilm production by select strains of *Clavibacter michiganensis* subsp. *sepedonicus* grown under optimal MBEC assay conditions.** Bacterial titers associated with biofilms were estimated by direct colony counts of viable cells (log VCC) or by extrapolation from plate readings of optical density at 590 nm ($OD_{590}$) using a standard curve of VCC versus $OD_{590}$. A) Actual biofilm-associated bacterial titer (log VCC) as determined by serial dilution plating is represented graphically. Error bars indicate standard error and letters indicate significance classes based on LSD tests. B) Calculated biofilm-associated bacterial titer by strain (log VCC). Error bars indicate standard error and letters indicate significance classes based on LSD tests.

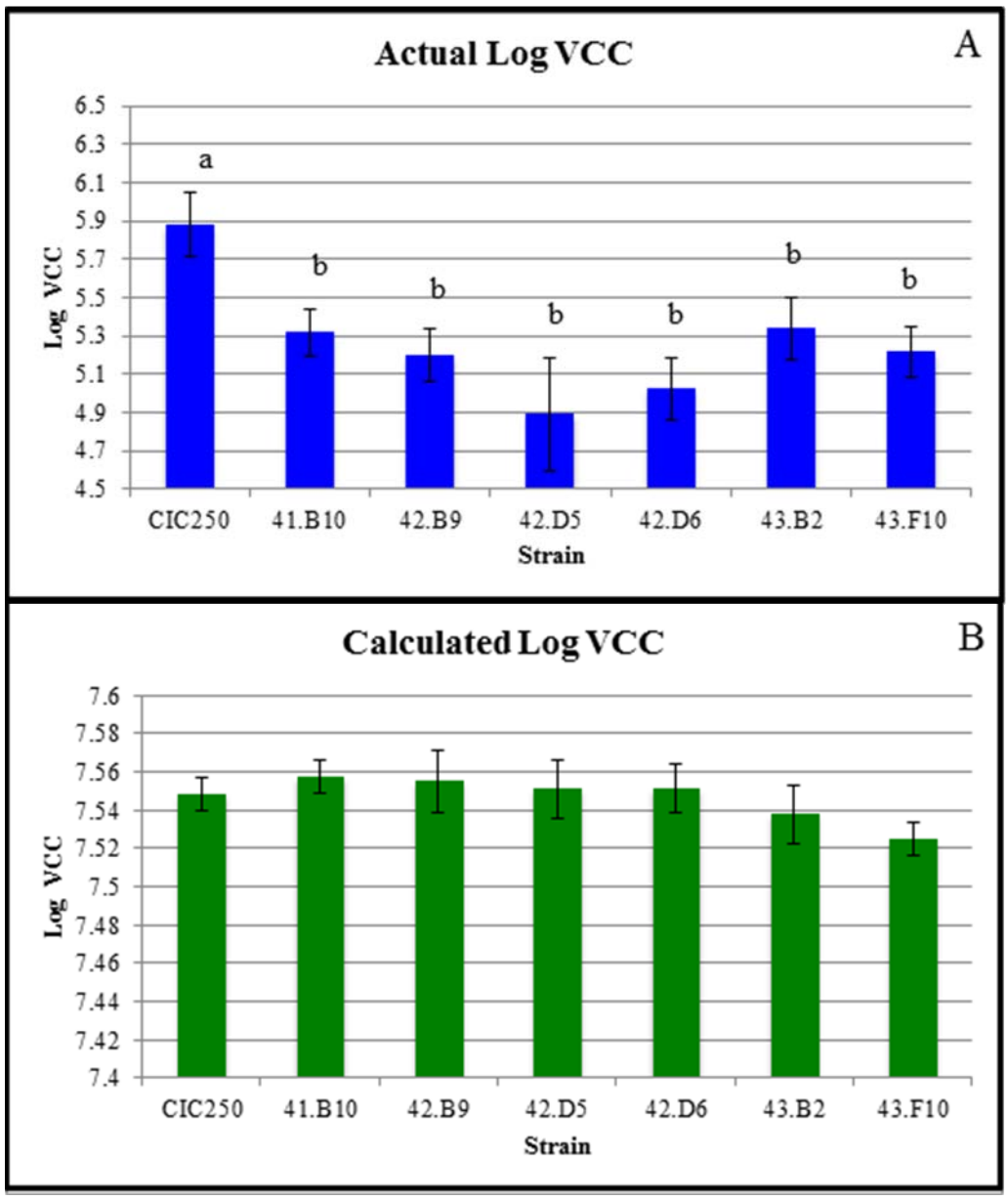


**Figure 4.4. Biofilm production by selected transposon mutants of *Clavibacter michiganensis* subsp. *sepedonicus*.** Six transposon mutants of *Cms* were selected as putative biofilm-deficient mutants and were rescreened to verify their biofilm phenotype. Bacterial titers associated with biofilms were estimated by direct colony counts of viable cells (log VCC) or by extrapolation from plate readings of optical density at 590 nm ($OD_{590}$) using a standard curve of VCC versus $OD_{590}$. A) Actual biofilm-associated bacterial titer (log VCC) as determined by serial dilution plating is represented graphically. Error bars indicate standard error and letters indicate significance classes based on LSD tests. B) Calculated biofilm-associated bacterial titer by strain (log VCC). Error bars indicate standard error and letters indicate significance classes based on LSD tests and the lack of letters indicates no significant differences observed.

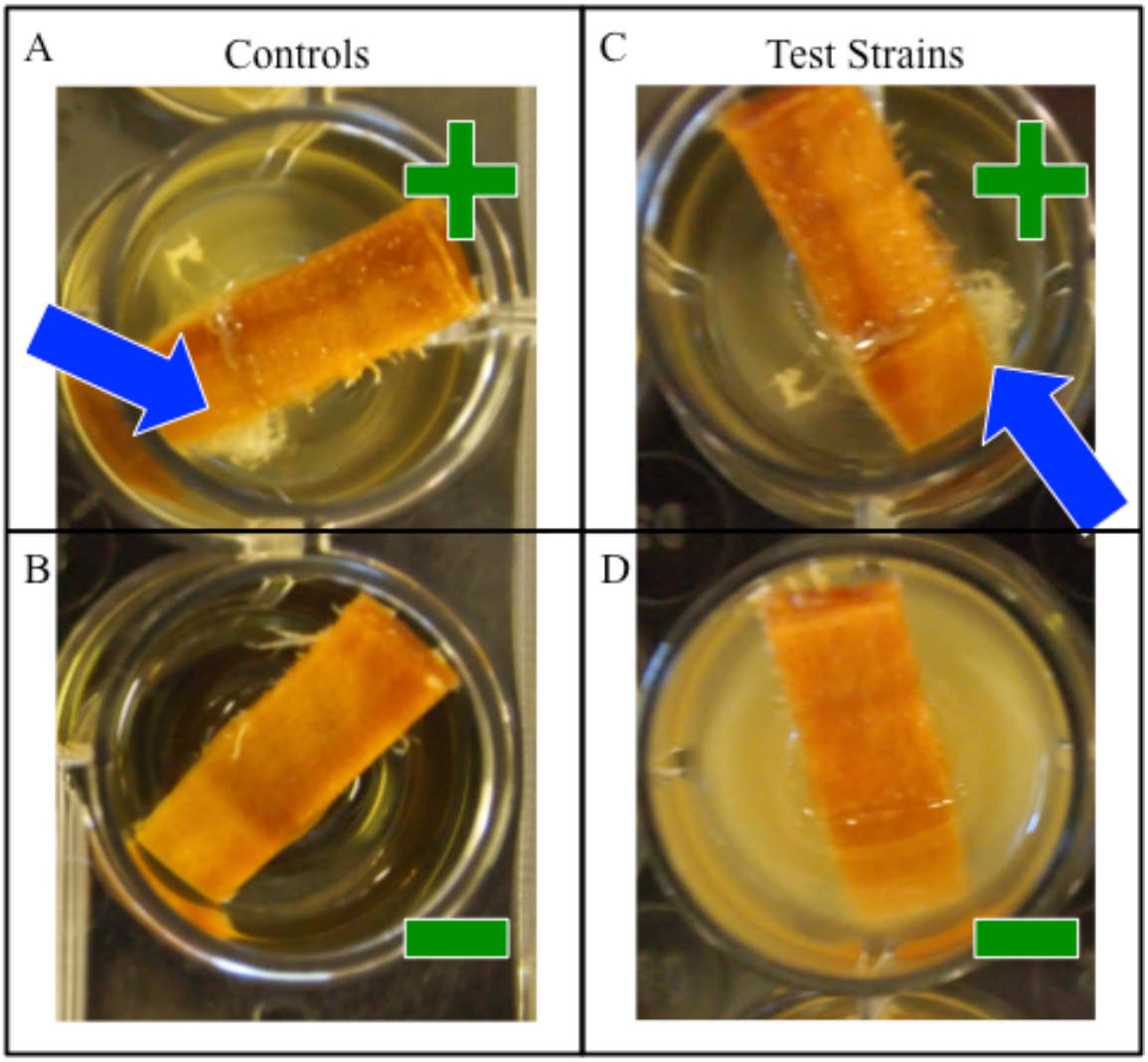


**Figure 4.5. Qualitative assay of biofilm formation by *Clavibacter michiganensis* subsp. *sepedonicus*.** Qualitative ratings of biofilms are shown where (+) indicates that a biofilms is present and (-) indicates that a biofilm is absent. A) An example image of the positive control ATCC33113. Biofilms indicated by blue arrows. B) An example image of the non-inoculated negative control. C) An example image of a biofilm-positive transposon mutant of *Cms*. Biofilms indicated by blue arrows. D) An example image of a putative biofilm-negative transposon mutant of *Cms*.

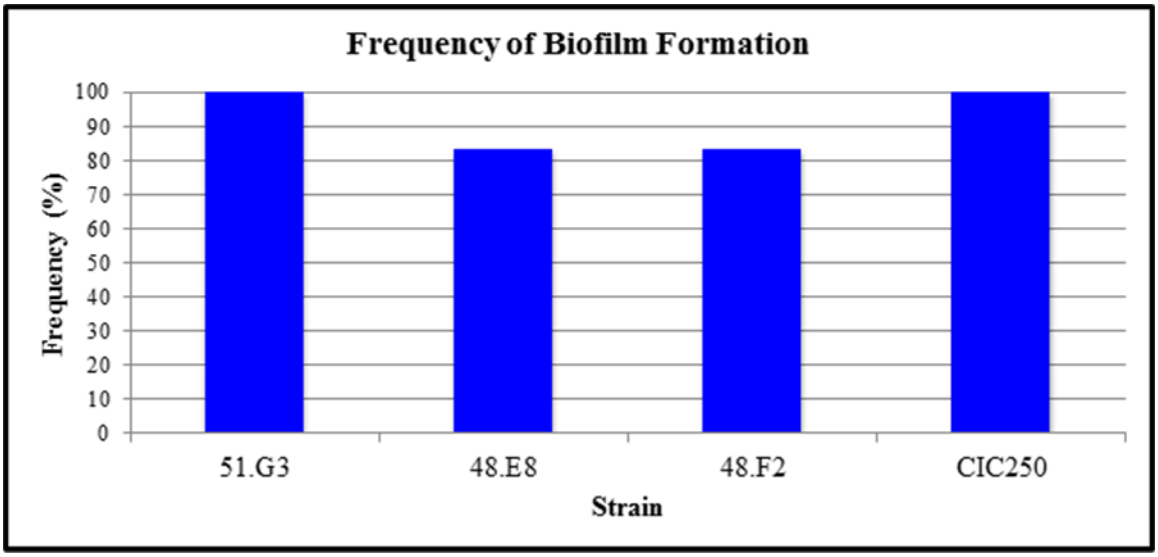


**Figure 4.6. Biofilm formation by select transposon mutants of *Clavibacter michiganensis* subsp. *sepedonicus*.** Putative biofilm-negative mutants from an initial screen were selected and rescreened with replication to verify their biofilm phenotype. Mutants were grown in YGM broth containing a piece of balsa wood for 10 days. Following growth, the presence (+) or absence (-) of biofilms was assessed visually. The frequency of biofilm formation by the putative biofilm-negative mutants of *Cms* over 12 replications is depicted.

## References


1. **Brown, S. E., A. A. Reilley, D. L. Knudson, and C. A. Ishimaru.** 2002. Genomic fingerprinting of virulent and avirulent strains of *Clavibacter michiganensis* subspecies *sepedonicus*. Current Microbiology **44:**112-119.
2. **Chalupowicz, L., E.-M. Zellermann, M. Fluegel, O. Dror, R. Eichenlaub, K.-H. Gartemann, A. Savidor, G. Sessa, N. Iraki, I. Barash, and S. Manulis.** 2010. Colonization and movement of gfp-labeled *Clavibacter michiganensis* subsp. *michiganensis* during tomato infection. Phytopathology **100:**252-261.
3. **De Boer, S. H., and R. J. Copeman.** 1980. Bacterial ring rot testing with the indirect fluorescent antibody staining procedure. American Journal of Potato Research **57:**457-465.
4. **Dow, J. M., L. Crossman, K. Findlay, Y. Q. He, J. X. Feng, and J. L. Tang.** 2003. Biofilm dispersal in *Xanthomonas campestris* is controlled by cell-cell signaling and is required for full virulence to plants. Proceedings of the National Academy of Sciences of the United States of America **100:**10995-11000.
5. **Harrison, J. J., R. J. Turner, L. L. R. Marques, and H. Ceri.** 2005. Biofilms. American Scientist **93:**508-515.
6. **Kang, Y. W., H. L. Liu, S. Genin, M. A. Schell, and T. P. Denny.** 2002. *Ralstonia solanacearum* requires type 4 pili to adhere to multiple surfaces and for natural transformation and virulence. Molecular Microbiology **46:**427-437.
7. **Lelliott, R. A., and D. E. Stead.** 1966. Methods for the diagnosis of bacterial diseases of plants, p. 216, Methods in Plant Pathology, vol. 2. T.F. Preece Series, British Society of Plant Pathology, Blackwell Scientific Publications, Oxford.
8. **Marques, L. L. R., H. Ceri, G. P. Manfio, D. M. Reid, and M. E. Olson.** 2002. Characterization of biofilm formation by *Xylella fastidiosa in vitro*. Plant Disease **86:**633-638.
9. **Marques, L. L. R., S. H. De Boer, H. Ceri, and M. E. Olson.** 2003. Evaluation of biofilms formed by *Clavibacter michiganesis* subsp. *sepedonicus*. Phytopathology **93:**S57.
10. **Merritt, J. H., D. E. Kadouri, and G. A. O'Toole.** 2005. Growing and analyzing static biofilms, p. 1B.1.1-1B.1.18. *In* R. Coico, T. Kowalik, J. Quarles, B. Stevenson, and R. Taylor (ed.), Current Protocols in Molecular Biology, vol. 22. J. Wiley & Sons, Hoboken, NJ.
11. **Mogen, B. D., A. E. Oleson, R. B. Sparks, N. C. Gudmestad, and G. A. Secor.** 1988. Distribution and partial characterization of pCS1, a highly conserved plasmid present in *Clavibacter michiganense* subsp. *sepedonicum*. Phytopathology **78:**1381-1386.
12. **Nissinen, R., Xia Y., Mattinen L., Ishimaru C. A.,, and D. L. Knudson, Knudson S. E., Metzler M., Pirhonen M.** 2009. The putative secreted serine protease Chp-7 is required for full virulence and induction of a nonhost hypersensitive response by *Clavibacter michiganensis* subsp. *sepedonicus*. Molecular Plant-Microbe Interactions **22:**809-819.

13. **Schneider, J. B., J.-l. Zhao, and C. S. Orser.** 1993. Detection of *Clavibacter michiganensis* subsp. *sepedonicus* by DNA amplification. FEMS Microbiology Letters **109:**207-212.
14. **Vidaver, A. K.** 1967. Synthetic and complex media for the rapid dection of fluorescence of phytopathogenic *Pseudomonads*: Effect of the carbon source. Applied Microbiology **15:**1523-1524.
15. **von Bodman, S. B., W. D. Bauer, and D. L. Coplin.** 2003. Quorum sensing in plant-pathogenic bacteria. Annual Reviews of Phytopathology **41:**455-482.

**Comprehensive Bibliography**


**Alfano, J. R., and A. Collmer.** 2004. Type III secretion system effector proteins: Double agents in bacterial disease and plant defense. Annual Review of Phytopathology **42:**385-414.

**Bentley, S. D., C. Corton, S. E. Brown, A. Barron, L. Clark, J. Doggett, B. Harris, D. Ormond, M. A. Quail, G. May, D. Francis, D. Knudson, J. Parkhill, and C. A. Ishimaru.** 2008. Genome of the Actinomycete plant pathogen *Clavibacter michiganensis* subspecies *sepedonicus* suggests recent niche adaptation. Journal of Bacteriology **190:**2150-2160.

**Bishop, A. L., and S. A. Slack.** 1987. Effect of innoculum dose and preparation, strain variation, and plant growth conditions on the eggplant assay for bacterial ring rot. American Potato Journal **64:**227-234.

**Brown, S. E., A. A. Reilley, D. L. Knudson, and C. A. Ishimaru.** 2002. Genomic fingerprinting of virulent and avirulent strains of *Clavibacter michiganensis* subspecies *sepedonicus*. Current Microbiology **44:**112-119.

**Burger, A., I. Grafen, J. Engemann, E. Niermann, M. Pieper, O. Kirchner, K. H. Gartemann, and R. Eichenlaub.** 2005. Identification of homologues to the pathogenicity factor *pat-1*, a putative serine protease of *Clavibacter michiganensis* subsp. *michiganensis*. Microbiological Research **160:**417-27.

**Chalupowicz, L., E.-M. Zellermann, M. Fluegel, O. Dror, R. Eichenlaub, K.-H. Gartemann, A. Savidor, G. Sessa, N. Iraki, I. Barash, and S. Manulis.** 2010. Colonization and movement of GFP-labeled *Clavibacter michiganensis* subsp. *michiganensis* during tomato infection. Phytopathology **100:**252-261.

**Davis, M. J., and A. K. Vidaver.** 2001. Coryneform plant pathogens, p. 218-235. *In* N. W. Schaad, J. B. Jones, and W. Chun (ed.), Plant Pathogenic Bacteria, Third ed. APS Press, St. Paul, MN.

**De Boer, S. H., and R. J. Copeman.** 1980. Bacterial ring rot testing with the indirect fluorescent antibody staining procedure. American Journal of Potato Research **57:**457-465.

**De Boer, S. H., and M. McCann.** 1990. Detection of *Corynebacterium sepedonicum* in potato cultivars with different propensities to express ring rot symptoms. American Potato Journal **67:**685-695.

**De Boer, S. H., A. Wieczorek, and A. Kummer.** 1988. An ELISA test for bacterial ring rot of potato with a new monoclonal antibody. Plant Disease **72:**874-878.

**Dow, J. M., L. Crossman, K. Findlay, Y. Q. He, J. X. Feng, and J. L. Tang.** 2003. Biofilm dispersal in *Xanthomonas campestris* is controlled by cell-cell signaling and is required for full virulence to plants. Proceedings of the National Academy of Sciences of the United States of America **100:**10995-11000.

**Dreier, J., D. Meletzus, and R. Eichenlaub.** 1997. Characterization of the plasmid encoded virulence region *pat*-1 of phytopathogenic *Clavibacter michiganensis* subsp. *michiganensis*. Molecular Plant-Microbe Interactions **10:**195-206.

**Dubeau, M.-P., M. G. Ghinet, P.-E. Jacques, N. Clermont, C. Beaulieu, and R. Brzezinski.** 2009. Cytosine deaminase as a negative selection marker for gene

disruption and replacement in the genus *Streptomyces* and other Actinobacteria. Applied Environmental Microbiology **75:**1211-1214.

**Ducey, T. F., Dyer D. W.** 2002. Rapid identification of Ez::Tn5$^{TM}$ transposon insertion sites in the genome of *Neisseria gonnorroeae*. EPICENTRE Forum **9:**6-7.

**Eichenlaub, R., and K. H. Gartemann.** 2011. The *Clavibacter michiganensis* subspecies: molecular investigation of Gram-positive bacterial plant pathogens. Annual Review of Phytopathology, Vol 49 **49:**445-464.

**Eichenlaub, R., K. H. Gartemann, B. Abt, T. Bekel, A. Burger, J. Engemann, M. Flugel, L. Gaigalat, A. Goesmann, I. Grafen, J. Kalinowski, O. Kaup, O. Kirchner, L. Krause, B. Linke, A. McHardy, F. Meyer, S. Pohle, C. Ruckert, S. Schneiker, E. M. Zellermann, A. Puhler, O. Kaiser, and D. Bartels.** 2008. The genome sequence of the tomato-pathogenic actinomycete *Clavibacter michiganensis* subsp *michiganensis* NCPPB382 reveals a large island involved in pathogenicity. Journal of Bacteriology **190:**2138-2149.

**Eichenlaub, R., K. H. Gartemann, and A. Burger.** 2006. *Clavibacter michiganensis*, a group of Gram-positive phytopathogenic bacteria, p. 385-421, Plant-Associated Bacteria. Springer, Netherlands.

**Gartemann, K.-H., and R. Eichenlaub.** 2001. Isolation and characterization of IS*1409*, an insertion element of 4-chlorobenzoate-degrading *Arthrobacter* sp. strain TM1, and development of a system for transposon mutagenesis. Journal of Bacteriology **183:**3729-3736.

**Gudmestad, N. C.** 1987. Recommendations of the national task force for the eradication of bacterial ring rot. American Potato Journal **64:**695-697.

**Gudmestad, N. C., and G. A. Secor.** 1984. Bacterial ring rot- the changing scene. Valley Potato Grower **49:**18-21.

**Harrison, J. J., R. J. Turner, L. L. R. Marques, and H. Ceri.** 2005. Biofilms. American Scientist **93:**508-515.

**Hogenhout, S. A., and R. Loria.** 2008. Virulence mechanisms of Gram-positive plant pathogenic bacteria. Current Opinion in Plant Biology **11:**449-456.

**Hogenhout, S. A., R. A. L. Van der Hoorn, R. Terauchi, and S. Kamoun.** 2009. Emerging concepts in effector biology of plant-associated organisms. Molecular Plant-Microbe Interactions **22:**115-122.

**Holtsmark, I., G. Takle, and M. Brurberg.** 2008. Expression of putative virulence factors in the potato pathogen *Clavibacter michiganensis* subsp. *sepedonicus* during infection. Archives of Microbiology **189:**131-139.

**Horsfall, J. G., and R. W. Barratt.** 1945. An improved grading system for measuring plant disease. Phytopathology **35:**655.

**Ishimaru, C. A., N. L. V. Lapitan, A. VanBuren, A. Fenwick, and K. Pedas.** 1994. Identification of parents suitable for molecular mapping of immunity and resistance genes in *Solanum* species. American Potato Journal **71:**517-533.

**Jahr, H., J. Dreier, D. Meletzus, R. Bahro, and R. Eichenlaub.** 2000. The endo-B-1, 4-glucanase *CelA* of *Clavibacter michiganensis* subsp. *michiganensis* is a pathogenicity determinant required for induction of bacterial wilt of tomato. Molecular Plant-Microbe Interactions **13:**703-714.

**Jones, J. D. G., and J. L. Dangl.** 2006. The plant immune system. Nature **444:**323-329.

**Kang, Y. W., H. L. Liu, S. Genin, M. A. Schell, and T. P. Denny.** 2002. *Ralstonia solanacearum* requires type 4 pili to adhere to multiple surfaces and for natural transformation and virulence. Molecular Microbiology **46:**427-437.

**Kirchner, O., K. H. Gartemann, E. M. Zellermann, R. Eichenlaub, and A. Burger.** 2001. A highly efficient transposon mutagenesis system for the tomato pathogen *Clavibacter michiganensis* subsp. *michiganensis*. Molecular Plant-Microbe Interactions **14:**1312-8.

**Laine, M. J., H. Nakhei, J. Dreier, K. Lehtila, D. Meletzus, R. Eichenlaub, and M. C. Metzler.** 1996. Stable transformation of the Gram-positive phytopathogenic bacterium *Clavibacter michiganensis* subsp. *sepedonicus* with several cloning vectors. Applied and Environmental Microbiology **62:**1500-1506.

**Lelliott, R. A., and D. E. Stead.** 1966. Methods for the diagnosis of bacterial diseases of plants, p. 216, Methods in Plant Pathology, vol. 2. T.F. Preece Series, British Society of Plant Pathology, Blackwell Scientific Publications, Oxford.

**Louws, F. J., J. Bell, C. M. Medina-Mora, C. D. Smart, D. Opgenorth, C. A. Ishimaru, M. K. Hausbeck, F. J. de Bruijn, and D. W. Fulbright.** 1998. Rep-PCR-mediated genomic fingerprinting: A rapid and effective method to identify *Clavibacter michiganensis*. Phytopathology **88:**862-868.

**Manzer, F. E., and C. J. Kurowski.** 1992. Bacterial ring rot disease development in resistant and susceptible cultivars. American Potato Journal **69:**363-370.

**Marques, L. L. R., H. Ceri, G. P. Manfio, D. M. Reid, and M. E. Olson.** 2002. Characterization of biofilm formation by *Xylella fastidiosa in vitro*. Plant Disease **86:**633-638.

**Marques, L. L. R., S. H. De Boer, H. Ceri, and M. E. Olson.** 2003. Evaluation of biofilms formed by *Clavibacter michiganesis* subsp. *sepedonicus*. Phytopathology **93:**S57.

**Merritt, J. H., D. E. Kadouri, and G. A. O'Toole.** 2005. Growing and analyzing static biofilms, p. 1B.1.1-1B.1.18. *In* R. Coico, T. Kowalik, J. Quarles, B. Stevenson, and R. Taylor (ed.), Current Protocols in Molecular Biology, vol. 22. J. Wiley & Sons, Hoboken, NJ.

**Mills, D., B. W. Russell, and J. W. Hanus.** 1997. Specific detection of *Clavibacter michiganensis* subsp. *sepedonicus* by amplification of three unique DNA sequences isolated by subtraction hybridization. Phytopathology **87:**853-861.

**Mogen, B. D., A. E. Oleson, R. B. Sparks, N. C. Gudmestad, and G. A. Secor.** 1988. Distribution and partial characterization of pCS1, a highly conserved plasmid present in *Clavibacter michiganense* subsp. *sepedonicum*. Phytopathology **78:**1381-1386.

**Morris, C. E., and J. M. Monier.** 2003. The ecological significance of biofilm formation by plant-associated bacteria. Annual Review of Phytopathology **41:**429-53.

**Nissinen, R., S. Kassuwi, R. Peltola, and M. C. Metzler.** 2001. *In planta* - complementation of *Clavibacter michiganensis* subsp. *sepedonicus* strains deficient in cellulase production or HR induction restores virulence. European Journal of Plant Pathology **107:**175-182.

**Nissinen, R., Y. Xia, L. Mattinen, C. A. Ishimaru, D. Knudson, S. E. Brown, M. Metzler, and M. Pirhonen.** 2009. The putative secreted serine protease Chp-7 is

required for full virulence and induction of a nonhost hypersensitive response by *Clavibacter michiganensis* subsp. *sepedonicus*. Molecular Plant-Microbe Interactions **22:**809-819.

**Parsek, M. R., and P. K. Singh.** 2003. Bacterial biofilms: an emerging link to disease pathogenesis. Annual Review of Microbiology **57:**677-701.

**Ramey, B. E., M. Koutsoudis, S. B. von Bodman, and C. Fuqua.** 2004. Biofilm formation in plant-microbe associations. Current Opinion in Microbiology **7:**602-609.

**Rozen, S., and H. J. Skaletsky.** 2000. Primer3 on the www for general users and for biologist programmers. *In* S. Krawetz and S. Misener (ed.), Bioinformatics methods and protocols: Methods in molecular biology. Humana Press, Totowa, NJ.

**Sands, D. C., G. Mizrak, V. N. Hall, H. K. Kim, H. E. Bockelman, and M. J. Golden.** 1986. Seed transmitted bacterial diseases of cereals: Epidemiology and control. Arab Journal of Plant Protection **4:**127-125.

**Schneider, J. B., J.-l. Zhao, and C. S. Orser.** 1993. Detection of *Clavibacter michiganensis* subsp. *sepedonicus* by DNA amplification. FEMS Microbiology Letters **109:**207-212.

**Stackebrandt, E., E. Brambilla, and K. Richert.** 2007. Gene sequence phylogenies of the family *Mircobacteriaceae*. Current Microbiology **55:**42-46.

**Stackebrandt, E., and P. Schumann.** 2006. Introduction to the taxonomy of Actinobacteria, p. 297-321, The Prokaryotes. Springer, New York, NY.

**Stahl, E. A., and J. G. Bishop.** 2000. Plant-pathogen arms races at the molecular level. Current Opinion in Plant Biology **3:**299-304.

**Stevenson, W. R., R. Loria, G. D. Franc, and D. P. Weingartner (ed.).** 2001. Compendium of potato diseases, Second ed. APS Press, St. Paul, MN.

**Stork, I., K.-H. Gartemann, A. Burger, and R. Eichenlaub.** 2008. A family of serine proteases of *Clavibacter michiganensis* subsp. *michiganensis*: *chpC* plays a role in colonization of the host plant tomato. Molecular Plant Pathology **9:**599-608.

**Sutherland, I. W.** 2001. Biofilm exopolysaccharides: a strong and sticky framework. Microbiology **147:**3-9.

**Team, R. D. C.** 2008. R: A language and environment for statistical computing. R Foundation for Statistical Computing, Vienna, Austria.

**Vidaver, A. K.** 1967. Synthetic and complex media for the rapid dection of fluorescence of phytopathogenic *Pseudomonads*: Effect of the carbon source. Applied Microbiology **15:**1523-1524.

**von Bodman, S. B., W. D. Bauer, and D. L. Coplin.** 2003. Quorum sensing in plant-pathogenic bacteria. Annual Review of Phytopathology **41:**455-482.

**Wilson, K.** 1997. Preparation of genomic DNA from bacteria. Current Protocols in Molecular Biology **27:**2.4.1-2.4.5.

**Woese, C. R.** 1987. Bacterial evolution. Microbiological Reviews **51:**221-271.